Reaction Kinetics of Carbonate Rocks with Chelating Agents/Seawater System

BY

Khaled Zidan Abdelgawad Ibrahim

A Dissertation Presented to the

DEANSHIP OF GRADUATE STUDIES

KING FAHD UNIVERSITY OF PETROLEUM & MINERALS

DHAHRAN, SAUDI ARABIA

In Partial Fulfillment of the
Requirements for the Degree of

DOCTOR OF PHILOSOPHY

In

Petroleum Engineering

December 2017

KING FAHD UNIVERSITY OF PETROLEUM & MINERALS

DHAHRAN- 31261, SAUDI ARABIA

DEANSHIP OF GRADUATE STUDIES

This thesis, written by **KHALED ZIDAN ABDELGAWAD** under the direction of his thesis advisor and approved by his thesis committee, has been presented and accepted by the Dean of Graduate Studies, in partial fulfillment of the requirements for the degree of **Doctor of Philosophy in Petroleum Engineering**.

Dr. Mohamed Mahmoud
(Advisor)

Dr. Dhafer A. Al Shehri
Department Chairman

Dr. Abdulazeez Abdulraheem
(Co-Advisor)

Dr. Salam A. Zummo
Dean of Graduate Studies

Dr. Sidqi A. Abu-Khamsin
(Member)

27/12/17

Date

Dr. Abdulaziz Al-Majed
(Co-Advisor)

Dr. Reyad A. Shawabkeh
(Member)

Surely my Prayer, all my acts of worship, and my living and my dying are for Allah alone, the Lord of the whole universe.

ACKNOWLEDGMENTS

Praise is to Allah, Lord of the Worlds, the most compassionate, and the most merciful who has given me the strength and patience to accomplish this work.

I would like to express my sincere thanks to my advisor Dr. Mohamed A. Mahmoud. I am grateful for his assistance and guidance throughout my studies and research, I am heartily thankful to him, whose encouragement, supervision and support from the preliminary to the concluding level enabled me to develop an understanding of this subject. I wish to extend my appreciation to Dr. Abdulazeez Abdulraheem, Dr. Abdulaziz Al Majid, Dr. Sidqi Abu-Khamsin, and Dr. Reyad Shawabkeh for devoting their invaluable time to review and evaluate my research work. Their comments during the course of my studies are highly appreciated. Many thanks to the Kingdom of Saudi Arabia for providing a scholarship during my studies at King Fahd University of Petroleum & Minerals. I would Like also to thank all the faculty, staff, and students in the College of petroleum engineering and geosciences and the center of integrative petroleum research.

I wish to express my love and gratitude to my beloved family; my Parents and my brothers. A special thanks to my wife for here understanding and infinite support she has shown through the last four years.

TABLE OF CONTENTS

LIST OF TABLES

LIST OF FIGURES

LIST OF ABBREVIATIONS

GLDA	N,N-Dicarboxymethyl glutamic acid
GLDA/SW	N,N-Dicarboxymethyl glutamic acid diluted from stock concentration using seawater
DTPA	Pentetic acid or diethylenetriaminepentaacetic acid
EDTA	Ethylenediaminetetraacetic acid
DTPA/DI	DTPA diluted from stock concentration using deionized water
DTPA/SW	DTPA diluted from stock concentration using seawater
EDTA/SW	EDTA diluted from stock concentration using seawater
EDTA/DI	EDTA diluted from stock concentration using deionized water
μ	Fluid viscosity, gm/cm^3
A	Surface area
BP	Back Pressure
C_b	Bulk concentration of the transferred species
C_s	Surface concentration of the transferred species
D_e	Diffusion coefficient cm^2/s
DI	Deionized water
HCl	Hydrochloric acid
HPHT	High pressure High temperature
IFT	Interfacial tension
in	Inches
J	Mass transfer flux
K_m	Mass transfer coefficient
mD	Milli-Darcy
NPV_{bt}	Normalized pore volumes to breakthrough

Nt_{bt}	Normalized time to breakthrough
ºF	Degree Fahrenheit
PDR	Pressure drop ratio at time t_i
pH	Potential of hydrogen
psi	Pound-force per square inch
PV	Pore Volume
PV_{BT}	Injected pore volume at the wormhole breakthrough
$PV_{bt.optimum}$	Optimum pore volumes to breakthrough
$PV_{bt.optimum}$	Maximum pore volume to breakthrough
RDA	Rotating Disk Apparatus
RPM	Revolution per minute
Sc	Schmidt number ((v / D_e),
SWDCA	Seawater diluted chelating agents
SEM	Scanning electron microscope
SW	Seawater
T	Temperature
t_{bt}	Time to breakthrough at a certain flow rate
$t_{bt.max}$	Maximum time to breakthrough
$t_{bt.min}$	Minimum time to breakthrough (time at optimum injection rate
v	Kinematic viscosity (μ/ρ), cm^2/s
ρ	Fluid density, gm/cm^3
ω	Disk rotational speed,

ABSTRACT

Full Name : Khaled Zidan Abdelgawad Ibrahim

Thesis Title : Reaction Kinetics of Carbonate Rocks with Chelating Agents/Seawater System

Major Field : Petroleum Engineering

Date of Degree : December, 2017

The drop in the oil and gas prices drives the oil and gas companies to enhance the productivity form the existing wells using well stimulation. Acid stimulation is a quick, cheap and easy solution for well depletion issues. In matrix acidizing, acid solutions are injected through the wellbore into the subsurface formation with a bottomhole injection pressure below the formation fracture pressure. A better understanding of reservoir matrix reaction with injected fluids allows the optimization of such treatments. The main objective of matrix acidizing is to Bypass the near-wellbore damage and improve well's performance using acids. Unfortunately, resulted corrosion due to the injection of hydrochloric acid (HCl) resulted in avoiding matrix stimulation practices in the industry early days until the discovery of corrosion inhibitors. Another issue of HCl acid in high temperature reservoirs, is the face dissolution by consuming the injected volume of acids at the formation face due to high reaction rates with carbonate rocks. High injection rates are required to allow acid penetration through the damaged near wellbore area and in same time are limited by the formation fracture pressure. In addition, it so difficult to handle safely huge quantities of HCl during field treatments. This requires the development of new treating formulations to meet such conditions. So much research was done to solve this problem using different acid systems

other than HCl. In most of those systems fresh water or even deionized water was used to prepare the treating fluids.

One of the environmental friendly stimulation fluid are those belong to the amine group known as chelating agents. This study focused on studying seawater effects on the reaction rate of chelating agents with calcite. In addition, the effect of porosity type on the reaction parameters was investigated. The optimum injection rate to propagate the wormhole was estimated from the reaction kinetics and the results were compared with the coreflooding experiments. The conducted experimental work results using different chelating agents showed that diluting the acid system using seawater had a significant effect on the fluid reaction with carbonate rock samples. The overall reaction of 20 wt% GLDA diluted using seawater (GLDA/SW) with Indiana limestone rock surface is inhibited with the presence of salt ions from seawater compared to GLDA diluted using fresh water (GLDA/DI). In addition, the reaction between 3.8 pH 20% GLDA/DI and Indiana limestone is surface reaction limited at 150^{o}F and mass transfer limited at 200 and 250^{o}F, however the reaction of 20% GLDA/SW with the same rock is mass transfer limited at 150-250^{o}F. The reaction between 3.8 pH 20% GLDA/SW and Austin chalk is surface reaction limited at 200^{o}F. 0.5 cm^{3}/min was estimated as an optimum injection rate for 20 wt. % GLDA/SW at 1000 psi and 250^{o}F from coreflooding experiments analysis compared to 0.43 cm^{3}/min using a mathematical model. For other chelating agents (DTPA, EDTA) the effect of seawater is different from GLDA indicating that the conclusion drawn from each fluid cannot be generalized for other fluids. This work, will help design successful HP/HT stimulation treatments using rotating disk results at the same lithology, pore geometry, pressure and temperature of the treated formations without any need for tedious coreflooding experiments.

ملخص الرسالة

الاسم الكامل: خالد زيدان عبد الجواد

عنوان الرسالة:

التخصص: هندسة البترول

تاريخ الدرجة العلمية:

يدفع انخفاض أسعار النفط ما إلي محاولة تحسين إنتاجية الأبار الموجودة وتقلل برامج الحفر والتكسير .غالبا ما تحول الشركات تركيزها لزيادة الإنتاج من الآبار القائمة عن طريق إستخدام السوائل الحمضية التي تعتبر أحد الحلول السريعة والرخيصة والسهلة لتحسين وزيادة الإنتاج. مع انتقال الصناعة من التعامل مع المكامن إلي محاولة الإنتاج من مكامن تنفية ذات ضغط ودرجة الحرارة الخزان مرتفعة، هناك ضرورة متزايدة لسوائل حمضية صالحة للعمل تحت هذه الظروف من الضغط والحرارة. خلال عمليا معالجة الأبار بالسوائل الحمضية، يتم حقن المحاليل الحمضية من خلال البئر إلي طبقات الأرض مع ضغط أقل من ضغط تكسير الطبقات. يؤدي الفهم الجيد للسوائل المستخدمة في عمليات المعالجة إلي القيام بها علي أفضل وجه ممكن. يعتبر تحديد المواد الكيميائية المستخدمة لمعالجة الطبقات بالإضافة إلي الكمية المطلو بضخها من أهم العوامل المهمة أثناء معالجة الطبقات لتحقيق الأهداف المنشوردة. يعتبرتحسين أداء الحقن والإنتاج في الآبار النفطية الهدف الرئيسي للتحفيز الكيميائي للأبار باستخدام الأحماض. يمكن أن تؤدي معالجة طبقات المكمن النفطي باستخدام حمض الهيدروكلوريك إلي زيادة الإنتاج بعدة أضعاف من الآبار المعالجة لكن استخدام حمض الهيدروكلوريك يؤدي إلي تأكل أنابيب إنتاج الأبار مما ترتب عليه تجنب استخدامه في الأيام الأولي لصناعة البترول إلي أن تم إكتشاف اكتشاف المواد الكيميائية المعروفة بمثبطات التآكل.

يعتبر معدل النفاعل السريع لحمض الهيدروكلوريك من المشاكل التي نواجه إستخداكه أيضا في معالدة الطبقات مما يتطلب مطلوب معدلات حقن عالية للسماح بتغلغل الحمض خلال الصخور مكا قد يؤدي إلي تكسيرها. وبالإضافة إلى ذلك، فإنه من الصعب جدا التعامل بأمان مع الكميات الهائلة من حمض الهيدروكلوريك خلال العمليات التي تتم في الحقول النفطية علي نطاق واسع. وهذا يتطلب تطوير تركيبات كيميائية جديدة لتلبية هذه الظروف. وقد تم إجراء الكثير من الأبحاث لحل هذه المشكلة باستخدام أنظمة حمض غير حمض الهيدروكلوريك. في معظم تلك النظم تم استخدام المياه العذبة أو حتى الماء منزوع الأملاح لإعداد السوائل المعالجة.

واحدة من سوائل التحفيز صديقة للبيئة هي تلك التي تنتمي إلى مجموعة Amino المعروفة باسم المركبات المخلبية. وسيركز هذا العمل البحثي علي دراسة تأثير مياه البحر على معدل التفاعل المواد المخلبية مع الصخور الكربوينة بما في ذلك تأثير درجة الحرارة. وبالإضافة إلى ذلك، سيتم التحقيق تأثير الملح الفردي على حركية المركبات المخلبية مع الصخور الكربونية وكذلك تأثير نوع المسامية. هذا العمل، مع في المنافسة، سوف تمكن من تصميم لعمليات تحفيز الأنتاج باستخدام النتائج المعملية التي تجري علي نفس نوع الصخر المراد معالجته.

CHAPTER 1

INTRODUCTION

1.1 Introduction

With the industry moving from moderate reservoir conditions to be more interested in producing High pressure and High temperature reservoir (HPHT), there is a growing need for HPHT matrix acidizing techniques. In matrix acidizing, acid mixtures are injected through the wellbore into the subsurface formation with a bottomhole injection pressure below the formation fracture pressure. A better understanding of the reservoir matrices reaction with injected fluids will allow the optimum design of such treatments. Two aspects of advance in matrix stimulations are the chemicals that are injected to the damaged zone and how such chemicals can be placed correctly to its destination.

Bypassing the near-wellbore damage and improving the performance of injection and production wells are the main objective matrix stimulation using acids. The history of matrix stimulation started back in 1895 when Ohio Oil Company used Hydrochloric acid (HCL) in the treatment of a limestone formation which resulted in increasing the production by several folds from the treated wells. Resulted casing corrosion due to the injection of HCl resulted in avoiding matrix stimulation practices in the industry until the discovery of corrosion inhibitors in 1931.

Generally, one can say that well acidizing is an intervention method to restore of improve flow into or out of a subsurface formation (infectivity or productivity improvement). The destination of the injected acids is the near will bore formation to either remove precipitated scales or dissolve part of the matrix itself creating wormholes that reduce the pressure drop across this part of the reservoir.

Producing different reservoirs in terms of lithology, downhole conditions, type of formation damage formed around producers and injectors require the development of new treating formulations to meet such conditions. Using mineral acids (HCl and HF) at HT reservoirs resulted in too rapid reaction rates which end up with consuming the injected volume of acids at the sandface and causing what is known as face dissolution. Also Mineral acids are difficult to handle safely and strongly affect the well tubular due to its corrosive nature. What is mentioned before requires the use of expensive corrosion inhibitors which significantly increase the cost of an acidizing treatment especially at higher temperature.

The formation lithology is a key factor when a stimulation formulation is to be designed. Worm holes (highly conductive pathways through the rock matrix) can be created easily in carbonate formations due to the high solubility of carbonate matrix in most of the used acids. They react with HCl at moderate temperatures generating wormholes through the rock matrix. Carbonates are rapidly dissolve in HCl and create products that are soluble in water.

The reaction of carbonate rocks with HCl is limited by Hydrogen ions diffusion to the rock surface whoever sandstones are slightly acid soluble. The shape, rate of growth the

wormhole depends on the acid type, strength, injection rate, formation temperature and the rock lithology. Under different conditions of controllable parameters, different dissolution patterns are formed.

The optimum dissolution pattern which is the target of all the treatments is the wormhole pattern in which the minimum volume of acid is injected to bypass the damaged region through the creation of long conductive wormholes as shown in

Figure 1.1.

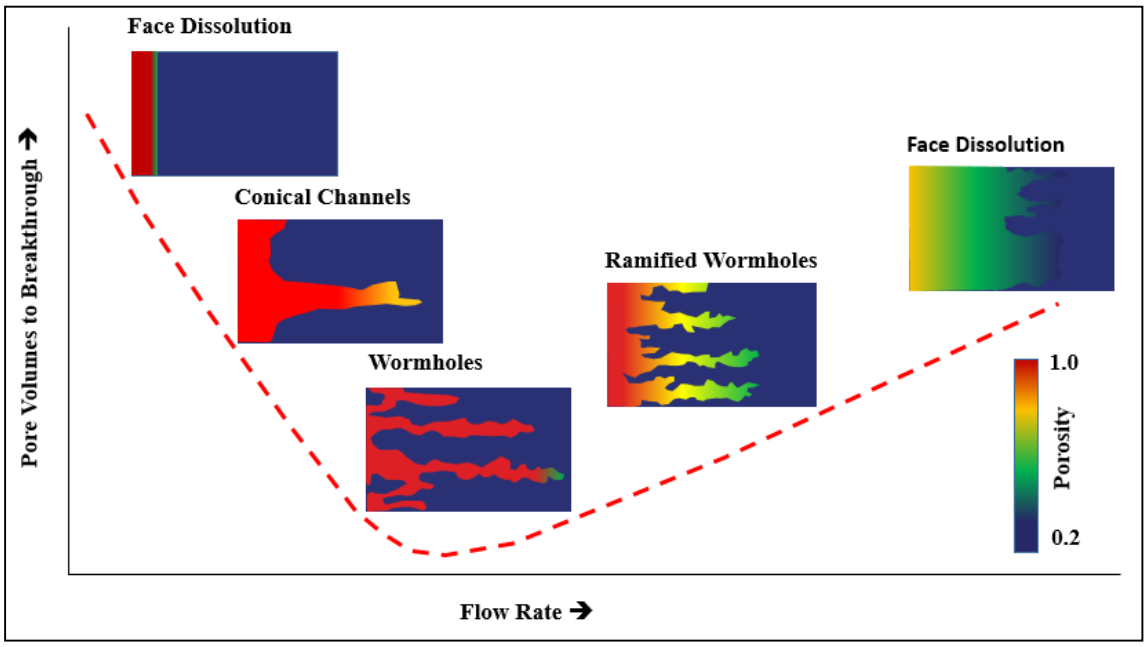

Figure 1.1—Carbonate Dissolution Patterns (After Al-Harthy el al, 2009).

The least efficient acidizing treatment in which the entire rock matrix is dissolved to advance the reaction front is known as face dissolution. If the flow rate is increased slightly so that face dissolution is avoided, conical channels can be created. At the required minimum acid pore volumes to penetrate the core sample, a dominating

wormhole extends from the core inlet to its outlet which is the most efficient permeability enhancement. The flow rate at which an optimized wormhole can be obtained using a certain formulation is found at the curve minimum. At rates higher than the optimum flow rates, several larger channels are created known as ramified wormholes which consume more acid volume. Finally, farther increase of the acid injection rate results in a uniform face dissolution (not entire matrix dissolution).

To overcome most of those challenges encountered during using HCl especially when low injection rate is required to avoid formation fracture, new stimulation fluids were developed to be used at high temperature environments. **Table 1.1** summarizes most of the fluids developed during the last fifty years as a requirement of the extension of matrix acidizing to HT formations.

Table 1.1—Developed matrix stimulation fluids for HT

Fluid	Mechanism
Organic acids	- Combination of organic acids (acetic and formic) used to minimize corrosion problems in high-temperature applications. - Dissolving power is equivalent to HC1with significantly reduced corrosion rates and the absence of Cl^- ions.
Emulsified acids	- Acid-oil emulsions slow down the acid reaction rate at HT by reducing D_e. - High viscosity which improves distribution in heterogeneous reservoirs. - Reduced tubular corrosion since the acid did not contact with it.
Retarded Acid Systems	- Polymers, Cross linked polymers, and viscoelastic surfactants are used to increasing HCl acid system viscosity.
Foamed acids	- Composed of gaseous N_2 and aqueous HCl - Prevent acid spending at the sandface allowing deeper penetration inside the formation and Promote the growth of wormhole - Foam acts to reduce the liquid permeability which decreases the volume of fresh acid leaked along the wormhole length.
Chelating Agents	- Lower toxicity and environment friendly. - Slow reaction rate - Deep penetration at HT - Low corrosion rate up to order or magnitude of mineral acids

1.2 Objectives

The aim of this study is to address the reaction of seawater diluted chelating agents (GLDA, DTPA and EDTA) with carbonate reservoir rock samples. Efficient determination of reaction parameters is an important step towards implementing seawater diluted chelating agents (SWDCA) in field operations. To achieve the main goal of this, work the following sub-objectives will be studied respectively:

(1) Defining the reaction controlling process for each fluid system whether mass transfer surface reaction limited.

(2) Studying the effect of seawater on the reaction rate of chelating agents with calcite.

(3) Comparing the results with the results available in the literature for the same chelating agents when diluted with deionized water.

(4) Investigating the effect of porosity type rock facies on the reaction parameters by using rocks with same porosity, lithology and different facies.

CHAPTER 2

LITERATURE REVIEW

2.1 Carbonate Stimulation

Organic and inorganic acids are often injected into subterranean formations to improve the oil and gas production rates. Those stimulation fluids are usually selected based on the type of formation being treated. In the case of stimulating carbonate formations, the acids can dissolve the carbonate rock matrix itself forming different dissolution features or structures depending in the type of the acid, injection rate, and formation conditions. At very low injection rates, the face of the rock is dissolved resulting in a face-dissolution patterns. At high injection rates, the retention time of acid in the rock is small and the rock is dissolved uniformly by forming narrow dissolution channels that might propagated throughout the rock or form more branches with continuous acid injection.

An optimum channel formed during acid injection is known as a wormhole which formed at the least amount of acid injected and give the most permeability increase. Other dissolution patterns can be present such as the conical wormholes (injection rate between face dissolution and wormhole patterns) and ramified wormholes (injection rate between wormhole and uniform dissolution patterns).

Face dissolution is the frequently occurring problem during the stimulation of carbonate formations using hydrochloric acid (HCl). Fluid loss along the wormhole increases with the acid penetration radius (Wang, 1993). Fluid loss can reach up to 63 % of the total rate

of the injected acid while the effective rate used in creating wormhole is the rest of the acid volume or less due to the consumption of acid at the rock face.

Wormhole penetration is of interest rather than the wormhole size as the deeper the acid can go the higher the permeability improvement. At low injection rate, fluid loss to the face of the created wormholes will increase and more face dissolution is expected due fast reaction of HCl. To solve the acid spending and face dissolution problems at low injection rates different acid systems have been used for carbonate formations stimulation treatment as shown earlier in. To overcome most of those challenges encountered during using HCl especially when low injection rate is required to avoid formation fracture, new stimulation fluids were developed to be used at high temperature environments. Fredd and Fogler (1998) investigated the reaction of different chelating agents with carbonate rock samples and evaluated the ability of these chemicals to form wormholes. They performed a linear coreflooding test using 4.3 pH 0.25M DTPA, and 4 and 13 pH 0.25M EDTA. Nonaggressive fluid having a very low corrosion rate as compared to HCl was tested by Wang et al. (2009) to stimulate carbonate reservoirs. The proved that Nonaggressive fluid can be used to stimulate heterogeneous reservoirs without any need of diverting agents as they reported using parallel coreflooding experiments utilizing their fluid system to treat both high and low permeability cores without adding any diverting agents.

Frenier et al. (2001) tested a 2.5, 4, and 9 pH solution of HEDTA (Ethylene diamine tri acetic acid at 300^{o}F and reported that the pH 4 sodium HEDTA was the best in terms of required breakthrough volumes while the pH 12 was not effective as required for stimulation treatments.

LePage et al. (2011) examined a readily biodegradable polyacidic chelate L-glutamic acid, N, N-diacetic acid or GLDA as a stimulation fluid. They compared GLDA with other chelating agents, including EDTA, HEDTA, NTA and EDG. They reported that GLDA was very effective for carbonate rock stimulation than other chelating agents and organic acids with a thermal stability of same order as HEDTA, matching the field requirements at high temperature.

2.2 Carbonate Rock Reaction Kinetics

Among the techniques used to evaluate stimulation fluid efficiencies for matrix acidulation is the rotating disk apparatus (RDA). RDA is used mainly for studying the reactions between fluids and rock surface. The rotating disk was first described in 1972 (Boomer 1972). The Rotating disk system is used to determine the reaction rate, the order of the reaction, and the diffusion coefficient associated with the dissolution (Fredd and Scott Fogler, 1998; Levich, 1962; Lund et al., 1975, 1973 and others). **Table 2.1** summarizes the previous reaction kinetics work done in the literature to determine the reaction parameters of carbonate rocks with different fluid systems.

As it become clear from my literature review that using seawater in stimulation operation ignored by the researchers specially when it comes to reaction kinetics area. The only work was done by Rabie et al. (2014) when they used seawater to dilute lactic acid and they concluded that the presence of salts (from seawater) reduced the rate of dissolution by lactic acid. Recently Assad (2015) performed cored flooding using seawater diluted chelating agents. The results of their work indicated that still even after the effect of the present salts, the solution was able to generate wormholes through Indiana limestone cores.

Table 2.1 —Reaction kinetics work done before for carbonate rocks with different fluid systems.

Author	Rock/Fluid System and conditions	Results
Sajjaat et al. 2015	- Emulsified acid (15 wt% HCl 0.7 acid Vol. fraction) - 0.5-2.0 Vol% emulsifier - Alabama marble (1.5" x 0.65" disk) - 1000 psi. - Temperature range 73-250°F. - 100 to 1500 rpm. - Experiment run for 10 minutes	- Dissolution rate of MSA with calcite was mass-transfer limited even at high rpm. - DC of a 5 wt% MSA at 150°F was 5.29×10^{-5} cm^2/s and - DC at 250°F was 3.03×10^{-4} cm^2/s. - The acid diffusivity increased with increasing system temperature.
Alkhaldi et al. 2010	- 1- 7.5 wt% Citric acid. - Calcite marble (1.5" x 0.65" disk). - 1000 psi at 25°C, 40°C and 50°C - 100 to 1000 rpm. - Experiment run for 50 minutes	- The effective D_e of citric acid reported as a function of the interaction between the calcium citrate precipitation and presence of the counter-calcium ions. - The effects of calcium citrate precipitation and counter-calcium ions on *De* were minimal at low citric acid concentrations.
Sayed et al. 2013	- 1- 7.5 wt% Citric acid. - Dolomite (1.5" x 0.75" disk). - 4.2 – 6.9 porosity - 1100 psi and 230°F - 100 to 1500 rpm. - Experiment run for 50 minutes	- Reaction of dolomite with emulsified acid at 230°Fwas found to mass transfer limited. - Compared to calcite dissolution rate of dolomite in emulsified acid is one order of magnitude. - DC of 1.413×10^{-10} cm^2/s emulsified acid with 0.5 vol% emulsifier and average droplet size of 8.118µm - DC of 8.367×10^{-10} cm^2/s emulsified acid with 0.5 vol% emulsifier and average droplet size of 2.82µm.
Taylor et al. 2003	- Calcite marble and dolomite marble - 23 and 50ºC. - 50 to 1000 rpm. - 0.1 N HCl with different additives	- Polymer changed the acid-rock reaction from mass transfer limited to surface reaction limited with both calcite and dolomite due to polymer adsorption. - Mutual solvent increased the acid dissolution rate by 9% for calcite and by up to 29% for dolomite. - 5,000 mg/L iron (III) resulted in surface deposition of iron (III) hydroxide which had an inhibiting effect on dissolution rate for both calcite and dolomite at low rpm. - 2 vol% corrosion inhibitor decreased the calcite dissolution rate by approximately 9%.

Table 2.1—Continued

Rabie et al. 2011	- Indiana limestone - Lactic acid (1, 5, and 10 wt. %) - Seawater diluted Lactic acid - 1000 psi and temperature (80-250^{o}F) - 100-1800 rpm - Experiment run for 30 minutes.	- Reaction was mass transfer limited at low rpm (up to 500) and surface reaction limited at higher rpm. - *Increasing the temperature increased D_e* - The Presence of salts (from seawater) reduced dissolution rate. - The recommended not to use lactic acid in seawater due to reduced D_e. - De of 5.91×10^{-7}, 1.1×10^{-5}, 1.47×10^{-5} cm^2/s at 80, 200, and 250^{o}F respectively.
Fredd and Fogler, 1997	- Calcite (5.3 x 0.65 cm disk). - 1.0 M HCl - 0.25 M EDTA (pH of 4 and 13) - 800 psi and room temperature	- With Mass transfer limited dissolution for HCl with D_e of 4.1×10^{-5} cm^2/s. - Reaction was surface reaction limited for pH 4.0 and 13, 0.25 M EDTA.
Fredd and Fogler, 1998	- 0.25 M CDTA, DTPA, and EDTA - Calcite - pH of 3.3- 12 - 800 psi and room temperature	- Dissolution rate is affected by the kinetics of the chelation and changes with type of chelating agent and pH. - Dissolution of Calcite by 0.25 M EDTA at pH 4.0 and 12.0 was surface reaction limited. - dissolution rate increased 2.7 times as the pH was decreased from 12 to 4, - At low concentrations (0.001 M EDTA pH of 12), the dissolution rate was mass transfer limited and D_e was 5.6×10^{-6} cm^2/s.
Nasreldin et al. 2006	- Calcite (1.5" x 0.65" disk). - 5 wt. % HCl - Polymer 0.5-2 wt. % - Corrosion inhibitor 0.2 wt. % - 1000 psi and 25 and 65^{o}C - 100-1000 rpm - Experiment run for 2 hours	- Dissolution rate significantly decreased as the polymer concentration increased from 0.5 to 1.5 wt%. - Gelled acids reaction with calcite was Surface reaction limited at room temperature, and mass transfer limited at 65°C. - Dissolution rate of calcite increased with temperature as a result of viscosity reduction.

Table 2.1—Continued

Qiu et al. 2014	- Marble (1.5" x 0.3" disk). - 15wt% HCl. - 1000 and 3000 psi and 150°F. - 250-1000 rpm. - Experiment run for 4 minutes.	- D_e for the same concentration of HC1 at 3000 psi is significantly lower than at 1000 psi to the order of 50%. - Carbon dioxide in solution acts to reduce the diffusion coefficient by "buffering" of hydrogen ions, resulting in slower mass transfer and therefore reaction rates. - De of 3.34 $\times 10^{-5}$ cm^2/s and 6.48 $\times 10^{-5}$ cm^2/s for 15% HCl at 3000 and 1000 psi respectively.
Qiu et al. 2014	- Silurian Dolomite (1.5" x 0.27" disk). - 15wt% HCl. - 10-19% porosity. - 1000 and 3000 psi and 150°F. - Experiment run for 4 minutes. - 250-1000 rpm.	- D_e of 5.52 $\times 10^{-7}$ cm^2/s and 7.15 $\times 10^{-7}$ cm^2/s for 15% HCl at 3000 and 1000 psi respectively - The reaction was mass transfer limited at low rpm and reaction limited at high rpm for low pressure and high pressure experiments using Silurian dolomite for spent 12.5 wt. % experiments however it was mass transfer limited over the entire range of disk rotational speeds for spent 10 wt. % and spent 7.5 wt. % experiments. - The reaction between calcite and HC1 was mass transfer limited for both fresh acid and various spent acid conditions.

2.3 Carbonate Rock Porosity Type

In any rock system porosity is defined as the proportion of pore space as a ratio of the total bulk volume regardless of the geometry. The pore geometry is highly affected by the rock genesis. Carbonate rocks origin can be clastic, chemical or biogenic which subsequently yields a very complex pore system. In addition, Carbonate minerals can experience rapid dissolution, cementation, recrystallization, and replacement at ambient conditions in a variety of diagenetic environments.

Carbonate porosity is a function of depositional process (winnowing or lime mud) as well as diagenetic process (pore filling and selective leaching). Intergranular, growth-framework, shelter and fenestral porosities are depositional porosities while Moldic, channel, inter-crystalline, fracture or vuggy porosities are formed during diagenesis. The porosity system in carbonate can be unimodal pore network (such as sucrosic dolomite, oolitic limestone, and micritic limestone) or bimodal pore network (such as sucrosic dolomite with relict fossil casts and lump limestone with intergranular porosity).

Porosity classification in carbonates were first developed by Archie (1952). Different carbonate rock porosity types are listed in **Table 2.2** The minor pore type should correspond to 20% or more of the porosity. The basic types of porosity can be either fabric selective (porosity is controlled by the crystals, grains, or any other physical structures in the rock and the pores do not cross those primary grains depositional fabrics), not fabric selective (porosity patterns can cross-cut primary grains and depositional fabrics), or fabric selective or not (Choquette and Pray, 1970).

Table 2.2 —Different carbonate porosity types (Lucia, 1995; Scholle and Dana, 2003)

Porosity system	Diagram	Photomicrographs
Intragranular (Ooid)	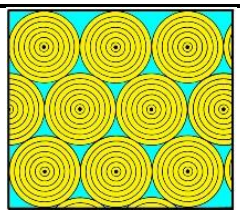	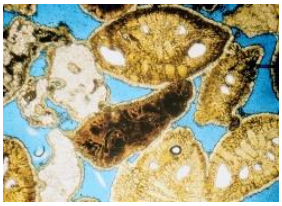 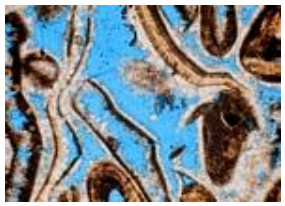
Intercrystalline	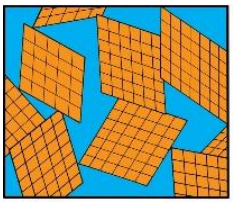	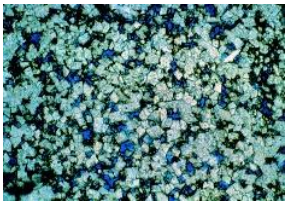 
Fractures	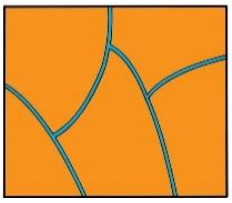	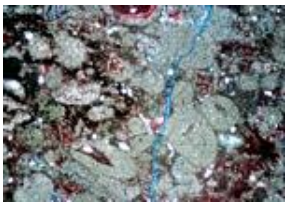 
Vugs	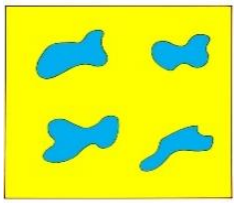	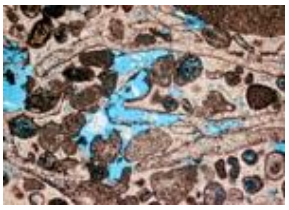 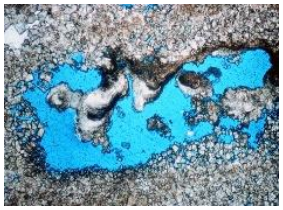
Moldic	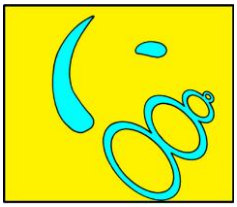	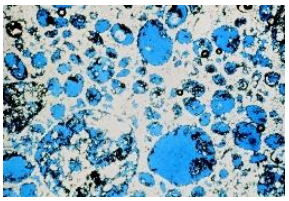 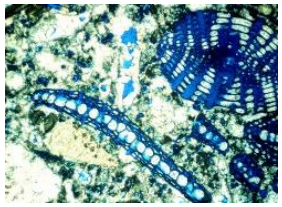
Channel	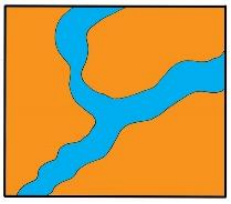	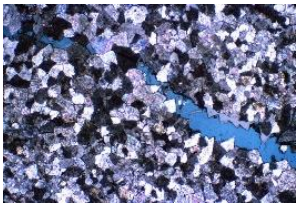
Shelter	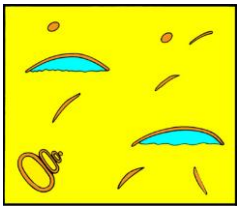	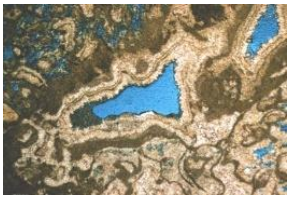

It’s even clear from the shown porosity types that different connectivity levels between the pore are found with in the same porosity system. As an example for this type is the vugs porosity type as it can be connected vugs or isolated vugs which significantly affects the overall rock connectivity. The high level of heterogeneity of carbonate formations require a detailed description of the formation to be treated and limit dealing with all formation as simple as single calcium carbonate lithology. In addition, as pore space geometry affects rock conductivity and fluid saturation, we think its effect should be considered during formation treatments using reactive chemicals. Microphotograph for thin section of Indiana Limestone, Pink Deseret limestone and Khuff limestone are shown in **Figure 2.1**.

Microphotograph for thin section of Indiana limestone (bioclastic grainstone).

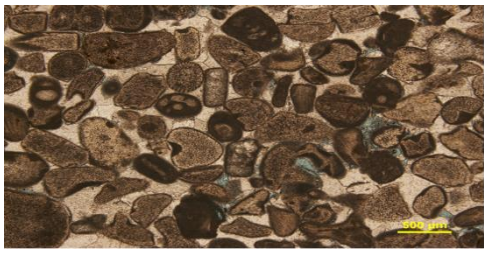

Microphotograph for thin section of Pink Deseret limestone.

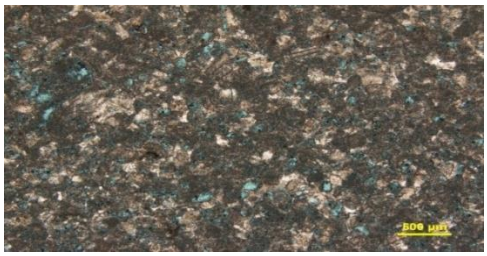

Microphotograph for thin section of Khuff limestone (oolitic grainstone).

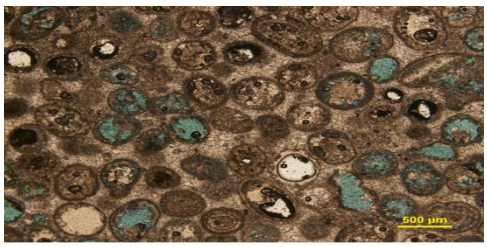

Figure 2.1—Microphotograph for thin section of Indiana Limestone, Pink Deseret limestone and Khuff limestone

2.4 Optimum Injection Rate and Wormhole Modeling

Many models are presented in the literature Investigate WH formation phenomena, Understand the propagation of WH during matrix acidizing, Describe Wormhole structure, Monitor wormhole propagation and even sometimes predict the dissolution structure of acid rock reaction and optimum injection rates for fluid-mineral systems. Carbonate Matrix Acidizing Models are based on one of the following approaches:

- Capillary tube approach (Buijse 2000)
- Damköhler number approach (Hofner and Fogler, 1988)
- Transition pore theory (Wang el al. 1993)
- Network models (Fredd and Fogler, 1998)
- Peclet number approach (Daccord and Lenormand 1987, and Frick et al. 1994)
- Semi-empirical approach (Buijse and Glasbergen, 2005 and Furui et al. 2012)
- Averaging continuum (two scale) approach (Liu et al. 1997)

An ideal model should output the efficiency of the treatment, optimum injection rate and wormhole propagation rate. In stimulation linear coreflooding experiments, core length is used to represent the required penetration depth when same acid system is to be used for field treatments (**Figure 2.2**). Optimum injection rate (Q_{opt}) to breakthrough the core length is determined through a series of liner coreflooding experiments. It has been proved that optimum injection rate is a function of core dimensions i.e. length and dimeter as shown in **Figure 2.3** (Furui et al. 2012).

The optimum injection rate can be estimate also by utilizing the diffusion coefficient obtained from rotating disk experiments for mass transfer limited dissolution reactions. This last approach save time of doing flooding experiments at several injection rates. In

addition, acid efficiency (minimum volume to breakthrough the core PV_{bt}) can be estimated using models based on kinetics and the optimum injection rate without any need for several flooding experiments for each core dimensions. Even laboratory determination is not accurate. In this study we can come up with a model to determine the PV_{bt} and Q_{opt} for the required damage radius to be removed and also for a specific temperature and carbonate mineralogy.

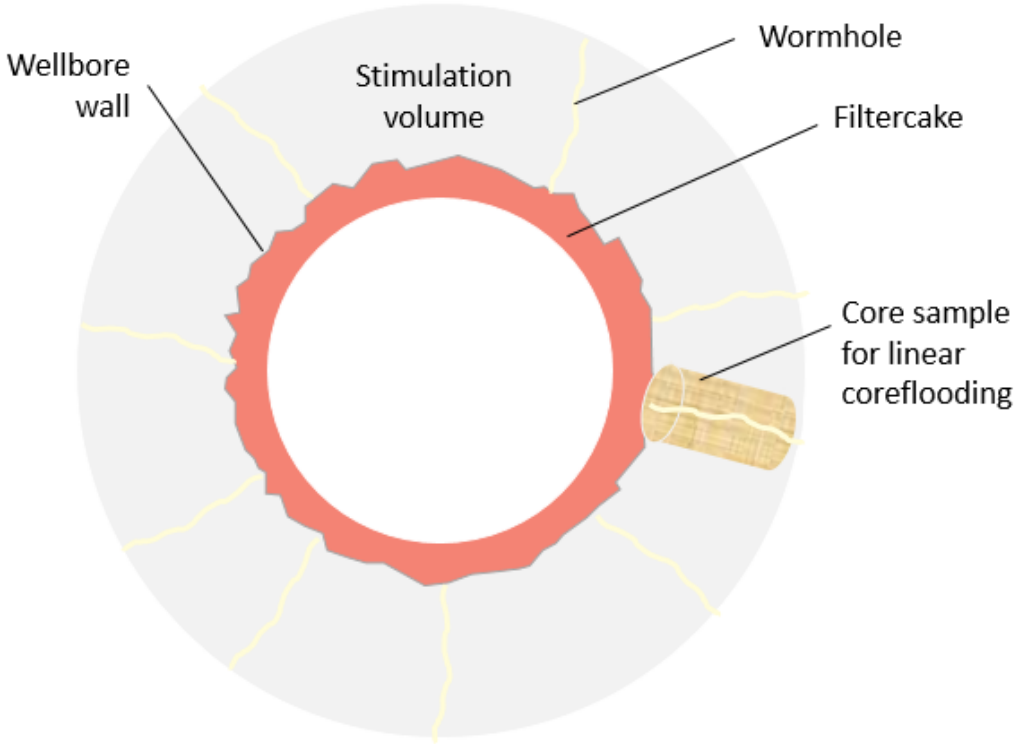

Figure 2.2—Radial and linear flooding for matrix acidizing

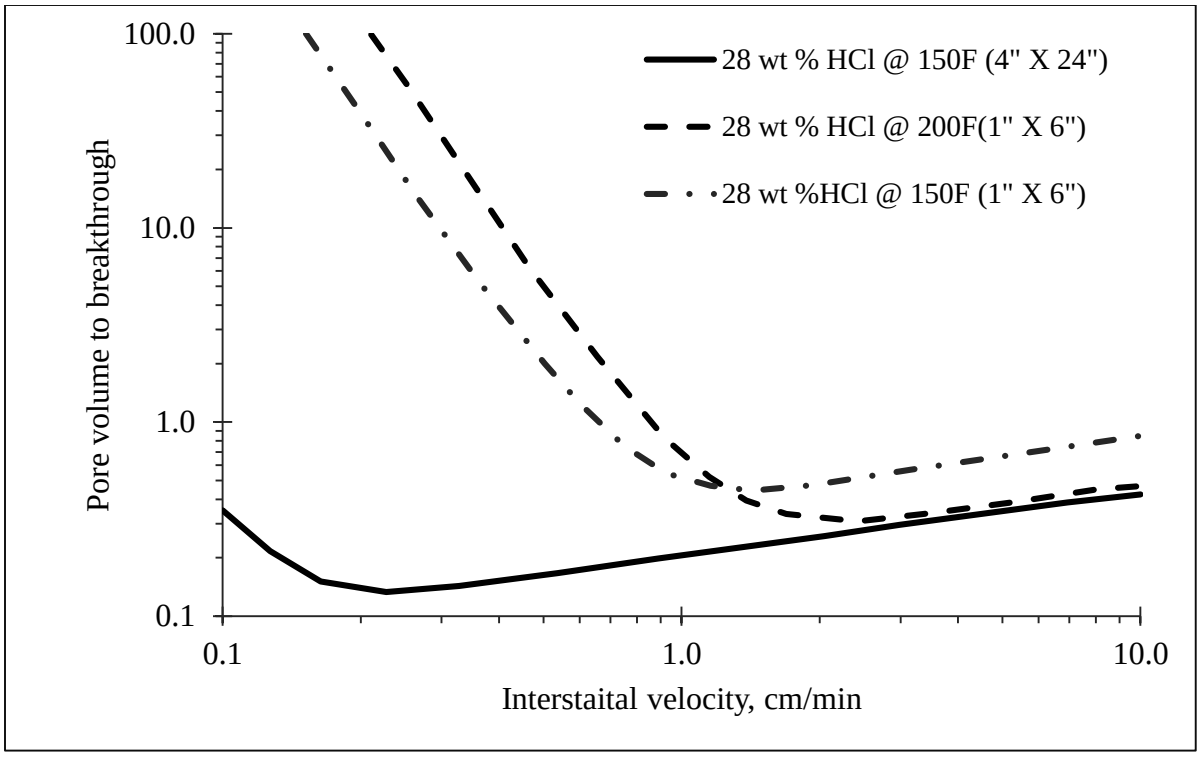

Figure 2.3—Linear acid flooding data for high porosity chalk.

2.5 Chelating Agents

Chelating agents contain different functional groups (carboxyl, hydroxyl, ether, primary amine, tertiary amine, thiol, nitro, nitroso, and sulphine etc.) which have the ability of sequestering the metal ion and form a stable complex. A chelate is defined as any metal that is attached to a negatively charged group (anion) with more than one attachment (**Figure 2.4**) while Chelation indicates that the anion has more than one separate sites to which the metal is attached or bonded. Site dissociated carboxyl group turns out to be the best sequestering group. Tertiary amine is the most promising group among the neutral groups (Bakken and Schöffel, 1996). The distribution of the ionic species of a chelating agent is a function of the equilibrium constants of it's the dissociation reactions and pH of the solution. The basic idea behind these chelating agents is the sequestration of metal ions

and preventing any metal precipitation in carbonate formations. The conjugate bases of the chelating agents have the ability to chelate different ions such as iron and calcite which present in reaction solutions. The stability of the calcium chelates influence the ability of the Chelant to dissolve more calcite. Typical chelants used in the upstream oil industry are shown in **Table 2.3**. Chelating agents include both Polyaminocarboxylic acids and Hydroxyaminocarboxylic acids. They consist of up to three nitrogen atoms surrounded by either COOH group or COOH and OH groups. DTPA is named the strongest chelating agent.

Chelating agents were first proposed to be used as a part of the stimulation formulation to control iron precipitation problem in 1989 by Dill et al. They used a chelating agents such as citric acid ($C_6H_8O_7$), Ethylenediaminetetraacetic acid (EDTA), or nitrilotriacetic acid (NTA) in an amount of from about 0.25 to about 5 percent by weight of the overall acid solution.

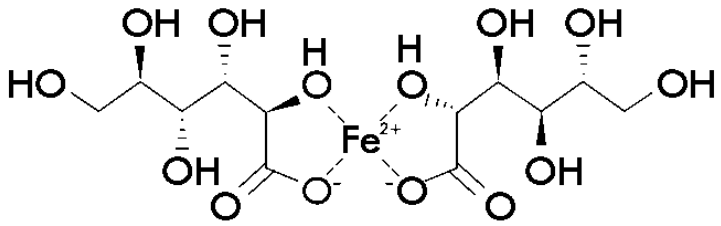

Figure 2. 4—Chemical structure of ferrous gluconate.

Table 2.3—Equilibrium constants for various metal/ligand chelates (Freiner 2001)

Polyaminocarboxylic acids	Ethylenediaminetetraacetic acid EDTA $N_2(COOH)_4$	Diethylenetraminepentaacetic acid DTPA $N_3(COOH)_5$
Hydroxyaminocarboxylic acids	Hydroxyethyliminodiacetic acid HEIDA $N(COOH)_2OH$	Hydroxyethylenediaminetriacetic acid HEDTA $N_2(COOH)_3OH$

The cleating agents form stable complexes with metal ions (Ca, Mg, Fe etc.). These complexes do not precipitate during the reaction of the stimulation fluid which in turn prevent formation damage. Strong calcium chelating agents such as CDTA, DTPA, and EDTA have a relatively high dissolution rate in 8.4 to 12 pH environment as reported by Fredd and Fogler (1998). Chelated mineral complexes with log K_F greater than 8 are stable chelates and from stable complexes with earth metals. From **Table 2.4**, it is clear that EDTA and DTPA form stable chelates with calcium and magnesium while HEDTA chelates with Calcium is more stable than its chelate with magnesium. The distribution of ionic species for EDTA at room temperature is shown in **Figure 2.5**. At a pH of approximately 4.5, EDTA is in the form of H_2Y^{-2}. EDTA successively deprotonates to the HY^{-3} and Y^{-4} species at higher pH values of 8.5 and 13 respectively. The used of chelating agents as a stimulation fluid does not depend only on its ability to bypass the damage and dissolve any precipitated scale in the near wellbore are but also on its stability and HP/HT conditions. The use of seawater diluted chelating agents will be limited by the solubility in seawater and the stability of the fluid system at stimulation conditions. Based on the stability tests done by Asaad (2015) EDTA, HEDTA, and DTPA are soluble in seawater and the solubility is affected by pH and acid concentration.

Table 2.4—Equilibrium constants for various metal/ligand chelates (Freiner 2001)

Ligand	MW	Log of stability constant (K_F) 1:1 complex				
	Acid	Fe(II)	Fe(III)	Mg(II)	Ba(II)	Ca(II)
NTA	191	8.3	15.9	5.5	4.8	6.4
HEDTA	278	12.2	19.8	7.0	6.2	8.4
EDTA	292	14.2	25.0	8.8	7.8	10.7
DTPA	393	16.5	28.0	9.3	8.9	10.9
HEIDA	177	6.8	11.6	3.5	3.4	4.8

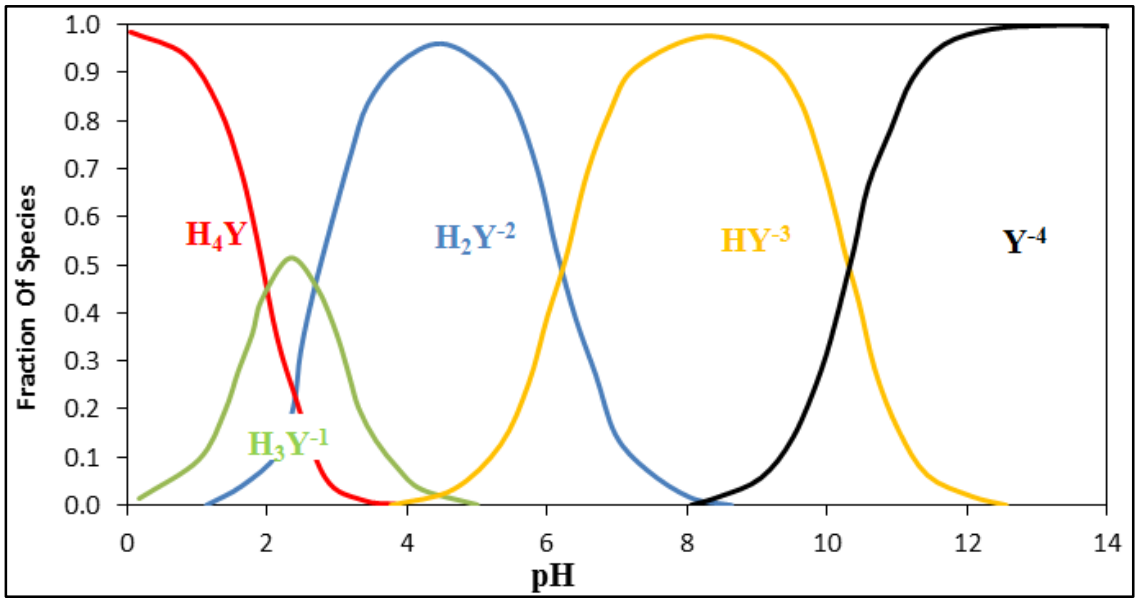

Figure 2.5—Distribution of ionic species of EDTA at room temperature (Freiner 2001).

2.6 Acid diversion

Regardless the lithology of the formations to be stimulated, the injected acids should target the less permeable or damaged zones. The presence of permeability contrast in layered reservoirs requires to injected fluids to be diverted from the most permeable layers to the less permeable or damaged ones. In many cases the operation achieved success ratio depend on the ability to divert the injected treatment fluids to the targeted formation and achieve the optimum fluid distribution within the desired treatment interval during the treatment. Acid diversion is generally made using mechanical or chemical techniques to alter the natural flow profile during injection by forcing the acid flow to be diverted from high-permeability or undamaged intervals to lower permeability or damaged intervals. Whoever mechanical methods are the surest way to guarantee fluid placement into a specific formation, they are time consuming and more expensive. Mechanical techniques (external diversion) depends in the zonal isolation include coiled tubing or drillpipe conveyed tools equipped with packers, bridge plugs, or both (Kalfayan and Martin, 2009). Mechanical methods for acid diversion can be applied in both sandstone and carbonate formations. Increasing the viscosity of the injected fluid upon interacting with the high permeability formation is the key concept behind many techniques to divert the flow to the targeted low permeability formation. Flow to the high permeability layers can be blocked using foam-acid diversion, surfactant-based acid diversion, polymer based acid diversion, Hydrajet acids, or solid based acid diversion (ball sealer diversion). A successful diverting agent should meet the following requirement:

- Must be compatible with the treatment fluids
- Must not react adversely with the formation fluids.

- Can flowed back to the surface and cleaned out after completing the treatment
- Stable physical properties at the reservoir conditions.

Self-viscosifying acid (SVA) or sometimes known as polymer based in-situ gelled acid composed of three components in addition to the acid system (HCL for example) and other functional additives (Johnson et al. 1988). The first component is a gelling agent usually from the polyacrylamide family such as hydroxyethylcellulose (HEC). The second component is a crosslinking agent, selected to initiate the crosslinking of the polymer at a certain pH value (2-4). Once the pH reaches a higher value (around 4) the third component known as a breaker activates and return the system viscosity to initial vales before crosslinking so that the fluid can flow out of the formation (Magee et al. 1997; Hill 2005). The speed at which this process of crosslinking and viscosity braking happens depends upon breaker and acid concentrations and bottomhole temperature, so the breaker loading needs to be specifically designed for each situation. Permeability reduction due to precipitation of the crosslinker was reported as one of the drawbacks of polymer based in-situ gelled acids in addition to the ability to completely cleanup the formation after the treatment (Lynn and Nasr-El-D 2001). Following are examples for polymers used in the industry to build stimulation and fracturing fluids system viscosity.

- Hydroxypropyl guar polymer (HPG)
- Xanthomonas campestris (XC) polymer
- AMPS based polymers
- Hydrolyzed polyacrylamide (HPAM)
- Thermo-viscosifying polymer (TVP)

Non-polymeric Viscoelastic surfactants **(**VES) are added to acids to form in-situ gelled acid solution with higher apparent viscosity. VES gelled aqueous fluids exhibit exceptionally high viscosity (thousands of cp) at very low shear rates and under static conditions. In carbonate formations, once the acid reacts with the formation matrix and the pH of the system increases, the surfactant forms rod-like micelles which build up the system viscosity. For some VES, the viscosity builds up by forming worm-like micelles once the injected system contacts formation brine containing KCl, NH_4Cl or $CaCl_2$ as shown in **figure 2.6**. During flow back, the VES in-situ gel breaks when the fluid is exposed to hydrocarbons, otherwise a mutual solvent post flush is injected to break the gel (Nasr-El-Din et al. 2008). It has been reported that wells cleanup is much better in case of VES than polymer based acid diversion (Lungwitz et al. 2007). One of the drawbacks of VES gelled acids is the high sensitivity to additives which might in some cases highly reduce the viscosity of the fresh and spent acid system (Nasr-El-Din et al. 2008). It important to highlight that in case of failure to break the VES gel due to absence of hydrocarbon fluids, the formation cleanup will be a hard operation. Huang and Crews (2008) showed that not all reservoir hydrocarbons will break VES fluid by simple contact and tried to solve this issue by using mineral oil as an internal breaker to degrade the viscosity of a spent dicarboxylic acid system.

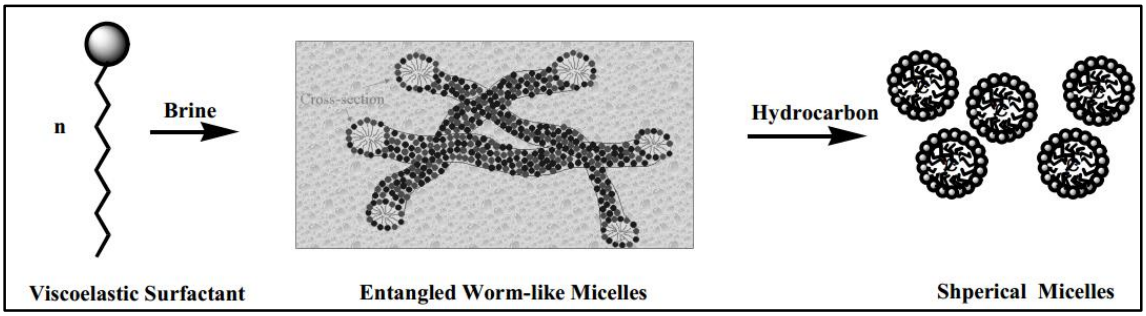

Figure 2.6—Creating of rod-like micelles by Viscoelastic surfactant and in-situ gel breaking when contacted with hydrocarbons during flowback (Chang et al. 1999).

Foam diversion is a routinely used diversion technique in sandstone and carbonate formations. This method advantages include easy practices of pumping foamed diversion treatments and clean it up after the treatment, along with excellent cleanup characteristics. Foam formed from three integral parts including a gas phase, a liquid phase, and a foaming surfactant, is used as for fluid diversion during matrix acidizing. The used surfactant gives the foam its stability. Foam quality is determined by the percentage of gas contained in the foam. Nitrogen is a typical gas used with either an acid or a non-reactive salt solution, representing the gas and liquid phases correspondingly.

Foams exist as a two-phase system of gas and liquid. Liquid is generally the wetting phase, and thus resides as a series of lamella bridging across pore throats and as thin films on rock surface. Gas is a discontinuous phase, residing in the larger void spaces in porous medium. The addition of surfactant allows the foam to maintain a stable two-phase configuration in which the lamella can break and reform during dynamic events (Glasbergen et al. 2006).

When foam enters a rock formation it causes an increase in gas saturation and a decrease in liquid saturation near the wellbore as it enters the rock due to the large amount of gas it contains. Consequently, liquid relative permeability in the zones where foam has entered is reduced. As a result, the resistance to liquid flow increases 100 to 1,000 times over the

resistance before foam entry (Bernadiner et al. 1992). After foam injection stage, injected acid stages can be diverted to low permeability zones where foam has not entered. Foam diversion works best in the range of 150 to 250°F as higher temperature affect the foam quality with Sandstone formations of 150 md permeability and above the suitable candidates for foam diversion practices (Poyyara et al. 2014). Foam diversion drawbacks are high friction pressure losses, and higher total cost as more equipment are required in the location (Glasbergen et al. 2006).

Ball sealers are small balls injected with the stimulation fluid to temporary block the perforations. Ball sealers of different materials have been used during well stimulation such as Hycar rubber, solid nylon balls, aluminum and rubber-covered aluminum balls, rubber-covered phenolic balls, and plastic-consolidated walnut shells.

Degradable particle diverting agent (DPDA) also have been used to control the fluid placement in sandstone and carbonate formations (Solares et al. 2008; Reyes et al. 2015; Gutierrez et al. 2015). DPDA are usually designed in different size groups of different particle size distribution to achieve perfect isolation of perforation tunnels and the formation itself by forming low permeability filter cake. DPDA can be used in open and cased hole. DPDA as a polymeric material can be degrade gradually when contacted by water thought hydrolysis process at temperatures higher than 100^{o}F. DPDA is usually injected with 6% KCl solution without affect the pH of the solution.

Temperature Control Viscosity Acids (TCA) are introduced to overcome the degradation and high leak off problems of gelled and emulsified acids at high temperature. Medium temperature is the key parameter for TCA, with increasing the temperature the gelling

agent undergoes polymerization and once the temperature exceeds a limit, the gelling agent molecules decomposes by broking chains (Zhou 2013).

Table 2.5 below gives a summary of the applicability of the acid diversion methods during matrix acidizing in both sandstone and carbonate formations. As shown in the table diversion can occur in the wellbore or in the formation after interaction with the diversion fluid and building high viscosity. It's clear that none of the "in-formation" techniques can work for sandstone except foam diversion.

Table 2.5—Matrix acidizing: summary of acid placement methods applicability for sandstone and carbonates

Diversion method	Wellbore		In the formation	
	Carbonate	Sandstone	Carbonate	Sandstone
Mechanical isolation			n/a	n/a
Ball sealers			n/a	n/a
Coild tubing			n/a	n/a
Foam				
Self-viscosifying acid	n/a	n/a		
Viscoelastic surfactants				

	Recommended
	Suitable, subject to specific circumstances
	Not recommended
n/a	Not applicable

As shown in **table 2.5**. acid diversion of the stimulation fluid using either viscoelastic surfactant (VES) or polymers based acids are not recommended in case of sandstone formations treatment. For most sandstones there is no enough calcite to react with these fluids to produce the gel diverting materials in case VES. Also permeability loss up to 80% would occur due to adsorption of polymers and surfactants by the sandstone formations (Friedmann 1986).

There is a need for adverting agents in both sandstone and carbonate reservoirs that has a low viscosity during mixing and pumping, which is favorable for large displacement due to its low frictional resistance and a high viscosity downhole to enhance acid.

CHAPTER 3

Research Methodology and Equipment

3.1 Introduction

The objective of this research is to study the effect of seawater in the reaction kinetics of chelating agents and carbonate rock samples. Also the effect of rock facies on the reaction of carbonate rocks with chelating agents. The phases and approach to reach our objectives is described in the **table 3.1** and **table 3.2** the following section

Table 3. 1—Approach, Tasks and Phases

Phase 1	**Task 1**	**Task 2**
Rock Analysis	Literature review Equipment and materials	Carbonate rock disks preparation (cutting, surface polishing and properties measurements, NMR, CT scan)
Phase 2	**Task 1**	**Task 2**
Reaction Kinetics study	Base system using DI water to dilute chelating agents at different pH values	Study system using seawater water to dilute chelating agents at different pH
Phase 3	**Task 1**	**Task 2**
Effect of porosity system & Mineralogy	RDA experiments using different porosity type carbonate sample.	Data Analysis and Write-up of the thesis

Table 3. 2—Approaches

Objective	Approaches
1. Defining the reaction controlling process for each fluid system whether mass transfer surface reaction limited overall dissolution process.	EDTA, and HEDTA diluted with DI water reaction with carbonate rock will be run a base cases at different pH and temperature.
2. Studding the effect of seawater on the reaction rate of chelating agents with calcite	Reaction kinetics experiments using EDTA and HEDTA diluted with seawater results will be analyzed to define the limiting phenomena of the overall dissolution rate. De will be defined for mass transfer limited reactions.
3. Comparing the results with the results for the same chelating agents when diluted with deionized water.	The effect of seawater can be highlighted within upon comparison of the results with the distilled or fresh water diluted chelating agents at same condones of (pH, temperature and acid concentration)
5. Investigating the effect of porosity type rock facies on the reaction parameters by using rocks with same porosity, lithology and different facies.	Carbonate porosity system s though to highly affect the reaction rate through the surface area difference form a system to another. Carbonate samples with different porosity systems will be used to examine their effect on the reaction rate with seawater diluted chelating agents.

3.2 Methodology

The rotating disk is preferred for studying fluid/rock surface reaction because:

- It requires small fluid volume (up to one litter maximum)
- Three-dimension flow system it represented by the rotation of the desk in an infinite fluid volume
- Heat and mass transfer constants are kept constant at the surface of the rotating disk

During rotating disk experiment a rock disk is attached to a rotating shaft, and submerged in a solution of reactant (acid). The reactant is transferred to the surface of the rock by convection and molecular diffusion. The overall dissolution rate is governed by the slower of these two processes. The rotating disk experiment can be summarized in the following points:

1- A cylindrical disk of rock, one-inch-thick and 1 or 1.5 in diameter, is attached to a metal mount and contained in the reaction vessel prior to the introduction of the reactant.

2- A bout one-inch gap is left between the fluid surface and the reaction vessel cap.

3- A pressure of 1000 psi is maintained above the fluid to keep CO_2 in solution.

4- The reaction vessel and acid reservoir temperature is set to the required value.

5- The rock is spun up to the desired rpm.

6- The reactant, (600 ml of acid) is transferred from the acid vessel to the reaction vessel at a higher pressure enough to create the1000 psi.

7- 3 ml fluid Sample are withdrawn every 2 minutes and the concentrations of targeted dissolved cations is measured and plotted vs time recorded.

8- Calcium flux from the rock surface to bulk solution is estimated from the slope of the straight line fitted to the measurements.
9- Same experiment is repeated at different rotation speed of the disk.
10- For each experiment, R is calculated from slope of Ca^{2+} vs. time plot.
11- Reaction rate is plotted as a function of disk rotation speed to determine the process controlling the overall dissolution.

If mass transfer of reactants or products is the limiting step, then increasing rotational speed would increase the mass transfer and the overall dissolution rate. If the mass transfer exceeds the consumption of the acid on the rock surface, then the overall dissolution is independent of rotational speed and known as surface reaction limited.

in moles/s.cm^2 using. The dissolution rate is calculated by dividing the slope of the straight line by the initial surface area of the disk.

$$R = \frac{1}{A_0}\frac{d(Ca)}{dt} \tag{3.1}$$

Where

R	Initial dissolution rate of dolomite or calcite in HCl (g moles/s.cm^2)
t	Time (sec)
A_o	Initial surface area

Initial surface area can be determined using the disk porosity (ϕ, fraction) from the weight method:

$$A_0 = (1 - \phi)A_c \tag{3.2}$$

It should be noted also that minimum of three samples should be withdraw from the rotating disk instrument to obtain dissolution rate for a single acid, a single rpm and a single

temperature. A minimum of three different rpm experiments are required for the same system to calculate the reaction rate. To determine the activation energy, reaction rate from three different temperatures is required for the same acid system. The previous described work will be repeated using Indiana limestone with GLDA/SW, DTPA/SW, and EDTA/SW systems to define the reaction rate limiting process at high and low RPM. Results will be compared with the base cases in which no seawater is used (GLDA/DI, DTPA/DI, and EDTA/DI). If a mass transfer limited reaction rate is reported, De will be estimated and utilized to predict the wormhole propagation and optimum injection rate under corresponding conditions.

3.3 Equipment

This section is descripting the equipment to be used for this research work. I will present the equipment in the same order to be used in our research.

3.3.1 Disk preparation equipment:

This work will start by preparing rock disk for reaction experiments. To cut rock disks and prepare their surfaces for reaction kinetics experiments, cutting, enface grinding, polishing, and sonic cleaning equipment shown in **Figure 3.1.** This surface preparation is done to correctly estimate the surface area at which reaction will occur. The objective is to obtain samples as shown in **Figure 3.2.**

Figure 3. 1—Disk preparation equipment

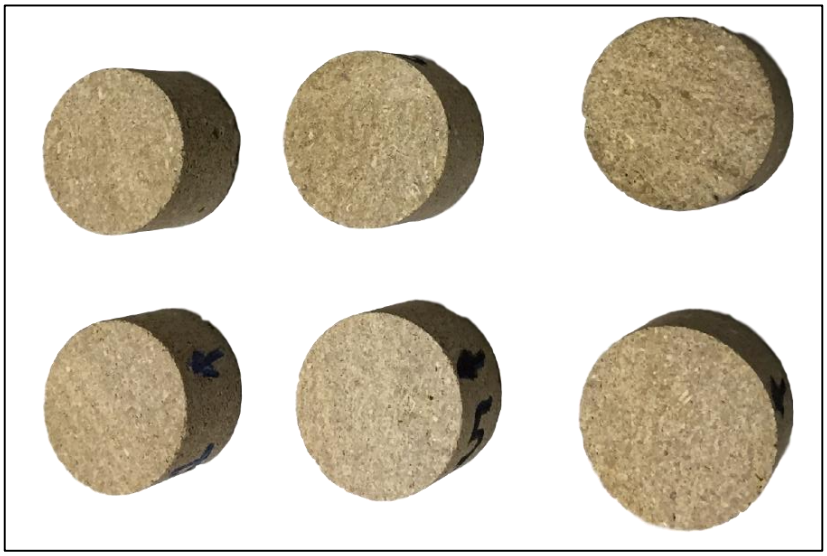

Figure 3. 2—Prepared rock samples for reaction kinetics experiments

3.3.2 Rotating Disk Apparatus (RDA):

Rotating Disc Acid Reaction System (**Figure 3.3**) is a computer controlled acid reaction system that allows for the controlled reaction of reservoir rock samples with acid fluids and the timed sequential collection of reactant fluid. From the chemical analysis of the reactant and the experimental and sample collection data from the RDA the reaction rates of carbonate samples can be calculated and the results used in the design of effective acid stimulation treatments of wells. The RDA available in KFUPM research institute has the specifications listed in **Table 3.3**. Rotating disc, disk drive system, temperature control system, sampling loops are controlled using data acquisition software. The software permits the collection of samples each of 3 ml volume at a selected time interval. **Figure 3.4** is a cartoon for different components of the RDA system.

Table 3. 3—RDA specifications (Courtesy of KFUPM CPM)

Parameter	Operating Range
Temperature	Up to 650^{o}F
Pressure	Up to 5500 psi
RPM	250-3000
Sample Volume	3 ml
Acid Volume	600 ml
Disk diameter	1" and 1.5"

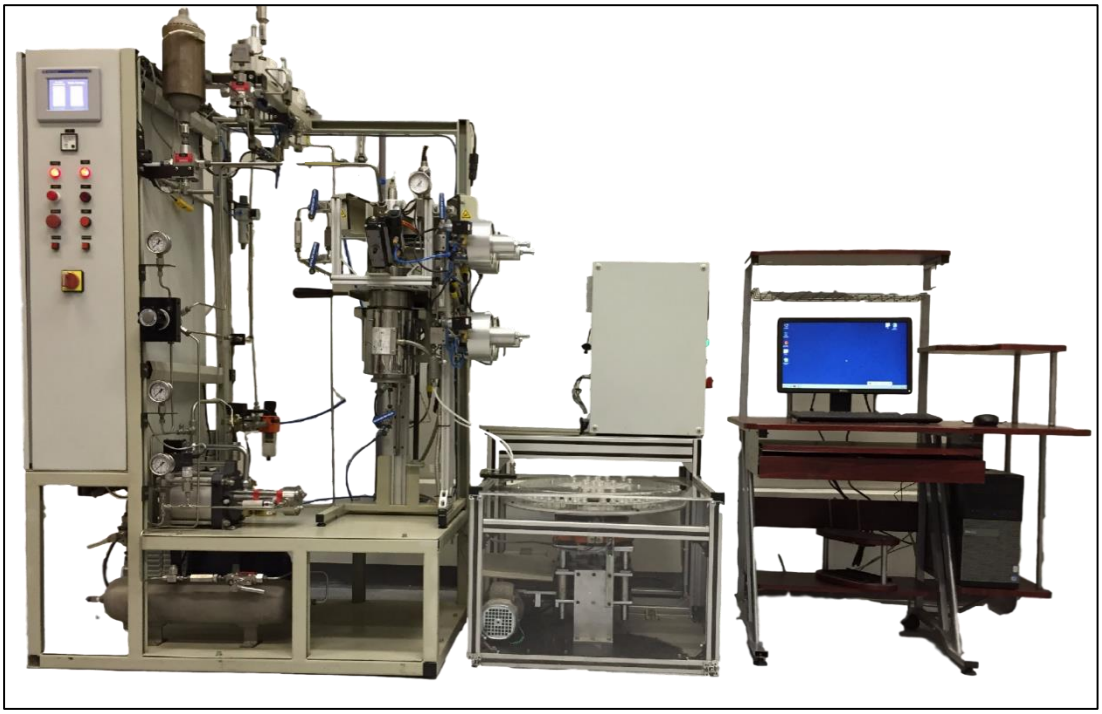

Figure 3. 3—Rotating Disk Apparatus (Courtesy of KFUPM CIPR)

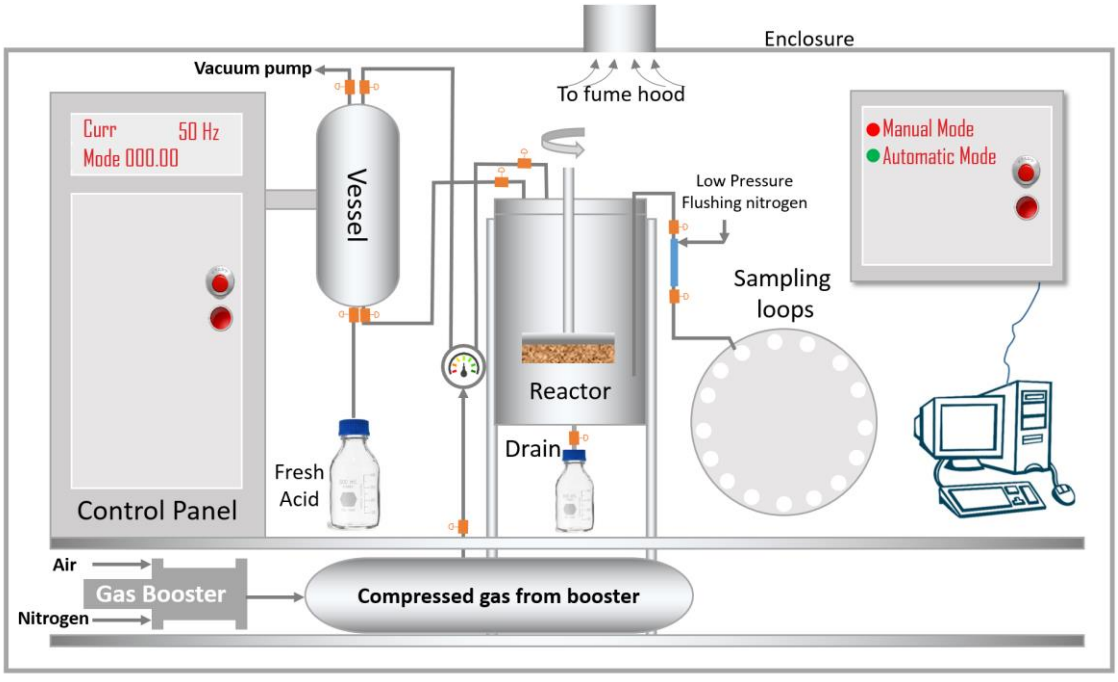

Figure 3. 4—Schematic of RDA components

For an acidizing treatment, involving a solid rock and a fluid acid system, the reaction rate determination process is greatly affected by:

- Reactant transport to the rock surface.
- Products transport away from the surface.

Therefore, the overall reaction comprises of three steps (**Figure 3.5**):

- Reactant transfer from bulk of solution to the solid surface.
- Reaction at the solid surface.
- Products transfer from the surface to the bulk solution again.

The slowest step of those three controlees the overall reaction kinetics and is referred to as the rate-limiting step. For a reaction system, if the mass transfer process is faster than the surface reaction rate, then it is a surface reaction limited, but if the rate of surface reaction is faster than diffusion to the surface, the process is mass transfer limited.

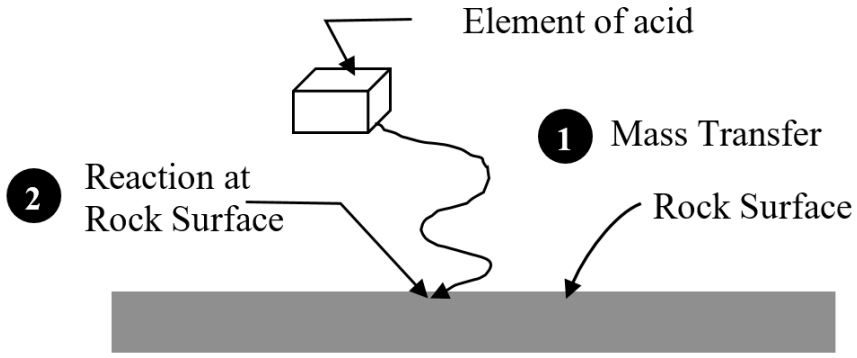

Figure 3. 5—Acid reaction with rock surface

As per the studies conducted by Levich (1962) and Newman (1966) For Newtonian fluids the rate of mass transfer (R_{MT}) of a reactant to the solid surface in a laminar flow regime ($Re < 3xl0^5$) is given by the following equation:

$$R_{MT} = \frac{J}{A} = K_m(\mathrm{C}_b - \mathrm{C}_s) \tag{3.3}$$

$$K_m = \frac{0.60248\ (S_c{}^{-\frac{2}{3}})\sqrt{\nu\omega}}{1 + 0.2980\left(S_c{}^{-\frac{1}{3}}\right) + 0.1451(S_c{}^{-\frac{2}{3}})} \tag{3.4}$$

Where:

J	Mass transfer flux
A	Surface area
C_b	Bulk concentration of the transferred species
C_s	Surface concentration of the transferred species
K_m	Mass transfer coefficient
ω	Disk rotational speed, $^{S-1}$
ρ	Fluid density, gm/cm^3
μ	Fluid viscosity, gm/cm^3
v	Kinematic viscosity (μ/ ρ), cm^2/s
Sc	Schmidt number ((v / D_e),
D_e	Diffusion coefficient cm^2/s

For a mass transfer limited regime, where the rate of mass transport is lower than the rate of reactant consumption at the surface (surface reaction rate), Due to the negligible concentration of reactant ants at the reaction solid surface (C_s=0). The final form of the mass transfer rate for a laminar flow of a Newtonian fluid can be expressed as:

$$R_{MT} = K_m(\mathrm{C}_b) = \frac{0.60248\ (S_c{}^{-\frac{2}{3}})\sqrt{\nu\omega}}{1 + 0.2980\left(S_c{}^{-\frac{1}{3}}\right) + 0.1451(S_c{}^{-\frac{2}{3}})}\,\mathrm{C}_b \tag{3.5}$$

$$R_{MT} = \frac{0.60248\ (S_c{}^{-\frac{2}{3}})\ \mathrm{C}_b\sqrt{\nu}}{1 + 0.2980\left(S_c{}^{-\frac{1}{3}}\right) + 0.1451(S_c{}^{-\frac{2}{3}})}\,\omega^{\frac{1}{2}} \tag{3.6}$$

$$R_{MT} = \frac{0.60248\,(\frac{\mu}{\rho D_e})^{-\frac{2}{3}}\,C_b\sqrt{\frac{\mu}{\rho}}}{1 + 0.2980(\frac{\mu}{\rho D_e})^{-\frac{1}{3}} + 0.1451(\frac{\mu}{\rho D_e})^{-\frac{2}{3}}}\,\omega^{\frac{1}{2}} \qquad (3.7)$$

It's clear that for a mass transfer limited regime, the rate of dissolution is linearly proportional to the square root of the disk rpm. D_e of the acid system can be determined by using the same equation. Plotting R_{MT} versus $\omega^{\frac{1}{2}}$ should yield a straight line with a slope that is proportional to the effective diffusivity raised to the power 2/3 which ensure that the dissolution rate is mass transfer limited. Lund et al (1973) described the surface reaction rate as a function of concentration by the following power-law model:

$$-r_{HCl} = kC_s^n = J_{mt} \qquad (3.8)$$

Where:

r_{HCl} : Dissolution rate of dolomite or calcite in HCl (moles/s.cm^2)

k : Specific reaction rate (moles /cm^2.s)(mole/cm^3)$^{-n}$

C_s : Surface concentrations of the transferring species

n : Dimensionless reaction order

The estimation of dissolution rate is done using the rotating disk system described before. Most of the reaction kinetics parameters are based on the dissolution rate determination (Taylor and Nasr-El-Din, 2007).

For the case of gelled acids used to assist acid diversion and enhance matrix stimulation, Hanford and Litt (1968) derived an expression (**Equation 3.9**) for mass transfer coefficient from a rotating disk to power-law liquids in terms of power low constants and system parameters.

$$k_m = \left[\phi(n)\,D^{\frac{2}{3}}\left(\frac{k}{\rho}\right)^{\frac{-1}{3(1+n)}}\,a^{\frac{1-n}{3(1+n)}}\,\omega^{\frac{1}{1+n}}\right] \qquad (3.9)$$

$$\phi(n) = \left(\frac{6n+6}{5n+7}\right)\left(\frac{a}{3}\right)^{\frac{1}{3}} \tag{3.10}$$

where:

n : Power-law behavior index, dimensionless

D : Surface area, cm^2/s

k : Power-law consistency index $g/cm\ s^{2-n}$

ω : Disk angular velocity ($2\pi N$, where N is the number of cycles/s), rad/s

ρ : Fluid density, gm/cm^3

a : Disk radius, cm

For a mass transfer limited reaction, where the rate of mass transport is lower than the rate of reactant consumption at the surface of the rock, due to the negligible concentration of reactants at the reaction solid surface ($C_s = 0$). The final form of the mass transfer of a non-Newtonian fluid can be expressed as follows:

$$J_{mt} = \left[\phi(n)\ \mathrm{D}^{\frac{2}{3}}\left(\frac{k}{\rho}\right)^{\frac{-1}{3(1+n)}} a^{\frac{1-n}{3(1+n)}}\ \omega^{\frac{1}{1+n}}\right]\mathrm{C}_b \tag{3.11}$$

After determining the surface area of the reacting rock disk, mass transfer rate can be determined. The dissolution rate is calculated by dividing the slope of the straight line fitted to each experimental results by the initial surface area of the disk.

$$J_{mt} = \frac{1}{A_0}\frac{d\ C_A}{dt} \tag{3.12}$$

where

R : Dissolution rate of calcite in acid per unit area ($mole/cm^2.s$)

C_A : Concentration of the substance A (Calcium in case of limestone rock)

t : Time (s)

A_o : Initial surface area (cm^2)

Initial surface area can be determined using the disk porosity (ϕ) and core surface area (A_c) as;

$$A_0 = (1 - \phi)A_c \tag{3.13}$$

During each experiment, the flux (J_{mt}) is determined from the analysis of the measured calcium ions concentration in the solution. Keeping all other parameters constant, the experiment is repeated at different rotational speeds (i.e. temperature and acid concentration). In the case of rotational speeds where mass transfer is the limiting step for the reaction is limited by mass transport, ($Cs << C_b$), the plot of the F function (**Equation 3.14**) versus $\omega^{\frac{1}{1+n}}$ will yield a straight line with a slope equal to $De^{2/3}$ (De Rozieres et al 1993).

$$F = \frac{J_{mt}}{\left[\phi(n)\left(\frac{k}{\rho}\right)^{\frac{-1}{3(1+n)}} a^{\frac{1-n}{3(1+n)}}\right] C_b} \tag{3.14}$$

If the mass transfer regime of reactants or products is the limiting step, then increasing angular velocity will increase the mass transfer and in turn, the overall dissolution rate will increase. If the mass transfer rate exceeds the consumption of the acid on the rock surface, then the overall dissolution is independent of angular velocity and known as surface reaction limited.

3.3.3 ICP-OES Spectrometer:

Inductively Coupled Plasma (ICP) Optical Emission Spectrometry (OES) is a well-established and powerful technique for the analysis and quantification of trace elements in both liquid and solid samples. ICP-OES Spectrometer (**Figure 3.6**) manufactured by PerkinElmer will be utilized for quantitative determination of the concentration of elements in the collected samples during the dissolution of carbonate rock disks for further analysis using the adsorption of optical radiation by free atoms. ICP-OES Spectrometer is a core equipment of the reaction kinetics experiment.

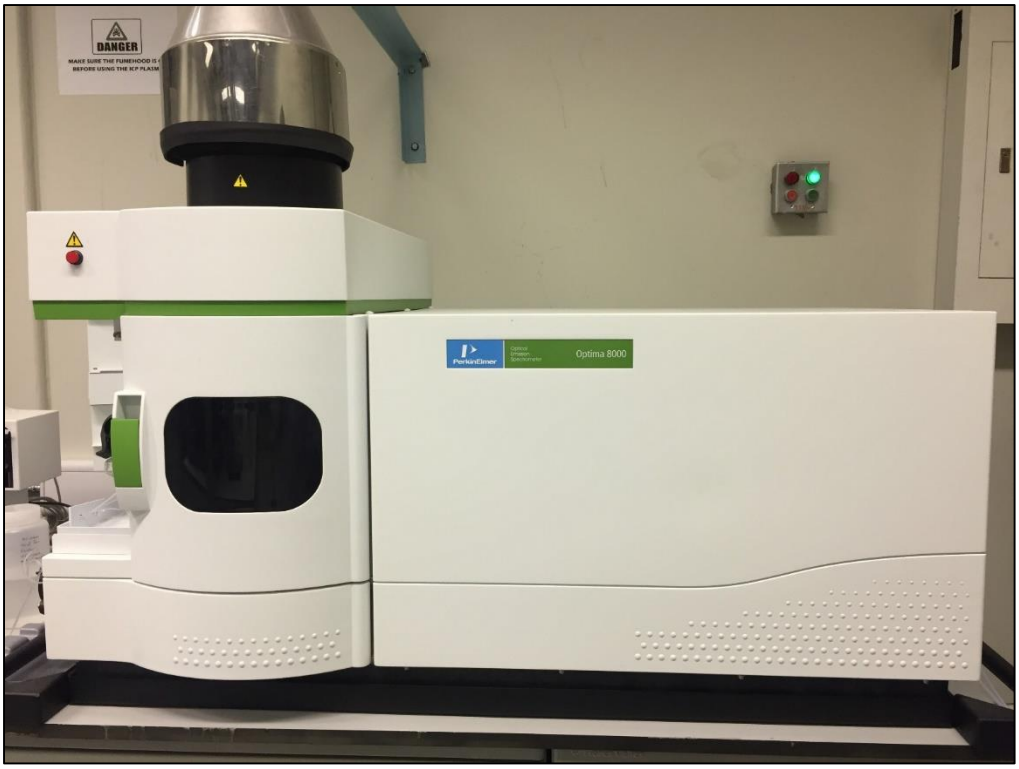

Figure 3. 6—PerkinElmer Optima 8000 ICP-OES Spectrometer

3.3.4 CoreFlooding System

Figure 3.7 shows the coreflooding set-up used to perform the acid treatment experiments in this study. The system is a fully automated coreflooding system designed to run linear coreflooding experiments under HPHT (up to 10000 psi and 150^{o}C). The system includes three fluid transfer vessels, very accurate versatile BFSP injection pump, nitrogen injection line, hydrostatic core holder, confining pump, back-pressure regulator, pressure measurement system, and data acquisition system. The pressure drop data and injection rate can be saved for each experiments for post analysis. Liquid permeability was measured using 3 wt% KCl (potassium chloride) solution at room temperature, then the system was heated up to the required temperature until equilibration is achieved.

Figure 3. 7—Coreflooding system

3.3.5 Computerized tomography (CT) X- Ray Scanner

The CT scanner (**Figure 3.8**) was used to characterize wormholes created during acid injection into carbonate rock samples. Toshiba Alexion TSX-032A medical X-ray CT scanner (resolution > 1 mm) shown in figure was used. The scans help to identify major wormholes inside the cores to better understand the acid rock interaction and define the optimum acid injection rate. All the scans run in this work were run at energy of 135kW/200mA with 1 mm resolution.

Figure 3. 8—Computerized tomography X-ray scanner

CHAPTER 4

Effect of Stimulation Fluid on Wormhole Connectivity

The optimum wormhole injection rate during acid stimulation treatment in a carbonate formation is defined as the injection rate that creates a dominant wormhole with the minimum acid volume. Wormholes are created to connect the reservoir to the wellbore by bypassing the drilling fluid damage and to enhance the wellbore productivity by increasing the effective wellbore radius in carbonate formations. Currently, the pressure drop and computed tomography scan (CT scan) are used to define the acid optimum injection rate and wormhole shape in the stimulated carbonate rock cores. However, these two techniques assess the interconnectivity of the created wormhole to the rest of the pore system in the reservoir in a coarse way.

In this chapter definitions and new approach to the optimum injection rate and wormhole evaluation during carbonate stimulation are summarized. Wormholes created using hydrochloric (HCl) acid, and chelating agents are compared and the effect of using preparing HCl in seawater is highlighted.

4.1 Introduction

Carbonate acidizing is a common practice in oil and gas producing wells and water injection wells to remove the damage due to drilling and to enhance the productivity/injectivity of the reservoir. Acids are used to create conductive channels (wormholes) that connect the undamaged regions in the reservoir to the wellbore. The generated wormholes facilitate the flow of oil and gas from the reservoir to the wellbore

by increasing the effective wellbore radius. In addition, they enhance the injectivity of water in water injection wells.

The productivity enhancement due to the acid treatment is a strong function of the acidized radial distance from the wellbore. Total recovery of the well productivity after acid stimulation requires acid penetration radius of 3 m from the wellbore in the case of a well that is not affected by damage in the near-wellbore area (Muskat 1947). To achieve this high penetration radius, the acid should be injected at the optimum wormholing conditions.

4.2 Different methods to determine the optimum wormholing conditions

4.2.1 Damkholer number (N_{Da})

Damkholer number (N_{Da}) is the ratio between the acid reaction rate to the acid injection rate and can be described as follows (Fredd and Fogler, 1998a, 1998b; Lund and Fogler 1975):

$$N_{Da} = \frac{\tau D_e^{2/3} L}{Q} \tag{4.1}$$

Where;

N_{Da} : Acid Damkholer number, dimensionless

τ : Rock tortuosity factor

D_e : Effective diffusion coefficient

L : Core length

Q : Acid injection rate

The latter equation is used to describe the Damkholer number when the reaction is controlled by the mass transfer rate. If the reaction is controlled by surface reaction (in

which the acid diffusion rate is very rapid compared to the acid reaction at the surface), the following equation can be used to describe the Damkholer number:

$$N_{Da} = \frac{\tau d \kappa L}{Q} \tag{4.2}$$

Where; τ, is the rock tortuosity factor, d, is the rock sample diameter, L is the rock sample length, κ is the overall dissolution rate constant, and Q is the acid injection rate.

Fredd and Fogler (1997) developed a modified Damkholer number that considers the effects of product transport, reactant transport, and reversible surface reaction as follows:

$$N'_{Da} = \frac{\pi D L \kappa}{Q} \tag{4.3}$$

Where; D is the diameter of the wormhole and L is the length of the wormhole. Fredd and Fogler (1997) concluded that the optimum dominant wormholes were created at modified Damkholer numbers of 0.17 for different acidizing fluids they tested. The tested fluids were 0.25 M DTPA (Diethylene tri amine penta acetic acid) at pH 4.3, 0.25 M EDTA (Ethylene diamine tetra acetic acid) at pH 13, 0.25 M CDTA (Cyclohexylenedinitrilotetraacetic acid) at pH 4.4, 0.25 M EDTA at pH 4, and 0.5 M HCl. They defined the optimum condition of the wormhole generation by the Damkholer number at which the wormhole is generated with the minimum volume of acid injected (minimum pore volume to acid breakthrough). Different fluids were tested at different concentration and different pH values and all of them revealed the optimum wormhole formation at 0.17 modified Damkholer number which means this number does not depend on the fluid type. Also they reported an optimum modified Damkholer number value of 0.3 at which dominant wormholes with less branches were formed with different fluids. it can conclude that, the optimum conditions of

wormhole formation can be obtained by controlling the modified Damkholer number of the acidizing fluid between 0.17 and 0.3.

Huang et al. (2000a, 2000b) introduced the following form of the optimum Damkholer number:

$$(N_{Da})_{opt} = \frac{\left(\frac{\pi}{20}\right)^{2/3} r_{max}^3}{k\bar{L}} \tag{4.4}$$

Where; r_{max} is the maximum pore radius, k is the rock matrix permeability, and $\bar{L}$ is the average pore length. This formula will give a specific Damkholer number for a fixed rock lithology.

4.2.2 Peclet number (N_{Pe})

The Peclet number is the acid convection rate divided by the acid diffusion rate and can be written as follows (Mahmoud et al. 2011):

$$N_{pe} = \frac{vL}{D_l} \tag{4.5}$$

Where; v is the Darcy velocity, L is the rock sample length, and D_l is the longitudinal dispersion coefficient. The Darcy velocity can be determined as follows:

$$v = \frac{Q}{A\,\phi} \tag{4.6}$$

Where; Q is the acid injection rate, A is the rock cross-sectional area and ϕ is the rock porosity. Based on their findings they showed that the optimum wormhole shape can be generated at higher Peclet number compared to that at low values of Peclet number. The Peclet number can be increased by injecting the acid at a higher rate and by reducing the acid dispersion to the wormhole walls. Longer wormhole length and low fluid loss to the wall can be obtained by increasing the Peclet number.

4.2.3 Optimum injection rate (Q_{opt}) and optimum acid flux (u_{opt})

The optimum injection rate in carbonate acidizing is defined as the injection rate at which the wormholes are generated with the minimum volume of the injected acid (Wang et al. 1993, Economides et al. 2014, Fredd and Fogler 1999, Glasbergen et al. 2009, Mostofizadeh and Economides 1994).

Wang et al. (1993) found that the optimum injection rate during carbonate acidizing is a strong function of acid concentration and temperature. They found out that the acid mass consumed to generate wormholes at the optimum injection rate was lower for low acid concentrations compared to higher acid concentrations. When 15 wt. % HCl acid was used the total mass consumed to generate wormhole at the optimum injection rate was 1.2 g and when 3.4 wt. % HCl was use the total mass consumed was 0.59 g. Also they found that increasing the temperature increased the value of the optimum injection rate. The shift in the location of the optimum injection rate with temperature can be attributed to the change in the reaction regime.

Huang et al. (2003) tested different acidizing fluids on carbonate rocks and located different optimum injection rates. They tested the same concentration, 10 wt. %, for Long Chain Carboxylic Acids (LCA), acetic acid, EDTA chelating agents and found different optimum injection rate because the different reactivity of each fluid with the rock.

The optimum acid flux (u_{opt}) for HCl acid can be related the optimum Damkholer number as follows (Huang et al. 2000a, 2000b):

$$u_{opt,HCl} = \frac{E_{f0} C_{HCl}^{m-1} \left(-\frac{\Delta E}{RT}\right)}{N_{Da,opt}} \tag{4.7}$$

Where; u_{opt} is the optimum acid flux, C is the acid concentration, E_{f0} is the reaction rate constant, ΔE is the activation energy, m is the reaction order, R is the gas constant, T is the

reaction temperature. Li et al. (2017) showed that the optimum acid flux at which the wormhole will be created is highly affected by the acid temperature. They did numerical simulation study and showed that the acid temperature effect on the wormhole creation was significant compared to the effect of the initial reservoir temperature. The volume required to generate the wormhole as well as the optimum injection rate of the acid increased with increasing the injected acid temperature. Gong and El-Rabaa (1999) showed the optimum injection rate at which the wormhole is created with the minimum injected acid volume is located on the transition from the mass transfer controlled regime to the surface reaction controlled regime. They showed that at low injection rates the wormhole propagation is restricted by the slow acid diffusion. At high injection rates the wormhole generation is controlled by the acid reaction rate at the rock surface. Mahmoud and Nasr-El-Din (2014) found that the optimum wormholing injection rate (Q_{opt}) in calcite rocks can be obtained for a mass transfer controlled reaction regime by the following equation:

$$Q_{opt\_L} = 102\ h_f\ L_{core}\ D_e \tag{4.8}$$

Where; h_f is the heterogeneity factor, which is defined as the ratio of wormhole length to core length. L_{core} is the core sample length, cm and D_e is the diffusion coefficient, cm^2/s. This equation can be used to predict the optimum injection rate required to generate wormholes in carbonate reservoirs to obtain a certain acid penetration radius. The standard deviation of this prediction with the laboratory experiments-determined optimum injection rate was found to be 5%.

4.3 Methods of wormhole characterization in carbonate rocks

4.3.1 Pressure drop across the core

During the acid reaction with the carbonate rocks the pressure drop in the generated wormhole is considered to be zero. The pressure drop during the acid flow and wormhole creation can be expresses as follows (Daccord et al. 1989):

$$p(t) = \frac{\mu Q}{k\pi r_o^2}\,[L - L_e(t)] \tag{4.9}$$

Where; p(t) is the pressure drop at time t, μ is the dynamic viscosity, Q is the acid injection rate, k is the rock sample permeability, r_o is the rock sample radius, L is the rock sample length, $L_e(t)$ is the wormhole length at time t. When the p(t) approaches zero, this means the breakthrough of the wormhole. The pressure drop during the acid reaction also is highly affected by the reaction products such as spent acid and CO_2. CO_2 forms secondary phase and this will restrict the mobility and flow of the acid due to the relative permeability effect and this could be misleading in the interpretation of the wormhole quantification and generation. The reaction products such as calcium chloride affects the solubility of CO_2 in the spent acid in the case of HCl acid. The higher the calcium chloride (resulting from the reaction of HCl with calcite), the higher the pressure required to dissolve CO_2 in solution. Cheng et al. (2016) studied the effect of pressure on the wormhole shape and generation in Indiana limestone rock samples. They found out that the wormhole propagation was highly affected by the CO_2 at injection rates lower than the optimum and the effect of CO_2 diminished at higher injection rates.

4.3.2 Computed tomography (CT) scan

Computed tomography (CT) scan was used extensively as a laboratory technique to characterize and describe the wormhole propagation in carbonate rocks using different

stimulation fluids. Gomaa and Nasr-El-Din (2010a, 2010b, and 2010c) used CT scan to study the wormhole propagation using in-situ gelled acid based on polymer and HCl. They found out that, gelled acid created branched wormhole compared to regular straight HCl acid which created dominant single wormhole in calcite cores at the same conditions of injection rate, pressure, and temperature. Gomaa et al. (2011) optimized the wormhole creation using gelled acid based on polymer using the CT scan. They identified the optimum injection rate using CT at which the gelled acid can penetrate through the parallel cores during parallel coreflooding experiments. They found out that at low permeability contrast the gelled acid worked better compared to high permeability contrast. At high permeability contrast between the two cores, the gelled acid did not fully penetrate the low permeability core.

Al-Ghamdi et al. (2009, 2010, 2014) and Yu et al. (2011) evaluated the wormhole generation in calcite rocks using CT scan. They used HCl acid based on viscoelastic surfactant (VES) to generate the wormhole in calcite cores. They carried out single as well as parallel coreflooding experiments. CT scan evaluation of this system showed that the HCl based on VES can create wormhole in heterogeneous cores that have a permeability contrast less than 10. For higher permeability contrast the VES system has to be designed carefully with additional diversion techniques to generate wormholes in low permeability zones in the reservoir.

Mahmoud et al. (2011a, 2011b, and 2017) used CT scan to assess the wormhole generation in calcite cores using chelating agents. They used chelating agents such as GLDA (Glutamic acid diacetic acid), EDTA (Ethylene diamine tetra acetic acid), DTPA (diethylene tri amine penta acetic acid), and HEDTA to acidize carbonate rocks. They

found out that different chelating agents created wormholes in calcite cores at low injection rates compared to those created by HCl and HCl-based acid systems. Also CT scan confirmed the diversion ability of the tested chelating agents because the wormhole path was not straight at the optimum injection rate.

Zakaria et al. (2012), Sayed and Nasr-El-Din (2013), and Sayed et al. (2013) used CT scan to evaluate the wormhole generated by emulsified acids in carbonate rocks. They found that emulsified acid has a retardation effect, it reduced the leak off rate to the generated wormhole; and the CT scan showed dominant less branched wormholes.

4.3.3 Nuclear Magnetic Resonance (NMR)

NMR tool is considered the most recognized formation evaluation tool. NMR can be used to determine the rock porosity without the need of lithology and because of that NMR is considered one of the primary porosity tools (Straley 1997; Kenyon 1992). The total amplitude of the measured H^1-NMR signal is a direct evaluation of the amount of hydrogen in the rock sample. Pores are filled with either water or hydrocarbon, therefore, NMR will yield the pores-filled porosity of the rock sample.

NMR also can be used to determine the pore size distribution and the type of pore systems in the rock samples. The T_1 relaxation time (spin lattice relaxation time) and T_2 (spin-spin relaxation time) are strong function of the pore size (Sørland 2007; Straley 1997; Kleinberg 1994; Kenyon 1992). The spin-lattice relaxation time (T_1) takes very long to measure. Therefore, the focus was paid to evaluate and measure T_2. T_2 relaxation time is used in well logging tools and laboratory NMR tools to determine the rock porosity and pore size distribution. The relation between T_2 and the rock pores can be described as following (Korringa 1962):

$$\frac{1}{T_2} = \frac{1}{T_{2B}} + \rho\frac{S}{V} + \frac{D_H}{12}(\gamma G \tau_e)^2 \quad (4.10)$$

Where T_2 is spin-spin relaxation time, T_{2B} is bulk relaxation time, ρ is the specific surface relaxivity, S is the surface area of the pores, V is the volume of the pores, D_H is the molecular diffusion of the hydrogen in the pores, G is the magnetic field gradient, γ is the gyromagnetic ratio of proton, and τ_e is the echo delay time.

The first and third terms in **equation 4.10** can be neglected when the controlling regime is the surface one not the diffusion under low magnetic field NMR (Kleinberg 1994). Under the surface controlling regime and low field NMR, surface area and volume of the pores (S/V) can be determined from the measured T_2 relaxation time when the rock surface relaxivity (ρ) is given. The pore size distribution also can be determined from the measured T_2 such as micro, meso, and macro pores with the connectivity between these different pores. The magnetization of the hydrogen nuclei in the connections between the different pore systems created what is called diffusion coupling (diffusion of magnetization) (Grunewald 2011; Toumelin 2003; Toumelin 2002; Freeman 1999; Ramakrishnan 1998). The diffusion coupling can be use to describe the degree of connectivity between the different pore systems in the rock.

4.4 Effect of Fluid System on Wormhole Connectivity

Mahmoud (2017) reported that the optimum injection rate of 15wt% HCl prepared in both fresh and seawater into Indiana limestone core samples (3 in long) was located at 2 cm^3/min and 100°C. **Figure 4.1** shows the optimum injection rate for the 15 wt. % HCl. The acid volume consumed to generate the wormhole at the optimum injection rate was 0.8 PV. The volume of 15 wt. % HCl diluted in seawater is little bit more than the required 15 wt. %

HCl diluted in fresh water due to the presence of salts in the seawater which reduced acid diffusion and reaction rate with calcite. The pressure drop at the optimum injection rate (2 cm^3/min) is fairly linear from the start of acid injection till the breakthrough of the wormhole (**Figure 4.2**).

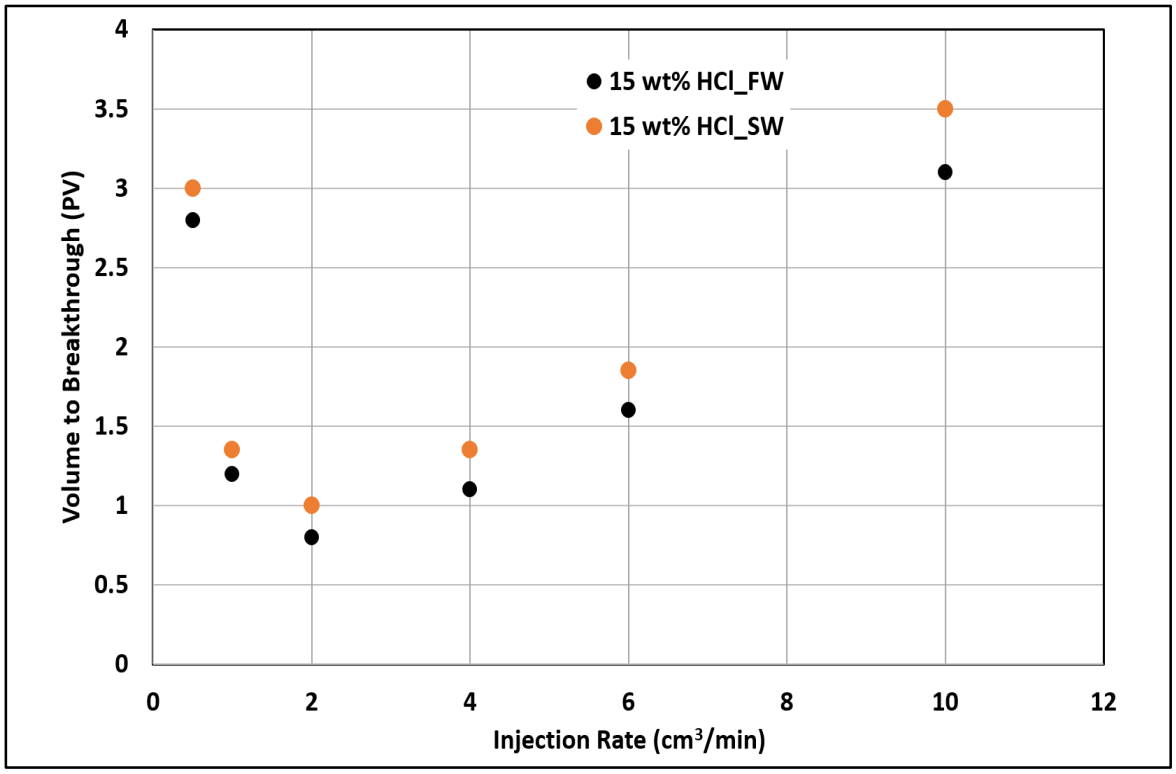

Figure 4. 1—Optimum injection rate for 15 wt. % HCl prepared in fresh water and seawater.

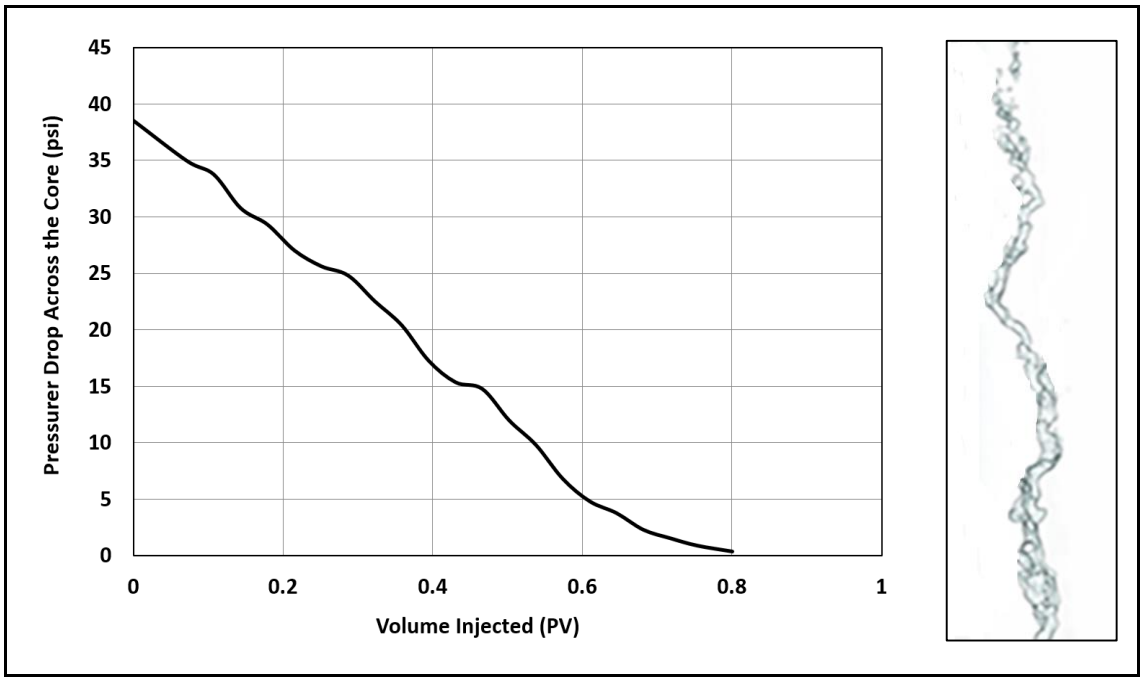

Figure 4. 2—Pressure drop profile and wormhole at the optimum injection rate (2 cm^3/min) for 15 wt. % HCl prepared in fresh water into Indiana limestone core sample at 100°C.

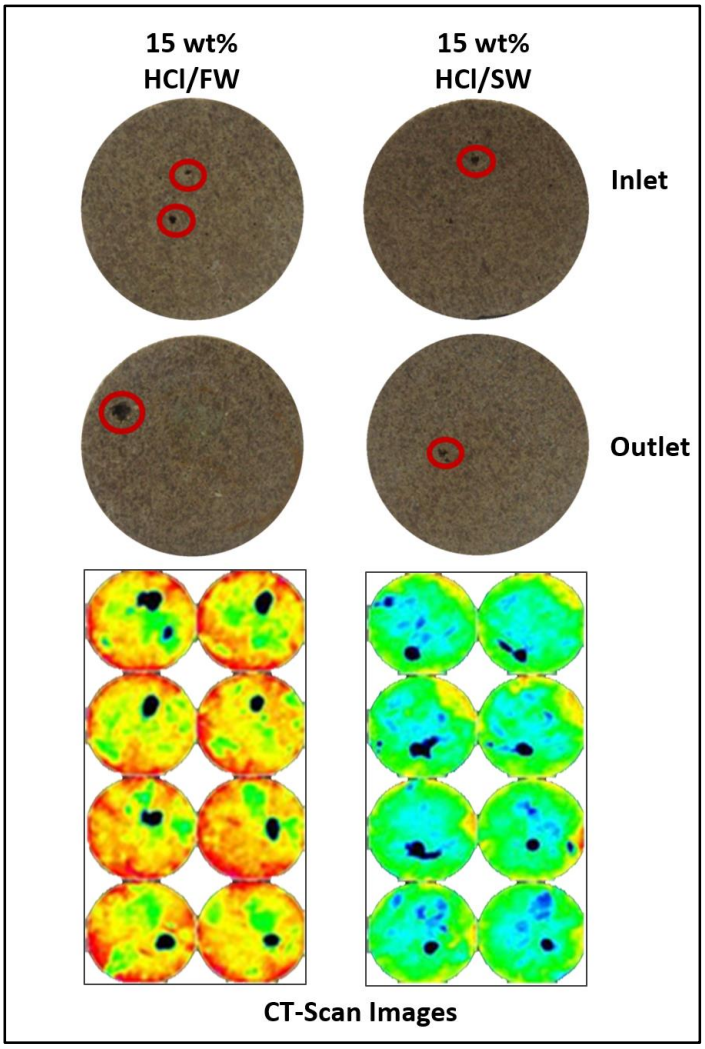

Figure 4. 3—Cores inlet and outlet faces and CT for Indiana limestone core samples flooded with 15 wt. % HCl prepared in fresh water (left) and seawater (right) at 100°C. Black spots in the CT scan images indicate the wormhole of an average CT number of zero.

However, Pressure drop and CT images (**Figure 4.3**) did not show any major difference between the core inlet and outlet faces in the cores stimulated by both HCl prepared in fresh water and seawater, NMR showed totally different results for the two cores (**Figure 4.4 and 4.5**). NMR indicated that the two cores have dual porosity system. In the two cases HCl injection yielded three pore system, micro, meso, and macro pores by created additional pore system (wormhole).

After the treatment the pore size distribution changed and yielded triple pore system (micro, meso, and macro-pores). The micro pores intensity increased due to the creation of more micro pores and a new pore system of meso-pores was created. The macro-pores were extended to bigger size due to the wormhole creation. The macro-pores relaxation time increased from 2000 to 3000 mSec due to the acid treatment and wormhole generation. diffusion coupling (Freeman et al. 1999) which is defined by the diffusion of magnetic field during the magnetization process of the NMR is located between the pore system. A high diffusion coupling indicates a well interconnected pore system is which the created wormhole is well-connected to the other pore systems in the core yielding high efficiency of the acid treatment.

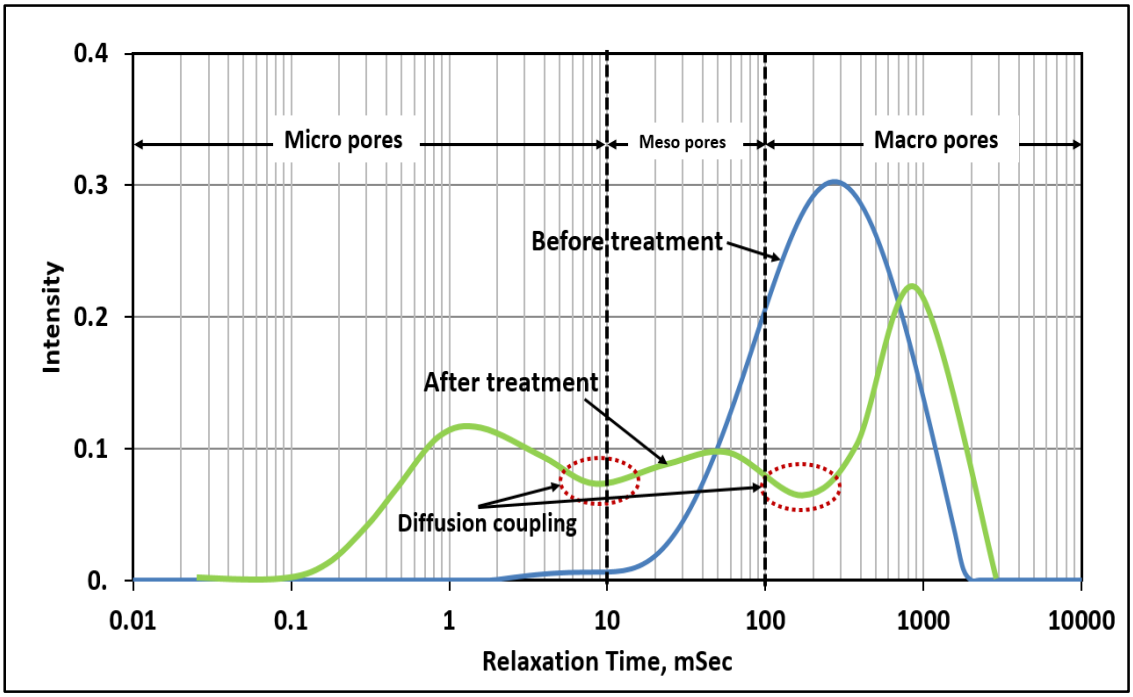

Figure 4. 4—NMR scans before and after acid treatment, in both cases the core was saturated by 3 wt. % KCl solution and stimulated using 15 wt. % HCl prepared in fresh water at 100°C.

Figure 4.5 shows the NMR profile for the core treated by 15 wt. % HCl prepared in seawater. After the treatment the generated wormhole due to the acid reaction enlarged the existing macro pores and relaxation time increased from 800 to 3000 msec. The reduced diffusion coupling to almost zero indicates pores plugging and isolation of the micro pores from the rest of the pore system in the core. As a result of the reaction of calcium (from HCl reaction with calcite) and sulfate from the seawater, Calcium sulfate scale was formed with a crystals ranges from 0.5 to 5 μm (Aliaga et al. 1992). Calcium sulfate scale can plug pore throats and pore sizes less than 5 μm.

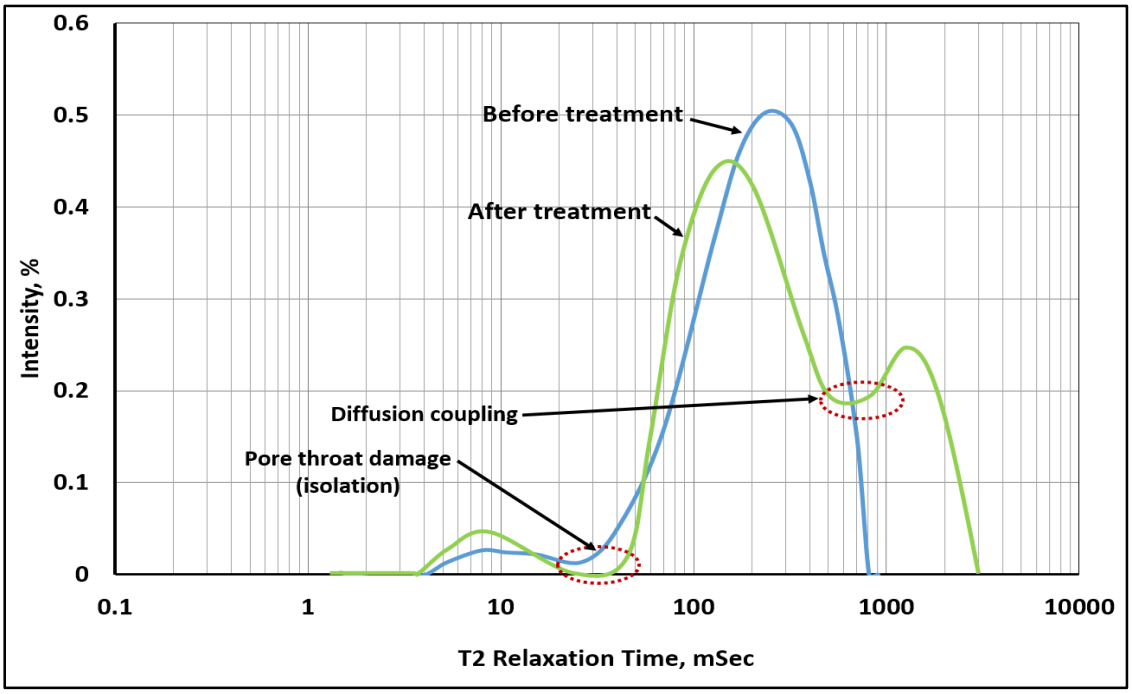

Figure 4. 5—NMR scans before and after acid treatment, in both cases the core was saturated by 3 wt. % KCl solution and stimulated using 15 wt. % HCl prepared in seawater at 100°C.

It can be concluded that HCl prepared in seawater should not be used to stimulate carbonate formations. Interconnectivity number (ICN) is a quantitative parameter is used to estimate the extent of connectivity of different pore systems within the rock samples before and after treatment. High interconnectivity number indicates good connectivity between the

generated wormhole and the rock matrix. The first ICN is calculated for the connection between micro and meso pores and the second one is calculated for the connection between meso and macro pores (wormhole). The following equation was used to determine the interconnectivity number (ICN):

$$ICN = \frac{\text{Intensity of the diffusion coupling}}{\text{Maximum intensity of the two pore systems}} \quad (4.11)$$

ICN can be used to assess the stimulation fluid for a rock with two pore system and ICN ratio will can be used for rocks with triple pore system. The ICN ratio can be determined as follows:

$$ICR_{Ratio} = \frac{ICN_{micro/meso}}{ICN_{meso/macro}} \quad (4.12)$$

Where:

$ICN_{micro/meso}$: the interconnectivity number between micro and meso pores

$ICN_{meso/macro}$: the interconnectivity number between meso and macro pores.

Table **4.1** is showing the parameters used to calculate ICR_{Ratio} for samples treated with 15 wt.% HCl prepared in fresh water and seawater from figures 4.4 and 4.5. It is clear that the zero ICR_{Ratio} in case of seawater is indicating a formation damage associated with the stimulation fluid which could not be located by CT scan and pressure drop.

Table 4. 1—Parameters used to calculate ICR_{Ratio} for Indiana limestone samples treated with 15 wt.% HCl prepared in fresh water and seawater at 100ºC

Parameter	After treatment with 15 wt. % HCl prepared in fresh	After treatment with 15 wt. % HCl prepared in seawater
Max. Intensity micro	0.12	0.05
Max. Intensity meso	0.1	0.45
Max. Intensity macro	0.225	0.25
Micro-meso diffusion coupling Intensity	0.625	0
Meso-Macro diffusion coupling Intensity	0.07	0.18
ICN (micro/meso)	0.625	0
ICN (meso/macro)	0.31	0.4
ICR_{Ratio}	2.016	0

For chelating agents, **Figure 4.6** shows the NMR profiles for the Indiana limestone sample treated by 20 wt. % EDTA chelating agent diluted in fresh water. EDTA created a third pore system and enhanced the connectivity between the three pore systems. The ICN between the micro and meso pores is 0.09/0.27 or 0.33, and the ICN between the meso pores and wormholes (macro pores) is 0.37. The ICN ratio is 89 % which indicates a very well connected wormhole to micro and meso pore systems without causing any damage to rock.

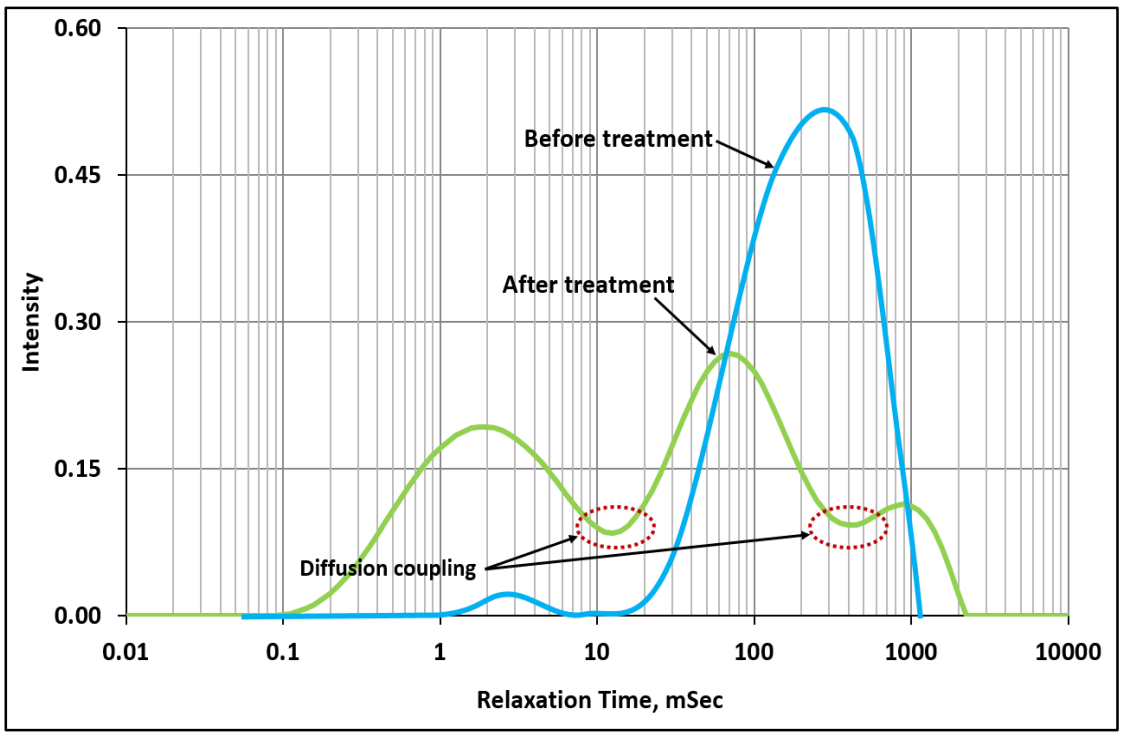

Figure 4. 6—NMR scans before and after acid treatment, using 20 wt. % EDTA diluted in fresh water at 2 cm^3/min, pH 4, and 100°C.

Figure 4.7 shows the summary of different coreflooding experiments for 20 wt% chelating agents diluted in both fresh water and seawater. Chelating agents prepared in seawater did not affect the interconnectivity between the pores and the created wormholes with high ICN ratio, which means that chelating agents diluted in fresh water or seawater can be used to stimulate carbonate reservoirs effectively compared to HCl that may lead to precipitation around the wormhole if prepared in seawater. In conclusion, HCl can cause formation damage when diluted in seawater for stimulation treatments by disconnecting different pore systems in the carbonate rock. Chelating agents can be used safely (No induced formation damage) for stimulation treatments when diluted in seawater. In the coming chapters the reaction of different chelating agents with carbonate rock samples will be studied at HPHT by conduction reaction kinetics and coreflooding experiments.

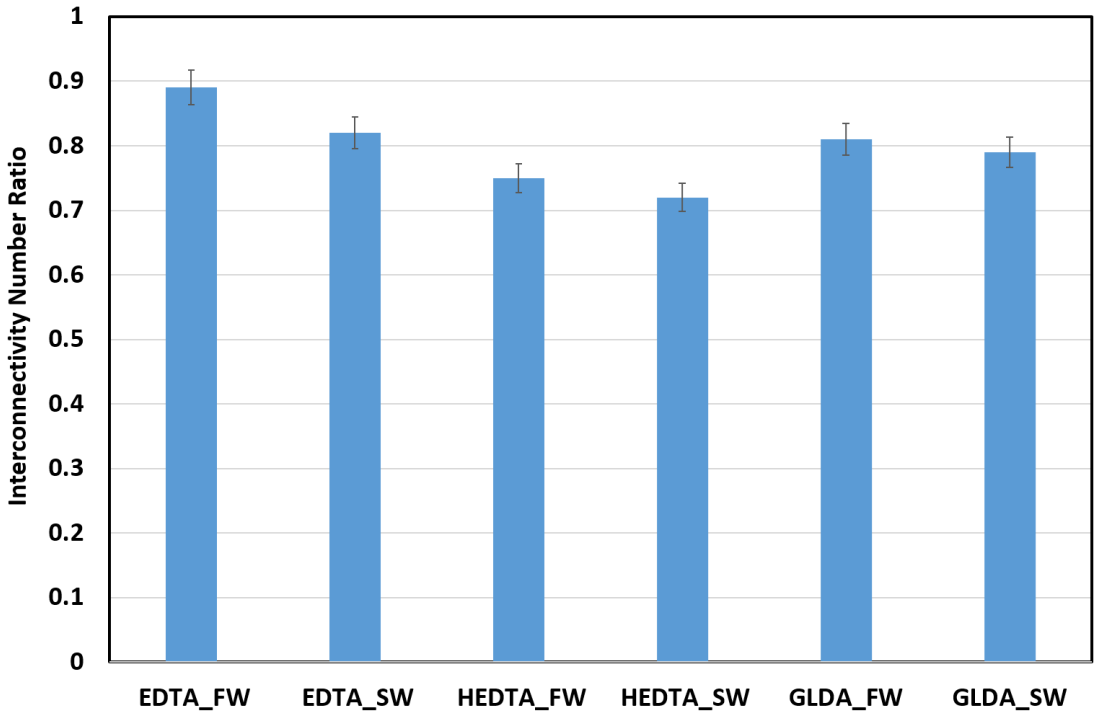

Figure 4. 7—Interconnectivity number ratio for 20 wt. % chelating agents diluted in fresh water (FW) and seawater (SW) at 2 cm^3/min, pH 4, and 100°C. The error bar is ±3%.

CHAPTER 5

GLDA Chelating Agents: Reaction Kinetics and Coreflooding Study

Hydrochloric acid (HCl) is commonly used as a stimulation fluid in oil and gas carbonate reservoirs. Using HCl acid during matrix acid treatment in high pressure high temperature carbonate acidizing has numerous limitations; namely, rapid tubulars corrosion, formation face dissolution due to fast uncontrolled reaction rate and low injection rates, and induced formation damage due to sludge formation in the presence of crude oil with high asphaltene content. There is also a difficulty of using HCl in stimulating multilateral and horizontal wells due to its fast reaction with the reservoir rock. Chelating agents were introduced as alternatives to HCl to alleviate the problems associated with HCl. GLDA (Glutamic acid diacetic acid) chelating agent was used previously to stimulate carbonate reservoirs at high pressure and high temperature (HPHT) conditions. GLDA was prepared in fresh water to stimulate these reservoirs.

In this paper, the effect of GLDA dilution using seawater on the reaction kinetics of low pH GLDA (3.8 pH) with different carbonate rocks under HPHT conditions was investigated using the rotating disk apparatus (RDA). The reaction experiments of GLDA solution with carbonate rocks in both fresh (GLDA/DI) and seawater (GLDA/SW) were carried out at 1000 psi and 150, 200, and 250^{o}F. Indiana limestone and Austin chalk carbonate rock samples were used to investigate the effect of rock facie on the reaction.

The reaction regime of GLDA chelating agent with calcite is mass transfer limited in both seawater and fresh water. Also the overall reaction rate and diffusion coefficient were highly dependency on the temperature. At 200^{o}F and 1000 psi the diffusion coefficient for the reaction of GLDA/SW with Austin chalk is an order of magnitude higher than the reaction of that with Indiana limestone.

The determined diffusion coefficients can be used to estimate the optimum injection rate required for stimulating high temperature carbonate formation. Highlighting the effect of porosity facies in the acid reaction with carbonate rock will lead to better understanding of the overall reaction of stimulation fluids with carbonate rocks of the same lithology but different porosity facies.

5.1 Introduction

Organic and inorganic acids are often injected into carbonate reservoirs to improve oil and gas production. These acids are usually selected based on the type of reservoir rock. In the case of stimulating carbonate formations, acids can dissolve the carbonate rock matrix and create different dissolution features or structures depending on the type of the acid, injection rate, and formation conditions (Williams et al. 1979; Daccord 1987; Hoefner and Fogler 1988; Wang et al. 1993; Daccord et al. 1993; Fredd and Fogler 1998; Bazin 2001). At very low injection rates, the face of the rock is dissolved resulting in a face-dissolution pattern (Fredd and Miller 2000). At high injection rates, the retention time of acid in the rock is small and the rock is dissolved uniformly by forming narrow dissolution channels that may propagate throughout the rock and form more branches with continuous acid injection (Fredd and Miller 2000; Golfier et al. 2002). An optimum channel formed during acid injection is known as a wormhole which is formed at the minimum volume of acid

injected and yield the highest permeability increase (Wang et al. 1993; Glasbergen at al. 2009; Maheshwari et al. 20013). Other dissolution patterns may present such as the conical wormholes (injection rate between face dissolution and wormhole patterns) and ramified wormholes (injection rate between wormhole and uniform dissolution patterns).

The acid type affects the structure of the generated wormholes during carbonate acidizing (Bazin 2001; Fredd 1998). Slow reacting acids such as chelating agents and other organic acids form wider, less branched wormholes, while highly reactive acids such as HCl form highly branched wormholes (Darren et al. 2010). The relative magnitudes of acid transport and reaction rates define the controlling step of the dissolution reaction whether kinetically controlled or mass-transfer controlled (Nierode and Williams 1971). As a result, the wormhole structure depends on the acid diffusivity and reactivity, in addition to the acid-injection rate (Mahmoud et al. 2016). To characterize the acid transport to rock surface during matrix acidizing, acid diffusion coefficient is an important parameter to be determined under reservoir conditions (Conway et al. 1999).

5.2 Chelating Agents

Chelating agents are organic molecules that can form stable ring-like structures and sequester metal ions through coordination bonds. The metal ions when chelated or sequestered by chelating agents are prevented from any further interaction with other ions present in the solution. A more stable complex depends on the chelating agent itself and the properties of the metal ion (Dwyer and Mellor, 1964).

Chelating agents have low corrosive nature and this feature has extended their use to different applications in the oil and gas industry. These applications in the upstream oil and gas industry include; removal of different types of scales from oil and gas reservoirs such

as calcium carbonate and calcium sulfate scales, and removal of the scale from electrical submersible pump in oil producers (Crabetree et al, 1999). Chelating agents were also used to prevent and inhibit calcium sulfate scale during seawater injection (Mahmoud et al, 2016). Recently, chelating agents were used as enhanced oil recovery fluids in carbonate and sandstone reservoirs (Mahmoud and Abdelgawad, 2016 and Attia et al, 2014).

GLDA is one of the Aminopolycarboxylic acids (**Figure 5.1**), which are able to form stable complexes with alkali earth metals (Ca, Mg, etc.) with a low corrosiveness nature to the equipment up to 300°F (De Wolf et al, 2016).

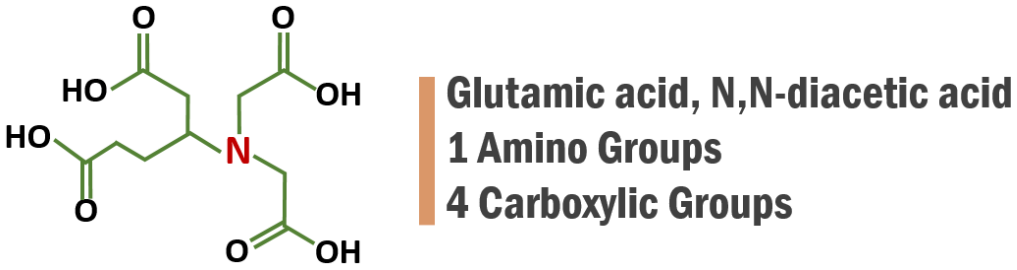

Figure 5. 1—Glutamic acid, N, N-diacetic acid (GLDA) chemical structure.

GLDA undergoes a stepwise loss of protons until it reaches the fully ionized state. GLDA dissociation reactions are as follows:

$$H_4Y \rightleftharpoons H_3Y^{-1} + H^+ \quad (5.1)$$

$$H_3Y^{-1} \rightleftharpoons H_2Y^{-2} + H^+ \quad (5.2)$$

$$H_2Y^{-2} \rightleftharpoons HY^{-3} + H^+ \quad (5.3)$$

$$HY^{-3} \rightleftharpoons Y^{-4} + H^+ \quad (5.4)$$

Where H_mY^{m-n} represents the chelating agent molecule, n is the number of carboxylic groups and m is the number of acidic protons. The ion species distribution for GLDA is shown in **Figure 5.2**.

GLDA is used to stimulate HPHT carbonate and sandstone reservoirs after showing promising results in many Laboratory studies (LePage et al. 2009; Mahmoud et al. 2011; De Wolf et al, 2016) and field treatments as well (Mahmoud et al. 2011, Nasr-El-Din et al. 2013; Nuñez et al. 2017). GLDA is used as an alternative to HCl to overcome the challenges in HPHT (high pressure high temperature) environments.

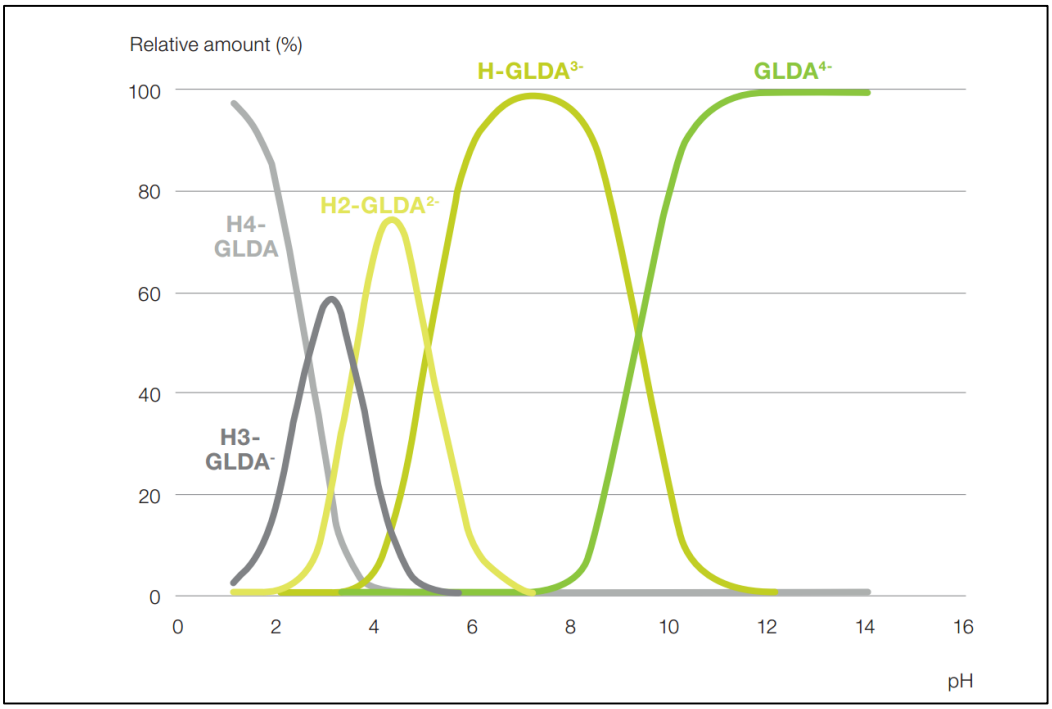

Figure 5. 2—The ion species distribution for GLDA

These challenges include; rapid corrosion of the well tubulars, face dissolution, very high and uncontrolled reaction rate, and formation damage in high clay content and iron-rich reservoirs. In addition, GLDA acts also as iron control agent and it is gentle to the well tubulars. HCl needs numerous additives and this will increase the cost of the acid treatment. HCl treatment should be loaded with the following additives; corrosion inhibitor, corrosion inhibitor intensifier, iron control agent, water wetting surfactants, anti-sludge agents, iron control agents etc. GLDA acid treatment does not require a single additive because it acts

as iron control agent, it has low IFT (interfacial tension, acts as surfactant). In addition, it does not cause asphaltene precipitation. Using GLDA will eliminate the need for the numerous additives used in the case of HCl.

Studying the reaction kinetics of stimulation fluids using RDA, eliminate the need for performing coreflooding experiments (which is tedious and expensive task). Several coreflooding experiments are needed to locate the optimum injection rate for each damage depth. Knowing the nature and limitations of the reaction between the stimulation fluid and a rock will facilitate the treatment design for any formation penetration radius. For example, the optimum Damköhler number and injection rate can be determined as a function of the diffusion coefficient of the mass transfer limited reaction that can be obtained from the reaction kinetics study.

Up to the author's knowledge, it is the first time to study the reaction kinetics of GLDA chelating agent prepared in seawater with calcite rock samples using the rotating disk apparatus at HPHT. The reaction regime is determined and the diffusion coefficient of GLDA are determined. In addition, the effect of porosity type on the rock fluid interaction is investigated by comparing the reaction of two different carbonate rocks with the same fluid system.

5.3 Rotating Disk Theory

For a matrix acidizing treatment where an acidic fluid is injected into the reservoir rock, the reaction regime is greatly affected by reactant transport to the rock surface and products transport away from the surface (Nierode and Williams 1971). The overall reaction consists of three steps as shown in **Figure 5.3**:

- Reactant transfer from the bulk solution to the solid surface.

- Reaction at the solid surface.
- Products transfer from the surface to the bulk solution.

The slowest step among the three controls the overall reaction kinetics and is referred to as "the rate-limiting step". For a reaction system, if the mass transfer process is faster than the surface reaction rate, then the overall reaction is controlled by surface reaction (Klaewkla et al. 2011). On the other hand, if the rate of surface reaction is faster than diffusion to the surface, the process is mass transfer limited.

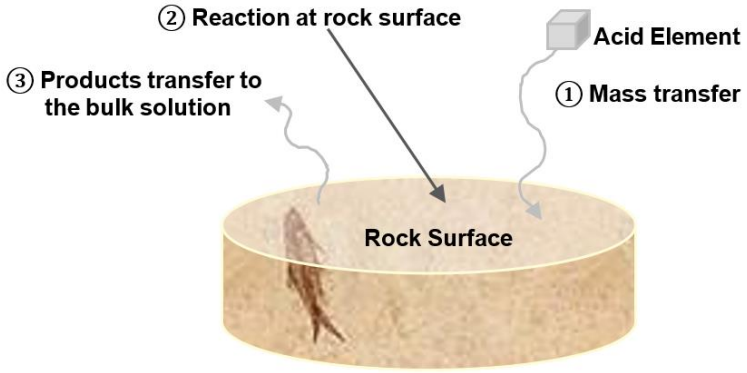

Figure 5. 3—Acid reaction with rock surface.

Levich (1962) showed that, for Newtonian fluids, the rate of mass transfer (R_{MT}) of a reactant to the solid surface in a laminar flow regime induced by a rotating disk geometry is given by the following equation:

$$\mathrm{J}_{mt} = k_m(\mathrm{C}_b - \mathrm{C}_s) \tag{5.5}$$

$$k_m = \frac{0.60248\ ({S_c}^{-\frac{2}{3}})\sqrt{\nu\omega}}{1 + 0.2980\left({S_c}^{-\frac{1}{3}}\right) + 0.1451({S_c}^{-\frac{2}{3}})} \tag{5.6}$$

where J_{mt} is the mass transfer flux, A is the Surface area (cm^2), C_b is bulk concentration of the transferred species, C_s is surface concentration of the transferred species, k_m is mass transfer coefficient, ω is disk angular velocity which is equal to $2\pi N$, where N is the

number of cycles/s (rad/s), ρ is the fluid density (gm/cm^3), μ is the fluid viscosity (gm/s.cm), ν is the kinematic viscosity (cm^2/s), D_e is the diffusion coefficient (cm^2/s), S_c is Schmidt number (ν / D_e), dimensionless.

For a mass transfer limited reaction in which the rate of mass transport is lower than the rate of reactant consumption at the rock surface, the concentration of reactants at the reaction solid surface can be neglected ($C_s = 0$). The final form of the mass transfer rate for a laminar flow of a Newtonian fluid can be expressed as follows:

$$J_{mt} = \frac{0.60248 \left(\frac{\mu}{\rho D_e}\right)^{-\frac{2}{3}} C_b \sqrt{\frac{\mu}{\rho}}}{1 + 0.2980 \left(\frac{\mu}{\rho D_e}\right)^{-\frac{1}{3}} + 0.1451 \left(\frac{\mu}{\rho D_e}\right)^{-\frac{2}{3}}} \omega^{\frac{1}{2}} \tag{5.7}$$

Levich (1962) defined the Reynold number for the flow around a rotating disk in laminar flow regime (R_e is in the order of 10^4-10^5) as:

$$N_{Re} = \frac{\omega R^2}{\nu} \tag{5.8}$$

Where R is the rotating disk radius (cm). Later, Yen et al. (1992) and Ellison and Cornet (1972) showed that for the rotating disk geometry, the laminar flow is controlled by Reynold's number less than 3 x 10^5 compared to 2000 in pipe flow. In this work, **Equation 4.7** was used, because N_{Re} is less than 10^4 (highest N_{Re} was 804 at 2000 rpm). Mahmoud et al. (2011) studied the viscosity of different chelating agents and they found that all chelating agents, within the studied concentrations, are Newtonian fluids with constant viscosity that is independent of shear rate. Lund et al. (1937) described the surface reaction rate as a function of concentration by the following equation:

$$-r_{HCl} = kC_{As}^n = J_{mt} \tag{5.9}$$

where r_{HCl} is the dissolution rate of calcite in HCl per unit area (moles/cm^2.s), k is the Specific reaction rate (moles /cm^2.s)(mole/cm^3)$^{-n}$, C_{As} is the surface concentrations of dissolving substance A, and n is dimensionless reaction order. After determining the surface area of the disk, the dissolution rate can be determined. The dissolution rate is calculated by dividing the slope of the straight line fitted to each experimental results by the initial surface area of the disk (Sayed et al. 2013).

$$R = \frac{1}{(1-\phi)A_{core}} \frac{d\,C_A}{dt} \tag{5.10}$$

where R is Dissolution rate of calcite in acid per unit area (mole/cm^2.s), C_A is concentration of the substance A (Calcium in our case), t is time (s), A_c is rock sample surface area exposed to acid (cm^2), and ϕ is rock sample porosity (fraction).

If the mass transfer regime of reactants or products is the limiting step, then increasing the angular velocity will increase the mass transfer and in turn, the overall dissolution rate will increase. If the mass transfer rate exceeds the consumption of the acid on the rock surface, the overall dissolution is independent of angular velocity and as the regime will be surface reaction limited (Taylor et al. 2004).

5.4 Materials and Methodology

Using the RDA shown in (**Figure 5.4**), 500 ml of the fluid are first charged into the vessel with the aid of vacuum pump. The fluid is then heated up to the required temperature using the heating jacket surrounding the vessel under a pressure of 500 psi on the top of the liquid to prevent any evaporation during the heating process. During each experiment, the rock sample is attached to the rotating disk using teflon shrinkage tube to isolate the sample from all sides except the face of the sample exposed to reaction with the acid. The reactor

is connected to the vessel to allow transfer of the fluid from the vessel to the reactor under pressure. Once the reactor body is heated to the same temperature of the acid system in the top vessel, the fluid is transferred into the reactor and the shaft is set to rotate at the required speed using a high revolution per minute (RPM) sensor controlled from the supervisory control and data acquisition (SCADA). After transferring the fluid to the reactor, the pressure in the reactor is increased to 1000 psi using nitrogen gas. The sampling loop is set to collect samples from the fluid inside the reactor every two minutes. A nitrogen line is connected to the sampling loop to ensure displacement of all the samples to collection tubes and to prevent mixing of consecutive samples inside the sampling line between the two-solenoid valves. A gas booster is used to provide high nitrogen pressure to the system.

During each experiment, the flux (J_{mt}) is determined from the analysis of the measured calcium ions concentration in the solution. Keeping all other parameters constant (such as temperature and acid concentration), the experiment is repeated at different rotational speeds.

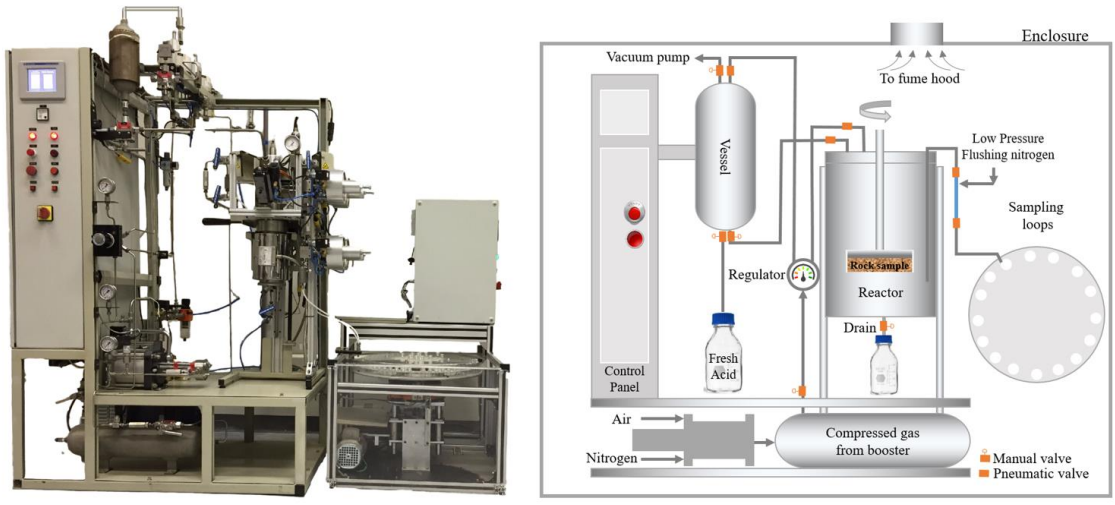

Figure 5. 4—Rotating disk apparatus with schematic showing main components.

The procedure for determining the limiting step for the reaction of 20 wt. % GLDA chelating agent at 3.8 pH solution with carbonate rock is shown in **Figure 5.5**. The calcium concentration in mg/L is plotted versus time and the dissolution rate is determined from the slope of a given set of experimental data. The dissolution rate is plotted versus the disk angular velocity to determine the limiting step of the reaction.

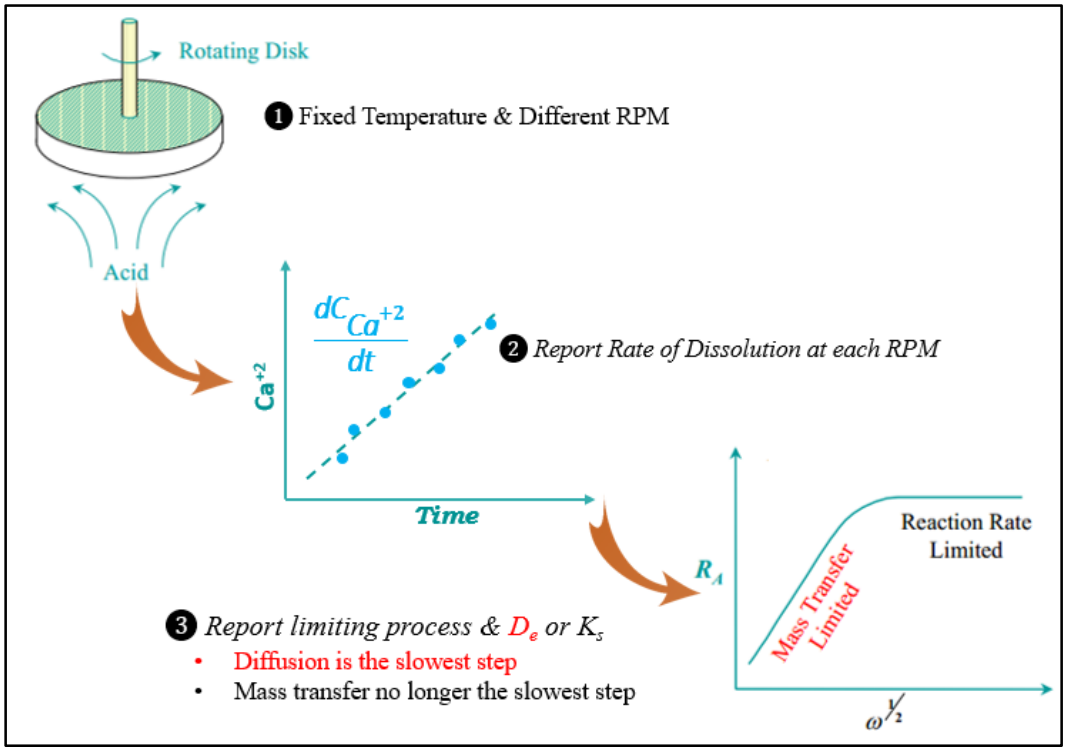

Figure 5. 5—The procedure for determining the reaction limiting step.

5.5 Experimental Work

The dissolution rate of carbonate rock using GLDA is estimated using two sets of experiments in the rotating disk apparatus. In the first set, GLDA diluted from stock concentration of 40 wt% to 20 wt% at (3.8 pH) using deionized water was used. In the second set of experiments, GLDA was diluted using synthetic seawater with the composition listed in **Table 5.1** at 20 wt%. Four experiments were carried out using each fluid/rock system at constant pressure and temperature and at different disk speeds (500, 1000, 1500, and 2000 rpm). A 500 ml of GLDA was used for each experiment. The density and viscosity of 20 wt% of GLDA/DI and GLDA/SW as a function of temperature are shown in **Figure 5.6**. These properties are required when **equation 5.7** is to be applied.

Table 5. 1—Synthetic seawater composition

Ions	Concentration (mg/l)
Sodium	18,300
Calcium	650
Magnesium	2,110
Sulfate	4,290
Chloride	32,200
Carbonate	0
Bicarbonate	120
Total dissolved salts (TDS)	57,670

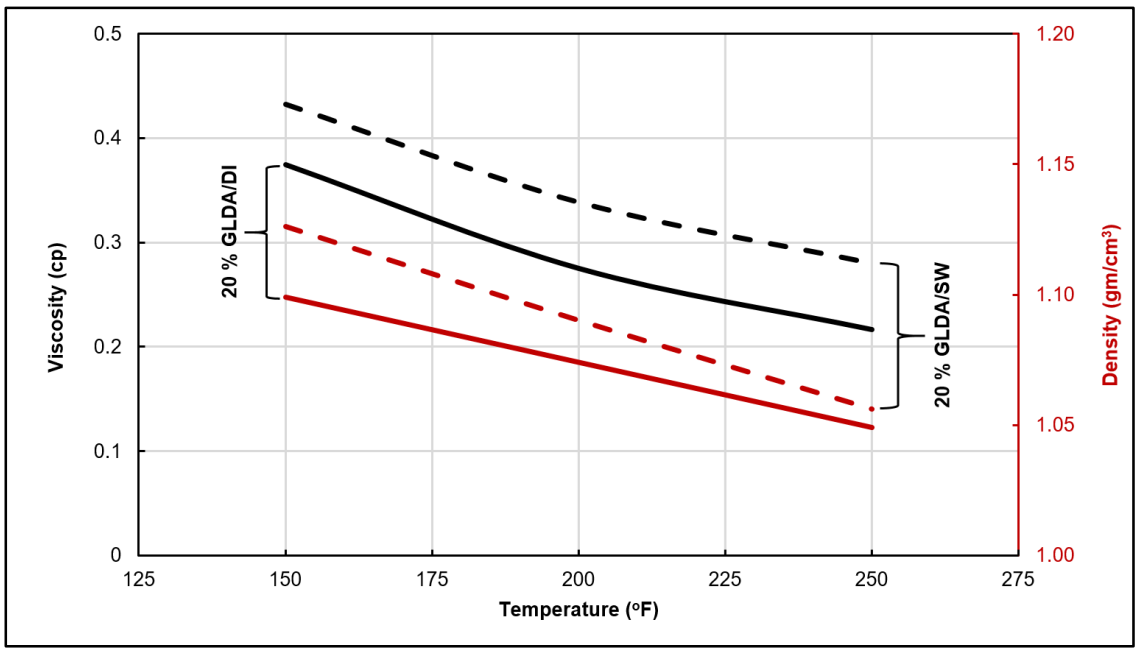

Figure 5. 6—20 wt% GLDA (3.8 pH) density (red) and viscosity (black) as a function of temperature.

During the experiment, a sample (3 ml) was collected every two minutes and the reaction was stopped after collecting 10 samples. After doing the required dilution especially for samples collected at high RPM, Inductively Coupled Plasma Optical Emission Spectroscopy (ICP-OES) was used to determine calcium concentration in each sample. The conducted experiments are listed in **Table 5.2**; all experiments were conducted at 1000 psi. Indiana limestone and Austin chalk core samples of 0.8-inch-long, 1.5-inch diameter were used in this study. The surface of each core sample was polished to assure smooth surface for reaction using end face grinding, polishing, and sonic cleaning to correctly estimate the surface area at which the reaction takes place. The porosity of each sample was calculated using dry and saturated weights and the cores were saturated with fresh water of 1 g/cm^3 density. Austin chalk samples were prepared similarly to Indiana cores.

Table 5. 2— Experiments using GLDA with Indiana limestone and Austin chalk rocks at different temperature conditions and 1000 psi.

Experiment No.	Fluid/Rock	Temperature (°F)	Disk Porosity (%)	Disk Angular Velocity (RPM)
1	20 wt% GLDA/DI /Indiana Limestone	150	6.82	500
2			6.82	1000
3			7.07	1500
4			7.15	2000
5		200	10.02	500
6			9.62	1000
7			10.14	1500
8			9.20	2000
9		250	9.08	500
10			9.99	1000
11			6.75	1500
12			9.46	2000
13	20 wt% GLDA/SW with Indiana Limestone	150	12.41	500
14			9.42	1000
15			9.75	1500
16			9.43	2000
17		200	9.30	500
18			9.55	1000
19			9.66	1500
20			6.916	2000
21		250	9.24	500
22			9.53	1000
23			9.53	1500
24			12.41	2000
25	20 wt% GLDA/SW with Austin chalk	200	26.07	500
26			22.45	1000
27			27.96	1500
28			26.79	2000

5.6 Results and discussion

5.6.1 Indiana Limestone

The analysis of the first four experiments (**Figure 5.7-a**) shows that the reaction regime for the 20% GLDA/DI and Indiana limestone rock samples is surface reaction. Increasing the temperature from 150^{o}F to 200^{o}F increased the surface reaction and turned the process to mass transfer limited regime (**Figure 5.7-b**). The same temperature effect is also obvious at 200^{o}F (**Figure 5.7-c**). **Figure 5.7-d** summarizes the results of 20% GLDA/DI reaction with Indiana limestone core samples at 150, 200, and 250^{o}F. Applying **equation 5.7**, diffusion coefficients of 4.59 x10^{-6} and 1.07 x10^{-5} cm^{2}/s are obtained at 200 and 250^{o}F respectively. On the other hand, the reaction of 3.8 pH, 20 wt% GLDA/SW with Indiana limestone core samples is mass transfer limited regime at all temperatures (150, 200, and 250^{o}F) as shown in **Figures 5.8-a** through **5.8-d**. This is attributed to the high mass transfer resistance due to high salinity. Applying **equation 5.7**, diffusion coefficients of 8.31 x 10^{-7}, 3.37 x 10^{-6} and 4.71 x 10^{-6} cm^{2}/s are obtained at 150, 200 and 250^{o}F, respectively. The diffusion coefficient in case of GLDA/SW is smaller compared to GLDA/SW because the chemical species diffusion is buffered by the salts presents in GLDA/SW system. The diffusion coefficient is this case can be correlated as a function of temperature as shown in **Figure 5.9** by **Equation. 5.11.**

$$D_e = 3.88 \times 10^{-8} T - 4.7 \times 10^{-6} \qquad (5.11)$$

The Temperature increase in case of GLDA/DI from 200 to 250^{o}F highly significantly increased D_e. The reduction in the acid diffusion can be attributed to the high salts which create can create a high resistive diffusive layer that slowed down the diffusion of GLDA making the mass transfer is the limiting step of the overall dissolution process.

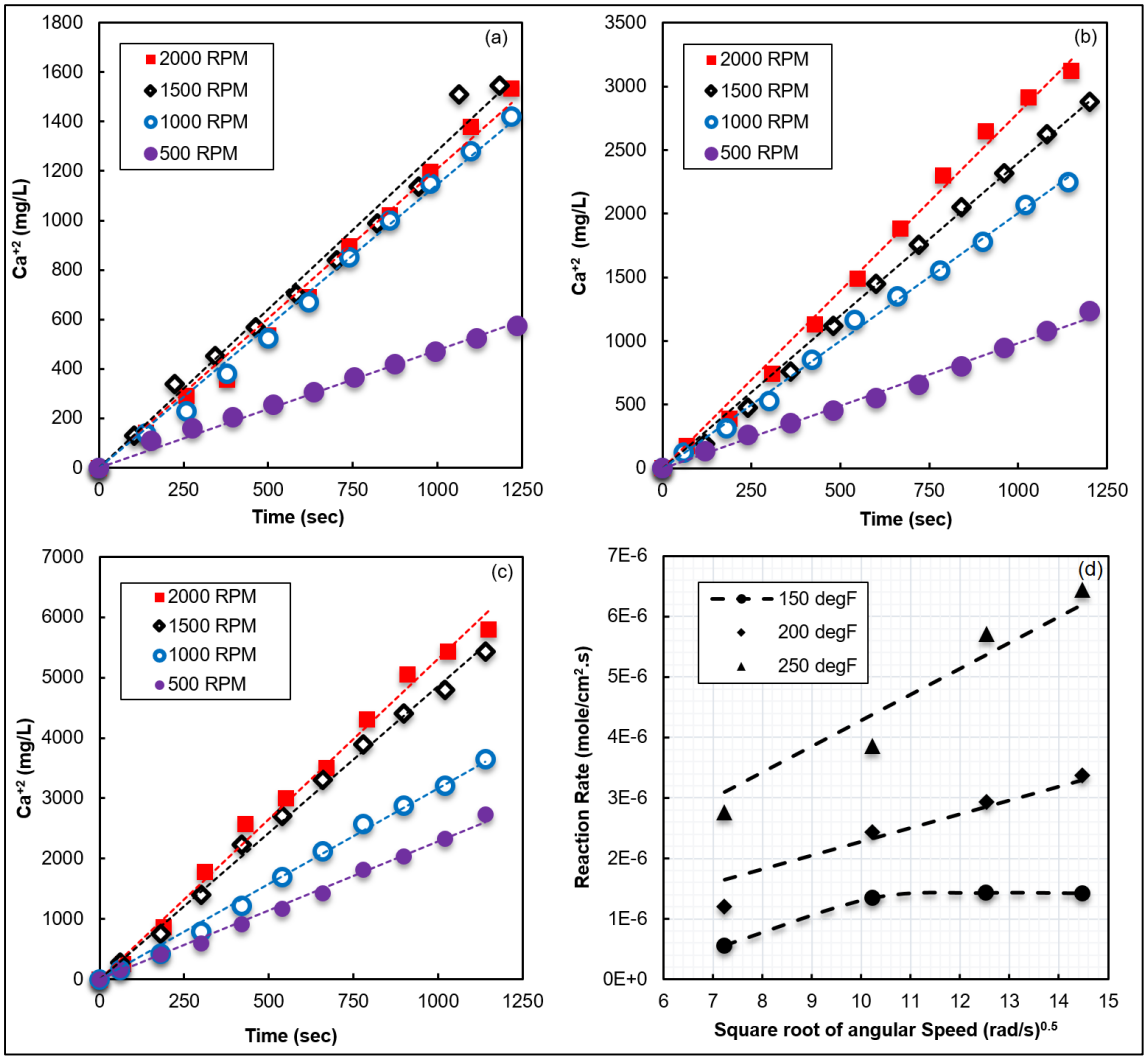

Figure 5. 7—Calcium concentration in the collected samples as a function of time and rotation speed using 20 wt% GLDA/DI solution at 150ºF (a), 200ºF (b), 250ºF (c), and Rate of calcite dissolution in 20 wt% GLDA/DI at pH 3.8 at corresponding temperatures (d).

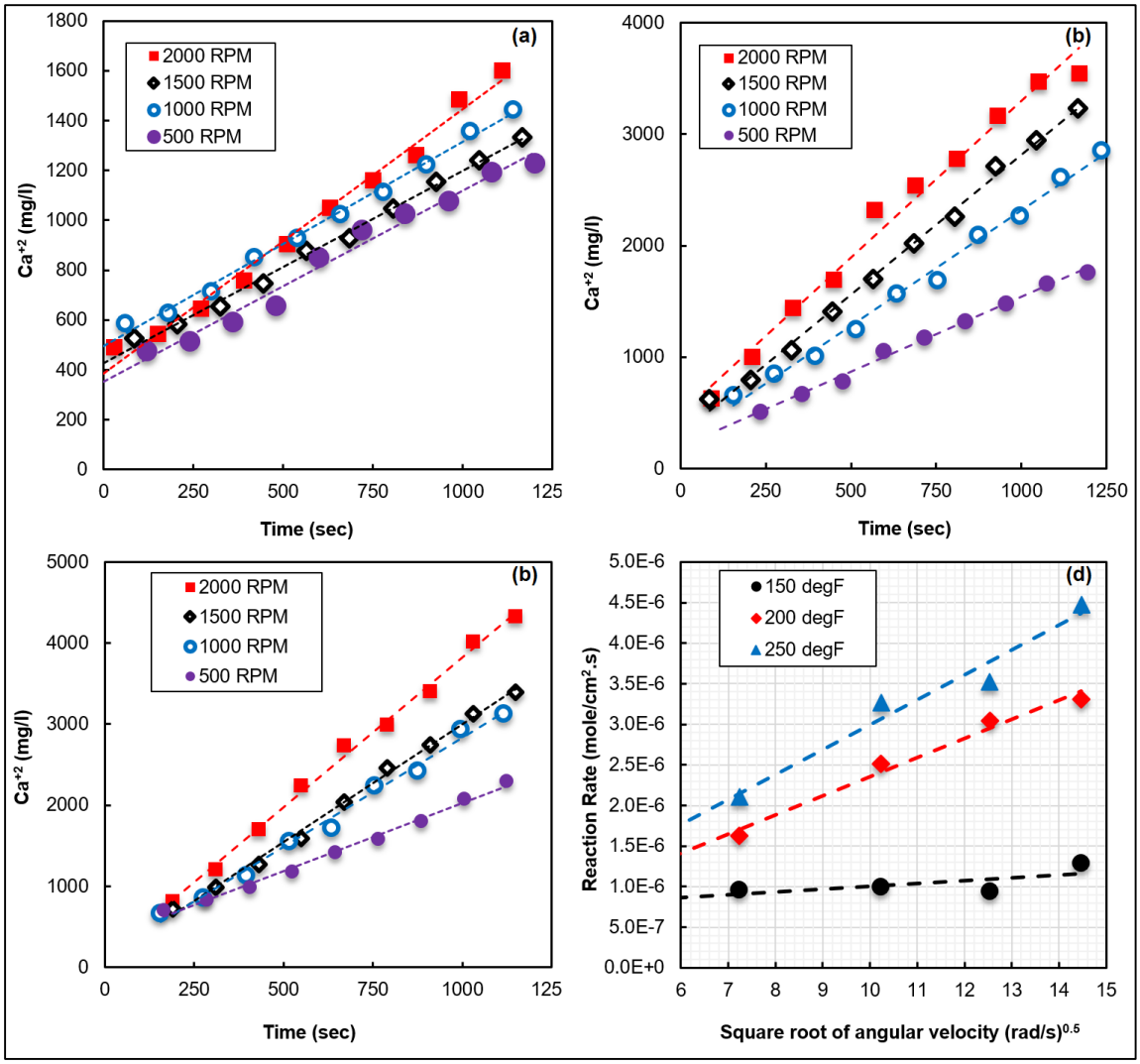

Figure 5. 8—Calcium concentration in the collected samples as a function of time and rotation speed using 20 wt% GLDA/SW solution at 150ºF (a), 200ºF (b), 250ºF (c), and rate of calcite dissolution by 20 wt% GLDA/SW at pH of 3.8 at corresponding temperatures (d).

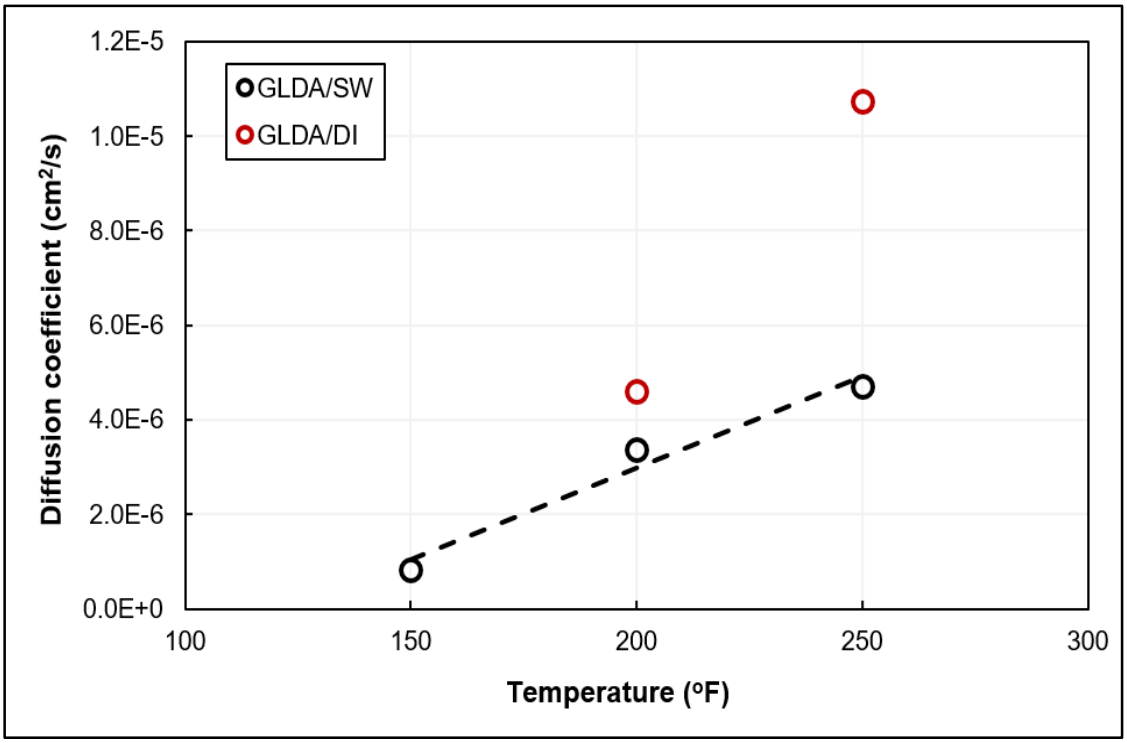

Figure 5. 9—Diffusion coefficient of 20 wt% GLDA/DI and GLDA/SW reaction with Indiana limestone as a function of temperature.

Comparing the rate of reaction of the two fluid systems with Indiana limestone at different RPM at 200°F **(Figure 5.10)**, it is clear that the two systems are almost same. The scanning electron microscopy (SEM) images for the samples cut from the rock surface (**Figure 5.11**) showed that the GLDA/DI only mainly reacted with fine grains in the rock surface while GLDA/SW reacted with both fine and coarse grains and made the reaction more uniform at the rock surface. Decreasing the acid diffusion will hinder the acid spending process and allows fresh acid to deeply penetrate the rock matrix more uniformly. Based on that, GLDA/SW system can stimulate cores in less injected acid volume at lower injection rate compared to GLDA/DI system.

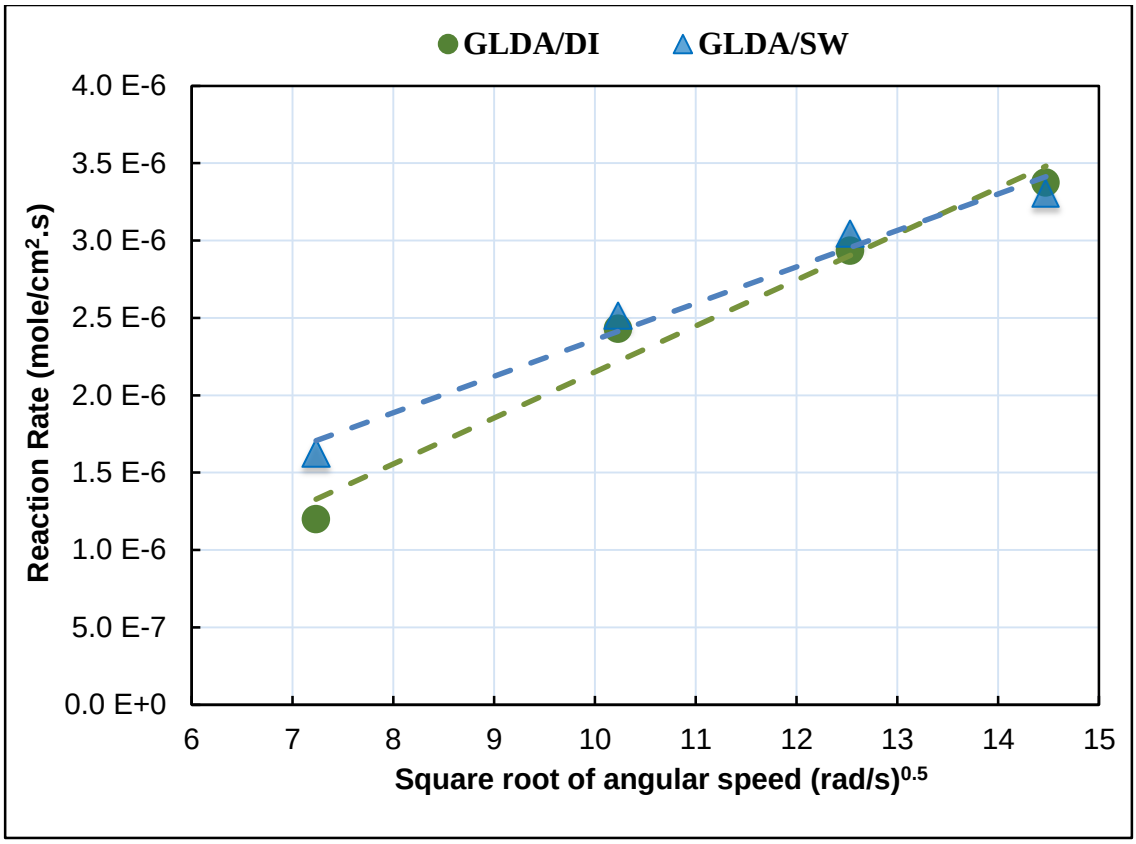

Figure 5. 10—Reaction Rate of 20 wt% GLDA/DI and GLDA/SW with Indiana limestone at 200°F (3.8 pH).

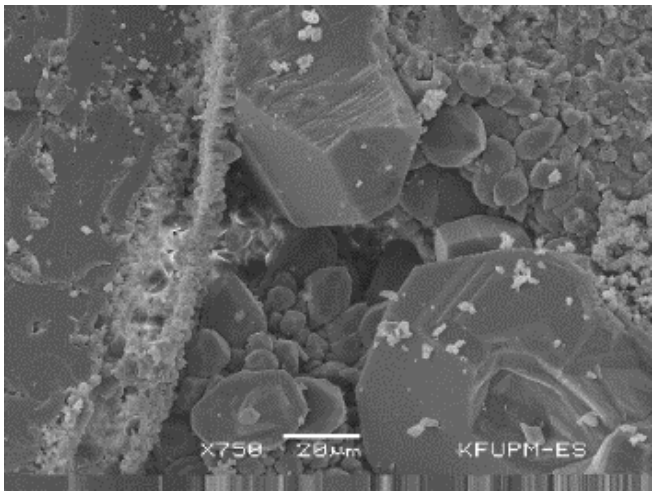

Before Reaction

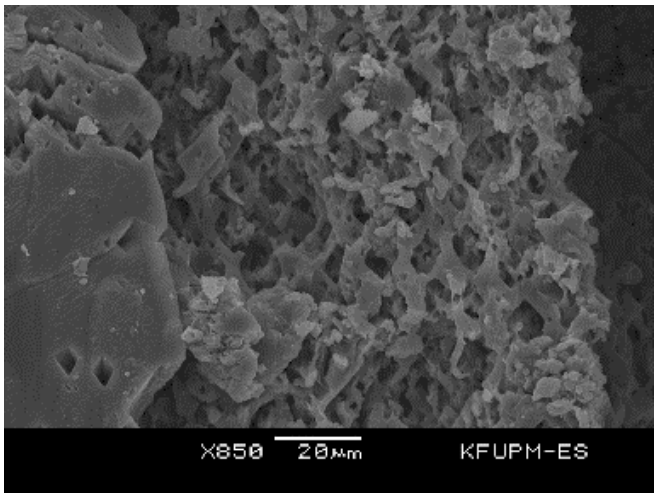

After Reaction with GLDA/DI

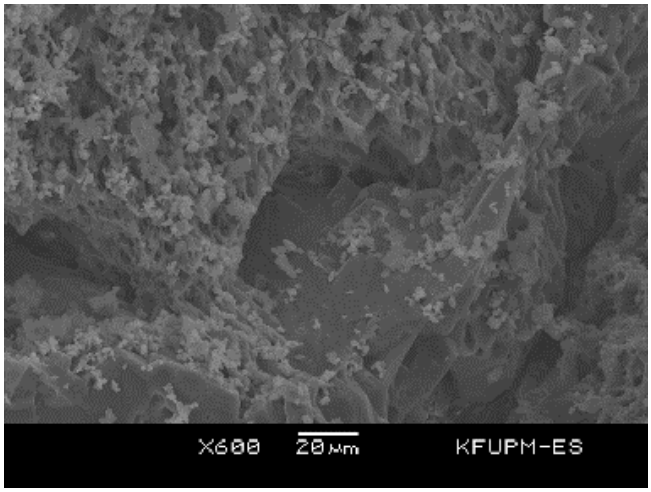

After Reaction with GLDA/SW

Figure 5. 11—SEM Surface Morphology of Indiana limestone rock surface before reaction and after reaction with GLDA/DI and GLDA/SW acid systems at 200ºF and 1000 RPM.

At 250^{o}F the GLDA/SW fluid system reaction with Indiana limestone is much less than in case of DLDA/DI system at the same temperature (**Figure 5.12**). Hubicki and Kołodyńska (2012) stated that the affinity of carboxylic groups for cations varies with Ionic size and charge of the cation. The affinity towards cation increases with increasing cation charge and increases with decreasing atomic size for different cations with same charge. This applies for GLDA because it has four carboxylic groups. Also Ivanov et al. (1996) proved that for carboxylic groups, the selectivity towards monovalent ions increases with temperature increase. This also applies for GLDA since it has four carboxylic groups in its structure. Based on that, the affinity of GLDA for Na^{+} will increase with temperature increase. Increasing the temperature from 200 to 250^{o}F the reaction rate of GLDA/SW is affected by the increased affinity of GLDA to Na^{+} compared to Ca^{2+} specially at higher concentration of Na^{+} in solution from seawater.

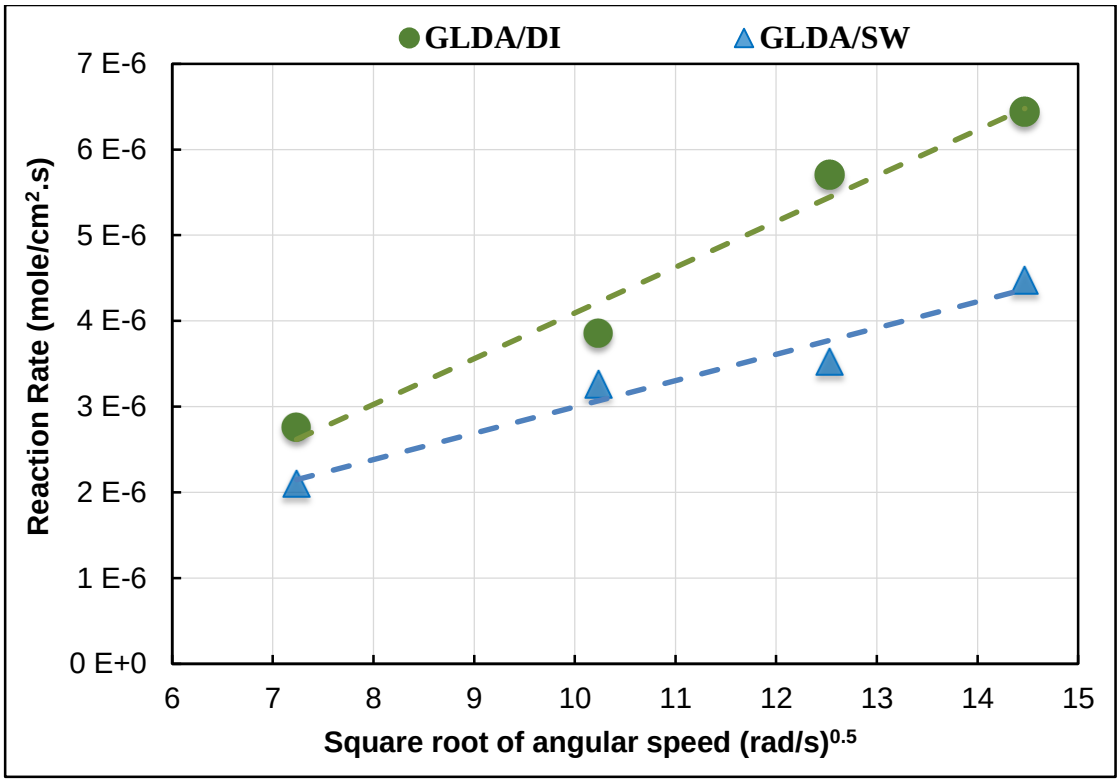

Figure 5. 12—Reaction Rate of 20 wt% GLDA/DI and GLDA/SW with Indiana limestone at 250°F (3.8 pH).

5.6.2 Austin Chalk

Four experiments were carried out using Austin chalk samples at 200°F in the same way described at similar conditions to Indiana limestone sample using GLDA/SW fluid system. The results are shown in **Figure 5.13**. From the behavior of the reaction rate versus square root of the disk angular speed, it is clear that the reaction regime is mass transfer limited with a reaction diffusion coefficient of 3.96x 10^{-5} cm^2/s. This diffusion coefficient value is an order of magnitude higher than the diffusion coefficient in the case of reaction with Indiana limestone at the same conditions.

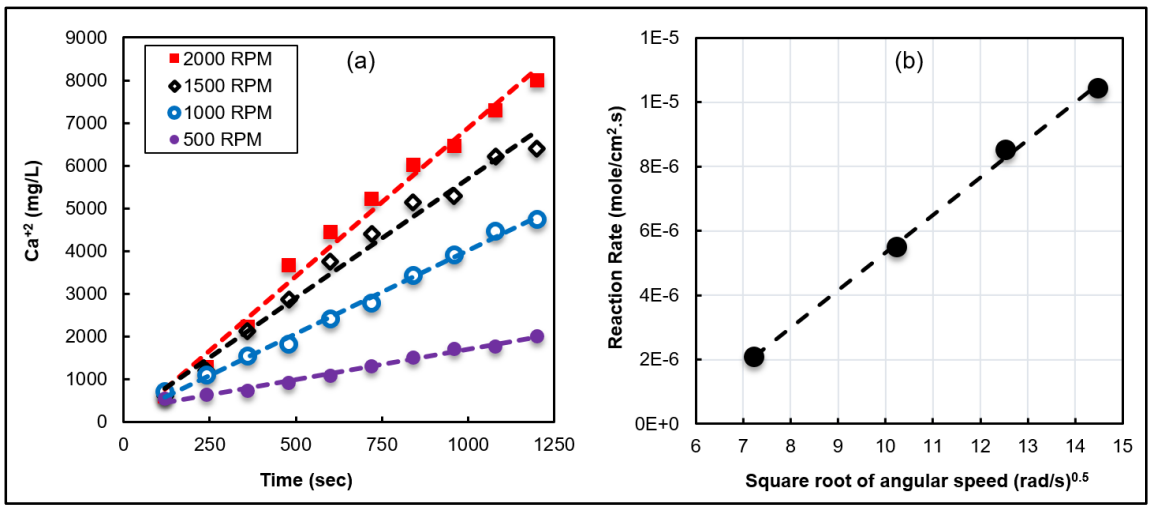

Figure 5. 13— (a) Calcium concentration in the collected samples as a function of time and rotation speed using 20 wt% GLDA/SW solution with Austin chalk disks at 200ºF, (b) Rate of calcite dissolution in 20 wt. % GLDA/seawater at pH of 3.8 at 1000 psi and 200ºF.

With the fact the both Indiana limestone and Austin chalk chemically composed of almost 100% calcium carbonate, therefore, the difference in reaction rates (**Figure 5.14**) can be attributed to the pore system geometry and to the bond between the rock grains as the unconfined compressive strength (UCS) of low permeability Indiana limestone is much higher compared to Austin chalk UCS.

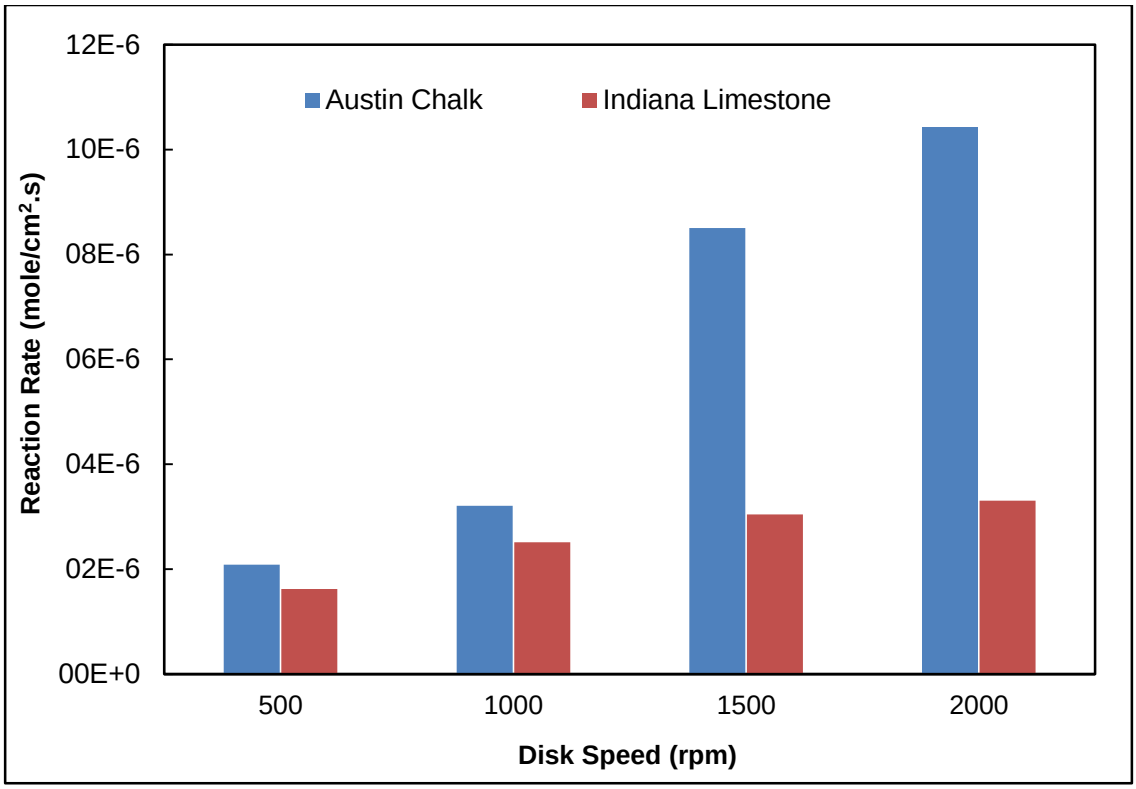

Figure 5. 14—Reaction rated of GLDA/SW with Austin chalk and Indiana limestone at 200ºF and 1000 psi.

Contrast resulted from different atomic number elements and their distribution is displayed by Scanning Electron Microscopy (SEM). The effect of acid system on the surface morphology of Austin chalk and Indiana limestone carbonate rocks used in this study is shown in **Figure 5.15**. Indiana limestone as a bioclastic coarse grained, cemented and mechanically compacted calcite rock is less reactive than the Austin chalk which is a microgranular fine grained calcite. Based on that, Austin chalk can be stimulated with low GLDA concentration, to avoid severe rock dissolution which may affect the rock integrity.

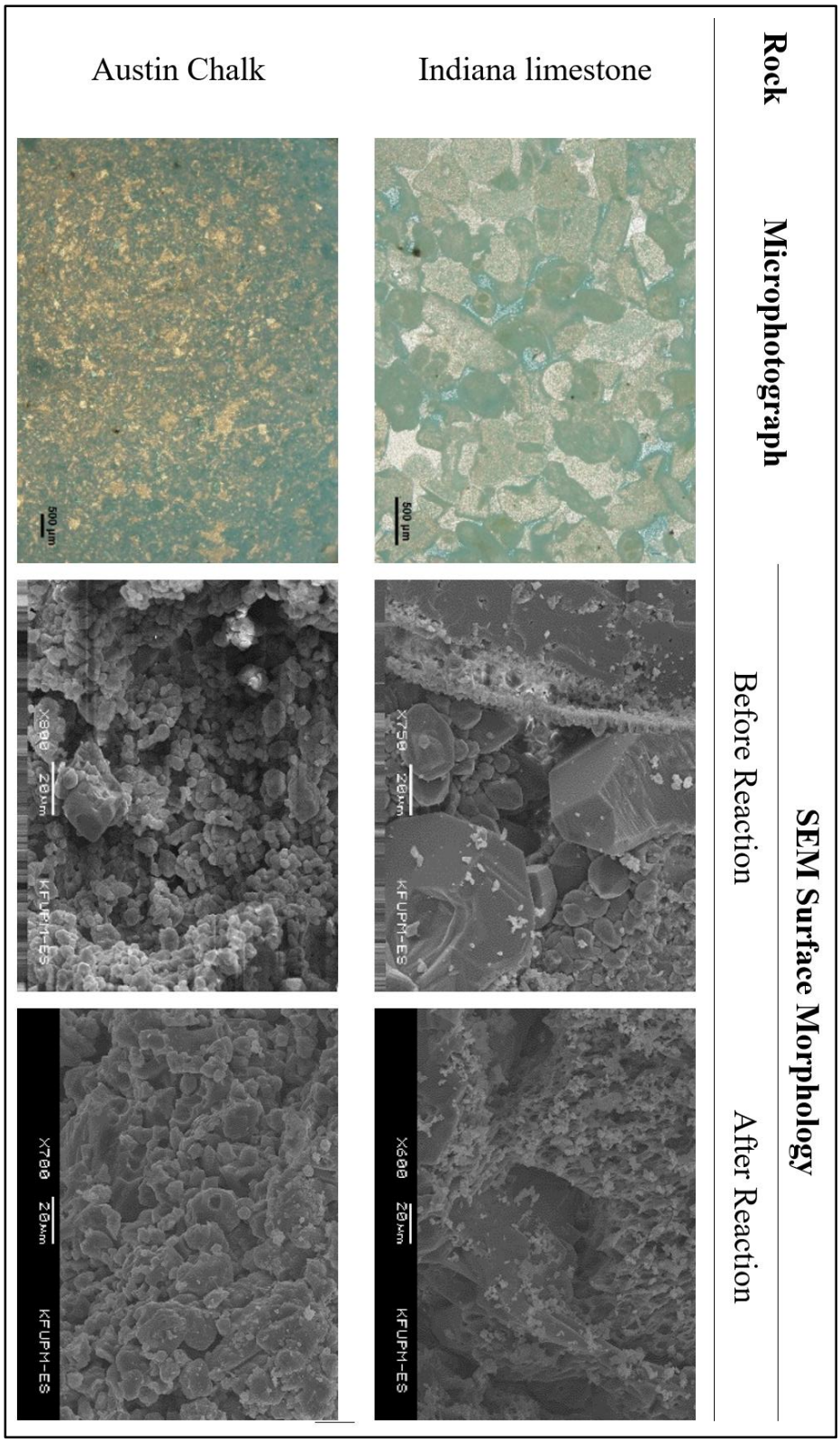

Figure 5. 15—SEM and Microphotograph for thin section of Indiana Limestone and Austin chalk before and after reaction with GLDA/SW system at 200°F and 1000 RPM.

5.6.3 Coreflooding Experiments

Four linear coreflooding experiments were performed to estimate the optimum injection rate using GLDA/SW system. A core sample of 1.5-inch diameter and 6-inch long Indiana limestone was used. Experimental parameters and flooding conditions are listed in **Table 5.3**. **Figure 5.16** shows the coreflooding set-up used to perform the acid treatment experiments in this study. Liquid permeability was measured using 3 wt% KCl (potassium chloride) solution at room temperature, then the system was heated up to 250^{o}F to allow temperature equilibration. The injection rate was then set to the desired rate (0.5, 1.0, 2.0 or 3.0 cm^3/min) with 3 wt% KCl solution. After steady state flow is achieved, the injected fluid is switched to GLDA/SW. The minimum pore volume required to create dominant wormhole in the core is the optimum injection rate. For each coreflooding experiment, the injected pore volume at the wormhole breakthrough (PV_{BT}) was reported corresponding to the pressure drop near zero (**Figures. 5.17** and **5.18**).

Table 5. 3— Properties of the Indiana limestone core samples used for coreflooding experiments and flooding conditions.

Experiment	L (cm)	D (cm)	ϕ (%)	K (mD)	Q (cm^3/min)	PV (cm^3)	T (^{o}F)	BP (psi)
1	15.09	38.1	8.30	0.51	0.5	14.30	120	1000
2	15.02	38.1	10.54	1.86	1.0	18.06	120	1000
3	15.03	38.1	9.55	0.75	2.0	16.37	120	1000
4	15.17	38.1	9.51	0.81	3.0	16.46	120	1000

(L) Length, (D) sample diameter, (ϕ) porosity, K permeability, (Q) Flow rate, (PV) pore volume, (T) Temperature, BP (back Pressure)

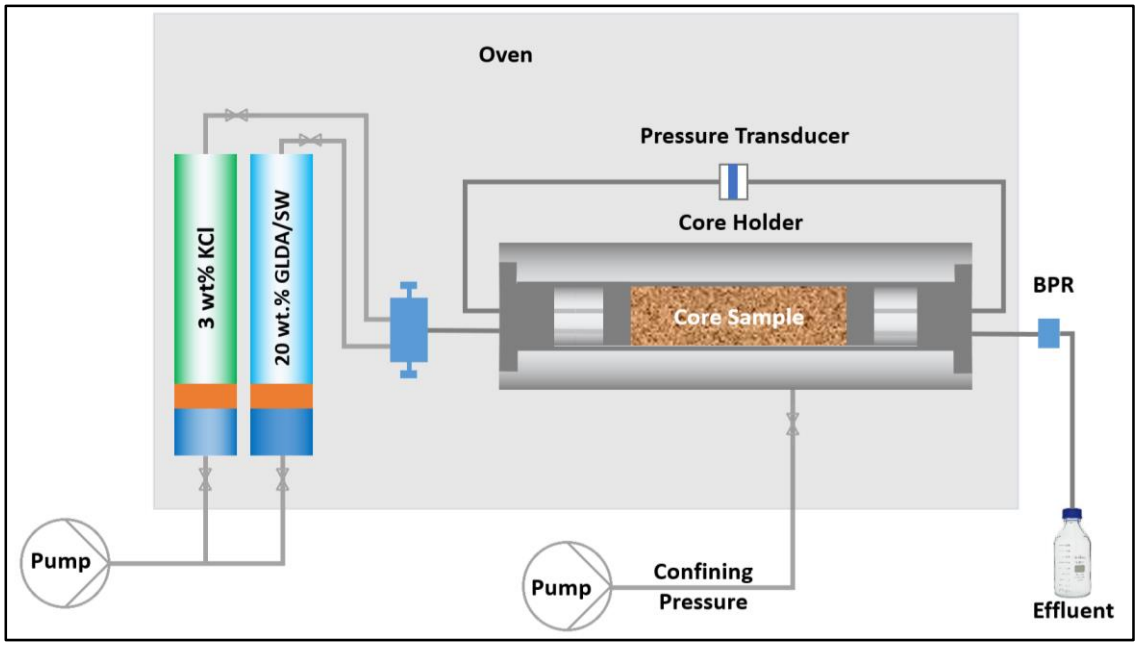

Figure 5. 16—Coreflooding system schematic

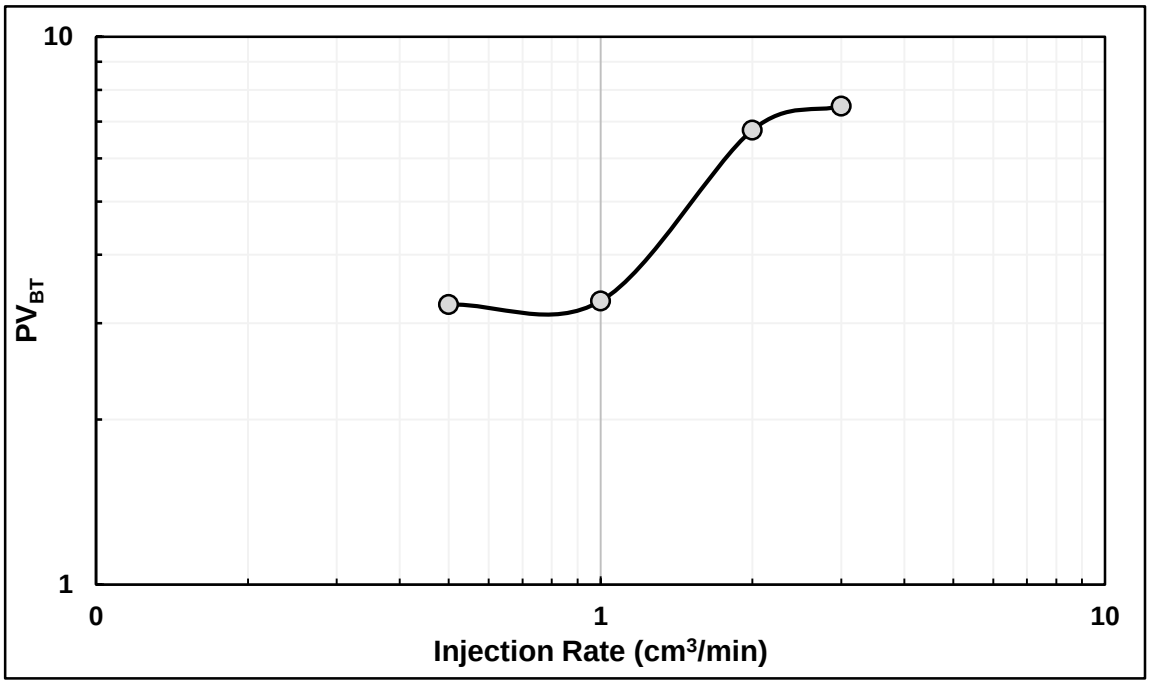

Figure 5. 17—Breakthrough curve of by 20 wt% GLDA/SW at pH of 3.8 in 6.0'' Indiana limestone core samples at 250°F.

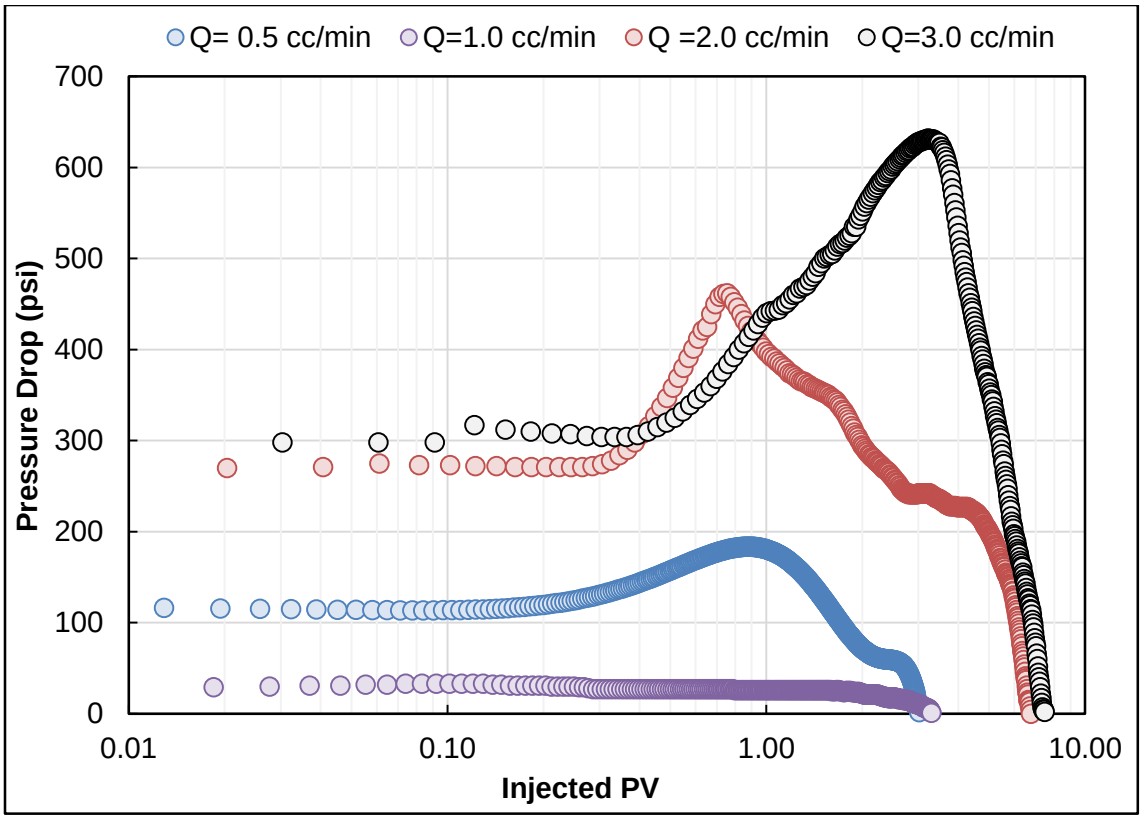

Figure 5. 18—Pressure drop variation during injection of 20 wt% GLDA/SW (pH=3.8) at 250ºF at different injection rates.

The wormholes were characterized using X-ray computed tomography (CT) scanner. CT-scans of the four samples were run at energy of 135kW/200mA with 1.0 mm resolution. **Figure 5.19** shows the wormhole path that confirmed the pressure drop results. It can be concluded from the CT scanned wormhole structures that the optimum injection rate is between 0.5 and 1.0 cm^3/min injection rates with thin, less ramified wormholes and minimum pore volumes (PVs) required to breakthrough. Dominant wormhole was created at 0.5 and 1.0 cm^3/min injection rates, the wormhole at 2.0 cm^3/min is wider than that at lower injection rate but higher acid volume is required to achieve breakthrough. At higher injection rates (3 and cm^3/min) more than one wormhole was initiated at the face of the rock but only one wormhole propagates with acid injection through the entire rock sample.

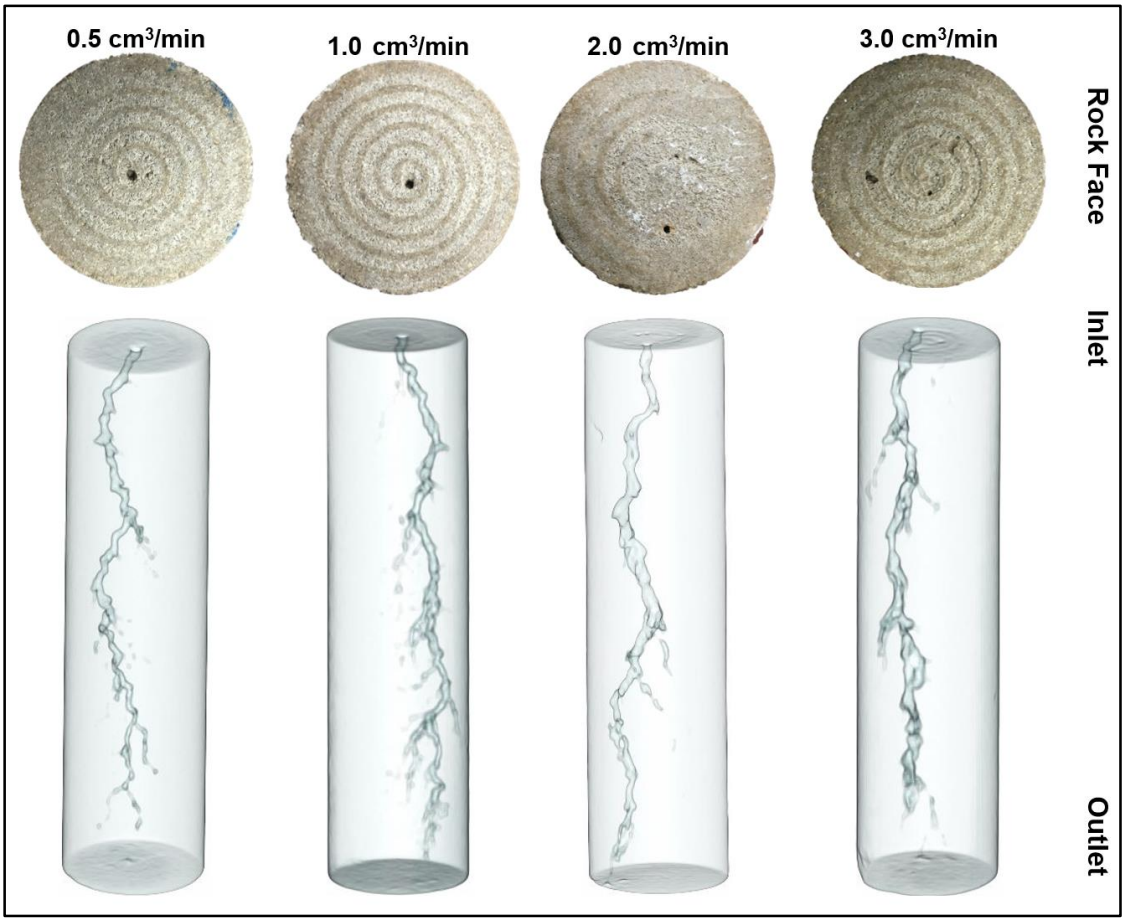

Figure 5. 19—Wormhole structure using CT scan for core samples stimulated using 20 wt% GLDA/SW at pH 3.8 at 250ºF.

As it become clear from Figure 5.19, unlike HCl, GLDA does not have a sharp optimum injection rate to be defined visually from the CT scans of the flooded core samples. A normalized pressure drop ratio (PDR) defined by **Equation 5.12** is used to accurately define the optimum injection rate. At the optimum injection rate, the minimum injected pore volume is used during the wormhole propagation to achieve the maximum value of pressure drop reduction from the maximum pressure drop encountered during the acid injection. PDR is defined as:

$$PDR_i = \frac{\Delta p_{max} - \Delta p_i}{\Delta p_{max}} \tag{5.12}$$

Where Δp_{max} is the maximum pressure drop for each injection rate, Δp is the pressure drop achieved at time t_i. For example, as shown in **Figure 5.20**, at injection rate of 0.5 cm^3/min about 2.0 PVs achieved 60% reduction of Δp_{max} where 3.0 PVs were required to achieve the same pressure drop reduction at 1.0 cm^3/min injection rate, 5.0 PVs at 2.0 cm^3/min and 6.0 PVs at 3.0 cm^3/min. Based on that, 0.5 cm^3/min can be selected as the optimum injection rate because of the earlier achieved PDR at minimum injected PVs compared to other injection rates.

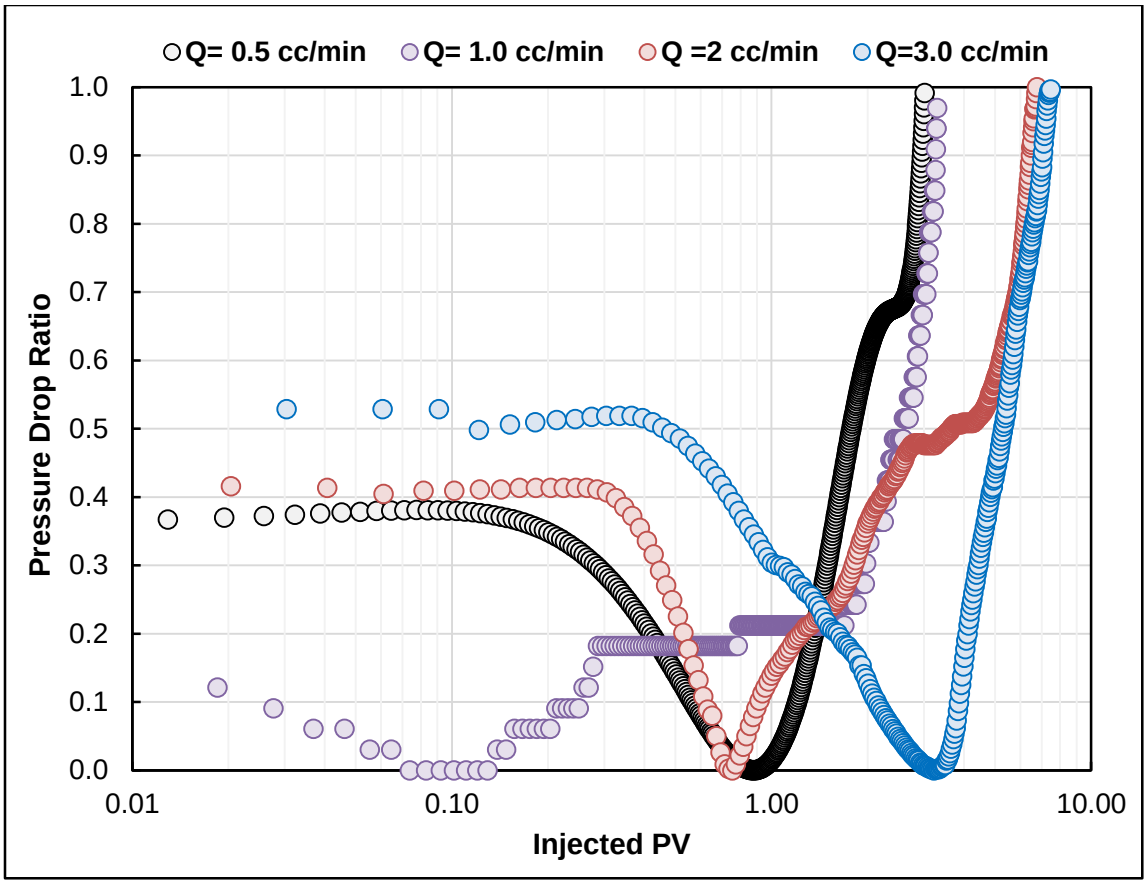

Figure 5. 20—Normalized pressure drop variation during injection of 20 wt% GLDA/SW (pH=3.8) at 250°F at different injection rates at pH 3.8 at 250°F.

For an effective stimulation treatment, the optimization process should include both factors, time and volume. In this study, new optimization tools were developed. Here, the normalized pore volume to breakthrough (NPV_{bt}) and the normalized time to breakthrough (NT_{bt}) were introduced. **Equations 5.13** and **5.14** are used to determine the two numbers.

$$NPV_{bt} = \frac{PV_{bt} - PV_{bt_{optimum}}}{PV_{bt_{max}} - PV_{bt_{optimum}}} \tag{5.13}$$

$$Nt_{bt} = \frac{t_{bt} - t_{bt_{min}}}{t_{bt_{max}} - t_{bt_{min}}} \tag{5.14}$$

Where PV_{bt} is the pore volume to breakthrough at each rate, $PV_{bt_{optimum}}$ is the minimum pore volume to breakthrough from **figure 5.20**, $PV_{bt_{max}}$ is the maximum pore volume required to breakthrough, t_{bt} is the time required to breakthrough at each injection rate, $t_{bt_{min}}$is the time required to breakthrough at the maximum injection rate, and $t_{bt_{max}}$ is the time required to breachthrough at the minimum injection rate.

Both NPV_{bt} and NT_{bt} have a range from zero to one. A value of zero indicates minimum volume and maximum time to breakthrough while a value of one indicates maximum volume and minimum time to breakthrough. The coreflooding results listed in **Table 5.4** were used to calculate both NPV_{bt} and NT_{bt} for each experiment. The point of intersection of NPV_{bt} and NT_{bt} in **Figure 5.21** represents the injection rate at which the wormhole can breakthrough the 15.24 cm (6-inch) Indiana limestone at the minimum injected volume and time simultaneously. The optimum injection rate, considering injected acid volume and injection time, is 1.1 cm^3/min compared to 0.5 cm^3/min when optimization is based only on the injected pore volume alone.

Table 5. 4— Coreflooding experiments results.

Q (cm^3/min)	Pore Volume at breakthrough	Time to breakthrough (min)	NPV_{bt}	NT_{bt}
0.5	3.25	92.8	0.00	1
1.0	3.30	59.5	0.011	0.357
2.0	6.80	55.3	0.831	0.276
3.0	7.50	41.0	1.000	0

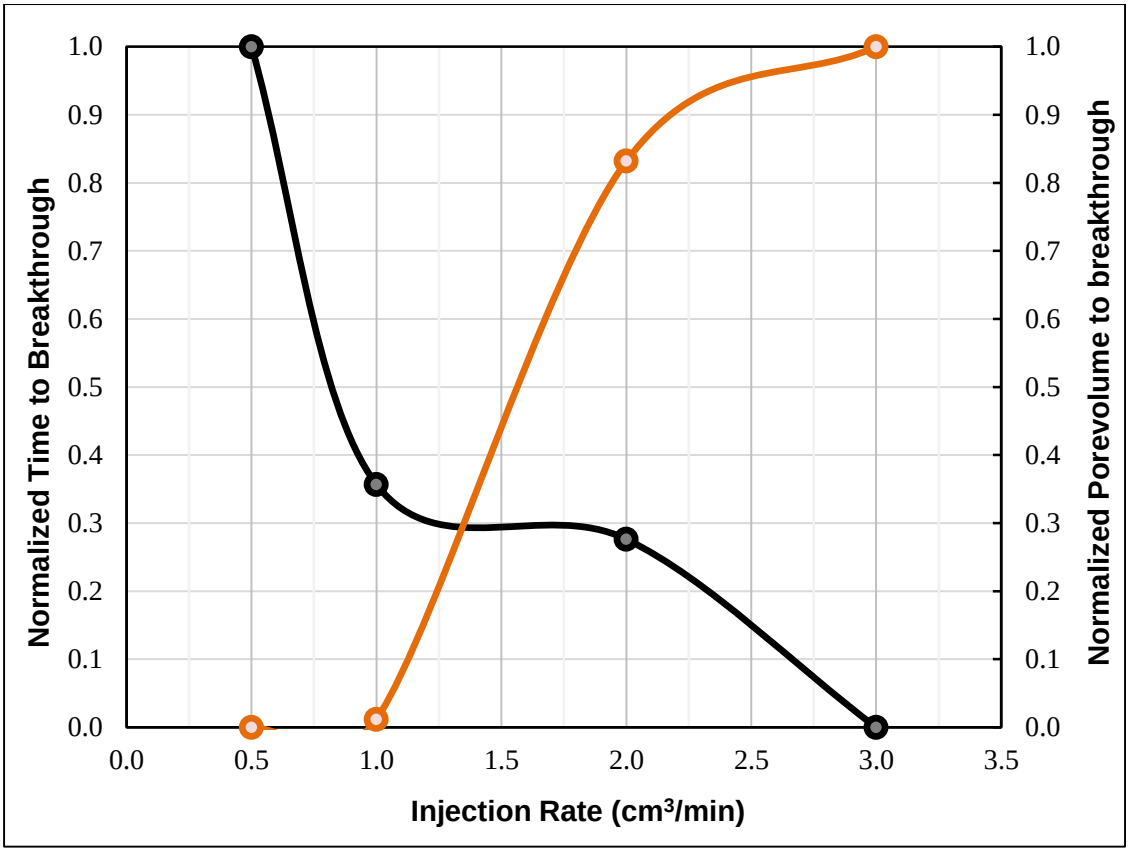

Figure 5. 21—Normalized pore volume and time to breakthrough during injection of 20 wt% GLDA/SW (pH=3.8) at 250ºF at different injection rates.

Using the model developed by Mahmoud and Nasr-El-Din (2014) to determine the linear optimum injection rate as a function of core length and diffusion coefficient as follows:

$$Q_{opt\_L} = 102\, h_f\, L_{core}\, D_e \tag{5.15}$$

Where h_f is the heterogeneity factor, which is defined as the ratio of wormhole length to core length. L_{core} is the core sample length, cm and D_e is the diffusion coefficient, cm^2/s. For a 6-inches core sample, and 4.71 $x10^{-6}$ cm^2/s diffusion coefficient, an optimum injection rate of 0.43 cm^3/min compared to 0.5 cm^3/min as reported from the coreflooding analysis. Based on that, the results of the rotating disk can be extrapolated to different temperature conditions and the optimum injection rate as a function of temperature and core length can be drawn (**Figure 5.22**). Figure 5.22 is a graphical representation for **Equation 5.15** for 1.5-inches dimeter Indiana limestone and 20 wt% GLDA/SW (pH 3.8) as a function of temperature. For example, if 20 wt% GLDA/SW is to be used to generate the optimum wormhole at 300°F through a 1.5-inches diameter 12-inches rock sample, an injection rate of 1.3 is to be used for that purpose.

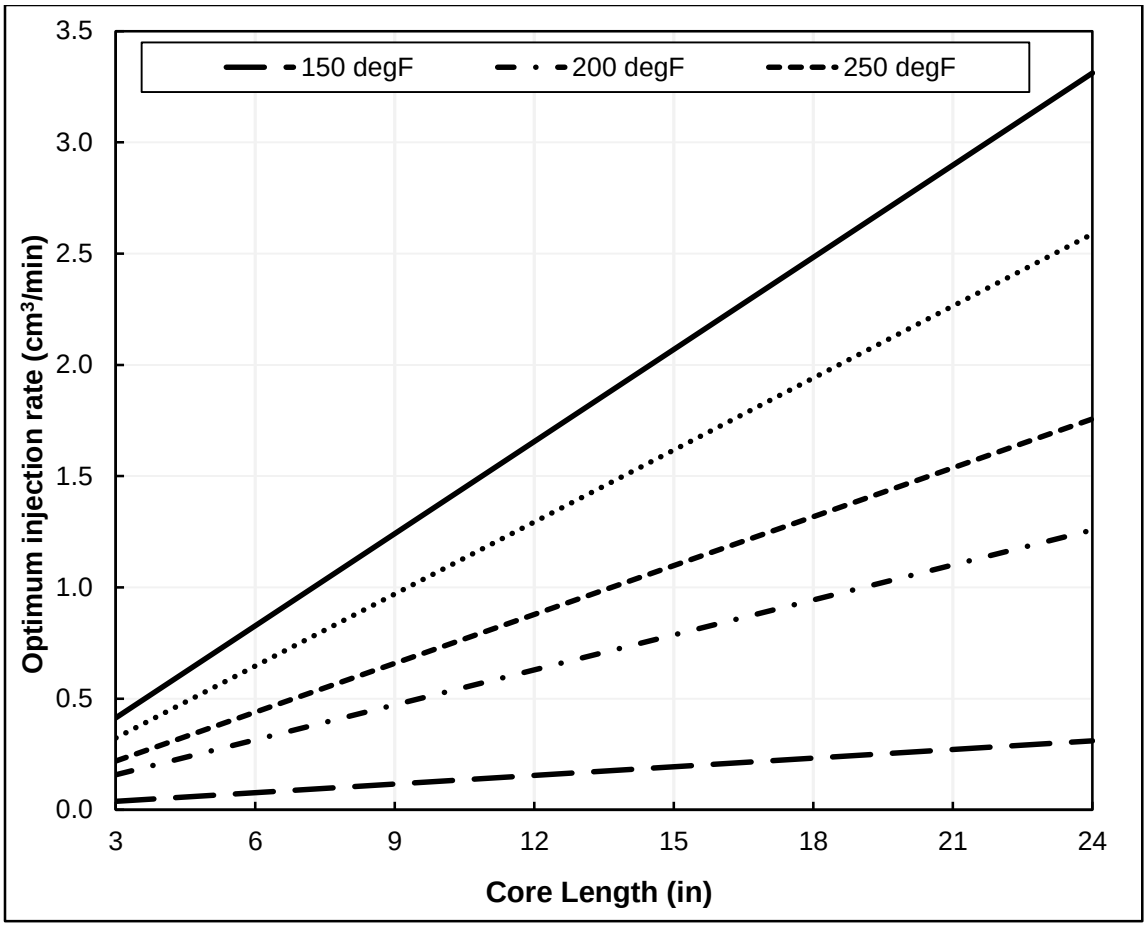

Figure 5. 22—Optimum injection rate of 20 wt% GLDA/SW at pH 3.8 as a function of temperature and core length.

5.7 Conclusions

After studying the reaction of Indiana limestone and Austin chalk with GLDA chelating agent diluted using seawater and fresh water, the reaction limiting process is defined for each system at reservoir conditions. The effect of porosity system was studied using Indiana limestone and Austin chalk which have almost has the same chemical composition of Indiana limestone but different porosity type resulted from the grain size distribution with in the rock matrix. The following conclusions can be drawn:

- The porosity type of the rock sample significantly affects the reaction rate with the same acid system even for the same chemical composition (Indiana limestone and Austin chalk as an example)
- The reaction between 3.8 pH 20% GLDA/DI and Indiana limestone is surface reaction limited at 150^{o}F and mass transfer limited at 200 and 250^{o}F, however the reaction of 20% GLDA/SW with the same rock is mass transfer limited at 150-250^{o}F.
- The overall reaction of GLDA/SW with Indiana limestone rock surface is inhibited with the presence of salt ions from seawater compared to GLDA/DI.
- Using pressure drop ratio enables an accurate determination of optimum injection rate of GLDA/SW which does not show a sharp optimum injection rate from the coreflooding results.
- The reaction between 3.8 pH 20% GLDA/SW and Austin chalk is surface reaction limited at 200^{o}F.
- 0.5 cm^{3}/min was estimated as an optimum injection rate for 20 wt. % SW/GLDA at 1000 psi and 250^{o}F from coreflooding experiments analysis compared to 0.43 cm^{3}/min using a mathematical model.

CHAPTER 6

DTPA Chelating Agents: Reaction Kinetics and Coreflooding Study

The use of hydrochloric acid (HCl) in gas well stimulation of high temperature reservoirs is currently facing different challenges. These challenges include rapid corrosion of the well tubulars, face dissolution, very high and uncontrolled reaction rate, and formation damage in high clay content and iron-rich reservoirs. In this study, water-soluble diethylene triamine penta acetic acid (DTPA) chelating agent is introduced as alternative to eliminate the risk associated with HCl at high temperatures. In addition, the potential of using seawater to replace fresh water in the stimulation process is explored to save the cost of fresh water transportation to deep offshore oil and gas wells. The effect of seawater on the reaction kinetics of DTPA with carbonate rocks under high pressure and high temperature conditions is investigated using the rotating disk apparatus. The reactions of DTPA solution diluted with fresh water (DTPA/DI) and seawater (DTPA/SW) with carbonate rocks were carried out at the same conditions. In the case of fresh water, the reaction is controlled by the surface reaction regime. Adding HCl to adjust DTPA pH did not turn the reaction into a mass transfer controlled reaction like the case of using HCl alone. The heavy matrix of seawater increased the resistance of ions diffusion, which resulted in a low reaction rate and transformed the reaction into a mass transfer limited regime.

Corrosion tests were carried out on production and coiled tubing coupons obtained from the gas wells and the results of the new DTPA/SW formulation is compared to the standard HCl formulation. DTPA showed very low corrosion rate of 0.0034 g/cm^2 without adding corrosion inhibitors compared to 0.205 g/cm^2 of 15 wt% HCl with 3% corrosion inhibitors while the industry limit is 0.0244 g/cm^2 in 6 hours. The reaction regime of DTPA chelating agent with calcite is identified to be mass transfer limited in seawater and surface reaction limited in fresh water. The rate expression for the dissolution of Ca^{2+} in DTPA/SW solution is obtained. Coreflooding experiments were performed to determine the optimum injection rate using low permeability Indiana limestone core samples. The optimum injection rate required to stimulate a very deep carbonate gas well was found to be 1.4 bbl/min after scaling up the coreflooding results to field scale. The application of the new DTPA/SW formulation in treating deep gas wells is expected to save the cost of fresh water and eliminate the cost of corrosion inhibitors.

6.1 Introduction

In matrix acidizing, the main target is to recover and enhance the permeability of the near-wellbore area by creating high conductivity channels (called wormholes) from the dissolution of carbonate rock matrix. Wormholes enable the hydrocarbon to flow from the oil reservoir to the wellbore. Wormhole penetration is of interest rather than the wormhole size, because the deeper the acid can go the higher the permeability improvement. At low injection rates, fluid loss to the face of the created wormholes will increase and more face dissolution is expected due to the fast reaction of HCl with carbonate rocks. Face dissolution, asphaltene sludge formation, the need for using costly additives to prevent sludge precipitation are some of the common problems in the stimulation of carbonate

formations using HCl. Different HCl alternatives were introduced for well stimulation purposes to avoid or minimize face dissolution problems especially in shallow and depleted formations. Fredd and Fogler (1998a and 1998b) and Fredd (1998) studied the reaction of different chelating agents with carbonate rock samples and evaluated their ability to create wormholes. They performed linear coreflooding experiments using 4.3 pH 0.25M DTPA chelating agent, and 4 and 13 pH 0.25M Ethylenediaminetetraacetic acid (EDTA). Wang et al. (2009) tested nonaggressive fluid, with a very low corrosion rate compared to HCl, for the stimulation of carbonate reservoirs. They proved that both high and low permeability core could be stimulated by nonaggressive fluid without adding diverting agents.

Frenier et al. (2001) tested 2.5, 4, and 9 pH solutions of HEDTA at 300^{o}F and reported that the pH 4 sodium HEDTA was more effective than the pH 12 in terms of the required volumes to breakthrough. LePage et al. (2009) examined a readily biodegradable poly acidic chelate L-glutamic acid, N, N-diacetic acid (GLDA) as a stand-alone stimulation fluid. They compared GLDA with other chelating agents, including EDTA, HEDTA, NTA and EDG. GLDA was very effective for carbonate rock stimulation compared to other chelating agents and organic acids and it has a thermal stability of the same order as HEDTA. However, using seawater as a base for stimulation fluid in stimulation operations was not fully studied in terms of its effect on the reaction kinetics. Rabie et al. (2014) used seawater to dilute lactic acid and they concluded that the presence of salts (from seawater) reduced the rate of dissolution by lactic acid. Recently, Barri (2015) performed coreflooding experiments using different seawater-diluted chelating agents and proved that the solutions were able to generate wormholes through Indiana limestone core samples.

Among the techniques used to evaluate stimulation fluid efficiencies for matrix acidizing is the rotating disk apparatus (RDA). RDA is used mainly to study the reaction kinetics of stimulation fluids with the reservoir rocks. The rotating disk was first introduced in 1972 (Boomer, 1972) and used to determine the reaction rate, the order of the reaction, and the diffusion coefficient associated with the minerals dissolution (Fredd and Fogler, 1998a; Wang et al., 2009; Lund et al., 1973). Studying the reaction kinetics of stimulation fluids can minimize the required coreflooding experiments needed to capture the optimum parameters for a stimulation treatment. With the fact that the optimum injection rate to bypass a formation damage of a certain depth changes with the damage depth. Several coreflooding experiments are needed to locate the optimum injection rate for each damage depth. Knowing the nature and limitations of the reaction between the stimulation fluid and a certain rock will facilitate the treatment design for any formation penetration radius. For example, the optimum Damköhler number and injection rate can be reported as a function of the diffusion coefficient of the mass transfer limited reaction.

The previous work that addressed the use of chelating agents as stimulating fluid was limited to room temperature. Currently, no work has been done to study the reaction kinetics of DTPA with carbonate rocks at high pressure and temperature typical of reservoir conditions. In addition, the potential of using seawater to replace fresh water in the stimulation process is explored to save the cost of fresh water transportation to deep offshore gas wells. Therefore, the reaction kinetics of DTPA chelating agent diluted with seawater and deionized water with carbonate samples are studied in rotating disk apparatus at elevated pressure and temperature. The reaction regime is determined and the diffusion coefficient of DTPA; along with the optimum injection rate required to treat deep gas wells

are identified for scale up purposes. The corrosion rate of DTPA/SW formulation at high pressure and high temperature (HPHT) conditions is measured using field samples of tubing coupons. Finally, the effectiveness of stimulations using DTPA and HCl formulations are compared.

6.2 Pentetic or Diethylenetriaminepentaacetic Acid (DTPA)

DTPA is one of the Aminopolycarboxylic acids, which are able to form stable complexes with alkali earth metals (Ca, Mg, etc.). DTPA is considered one of the strongest chelating agents due to the presence of 5 carboxylic groups and three nitrogen atoms, **Figure 6.1.** The higher the equilibrium constant for the metal/ligand complex, the higher its stability. DTPA forms stable calcium and magnesium complexes with equilibrium constant of 10.34 and 9.3, respectively (Anderegg et al 2009).

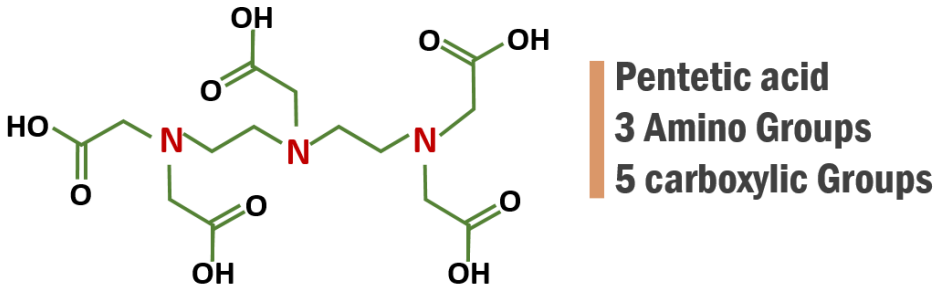

Figure 6. 1—DTPA chemical structure.

DTAP undergoes a stepwise loss of protons until it reaches the fully ionized state. DTPA dissociation reactions are as follows:

$$H_5Y \rightleftharpoons H_4Y^{-1} + H^+ \quad (6.1)$$

$$H_4Y^{-1} \rightleftharpoons H_3Y^{-2} + H^+ \quad (6.2)$$

$$H_3Y^{-2} \rightleftharpoons H_2Y^{-3} + H^+ \quad (6.3)$$

$$H_2Y^{-3} \rightleftharpoons HY^{-4} + H^+ \quad (6.4)$$

$$HY^{-4} \rightleftharpoons Y^{-5} + H^+ \quad (6.5)$$

where H_mY^{m-n} represents the chelating agent molecule, n is the number of carboxylic groups and m is the number of acidic protons. The ion species distribution for GLDA is shown in **Figure 6.2**.

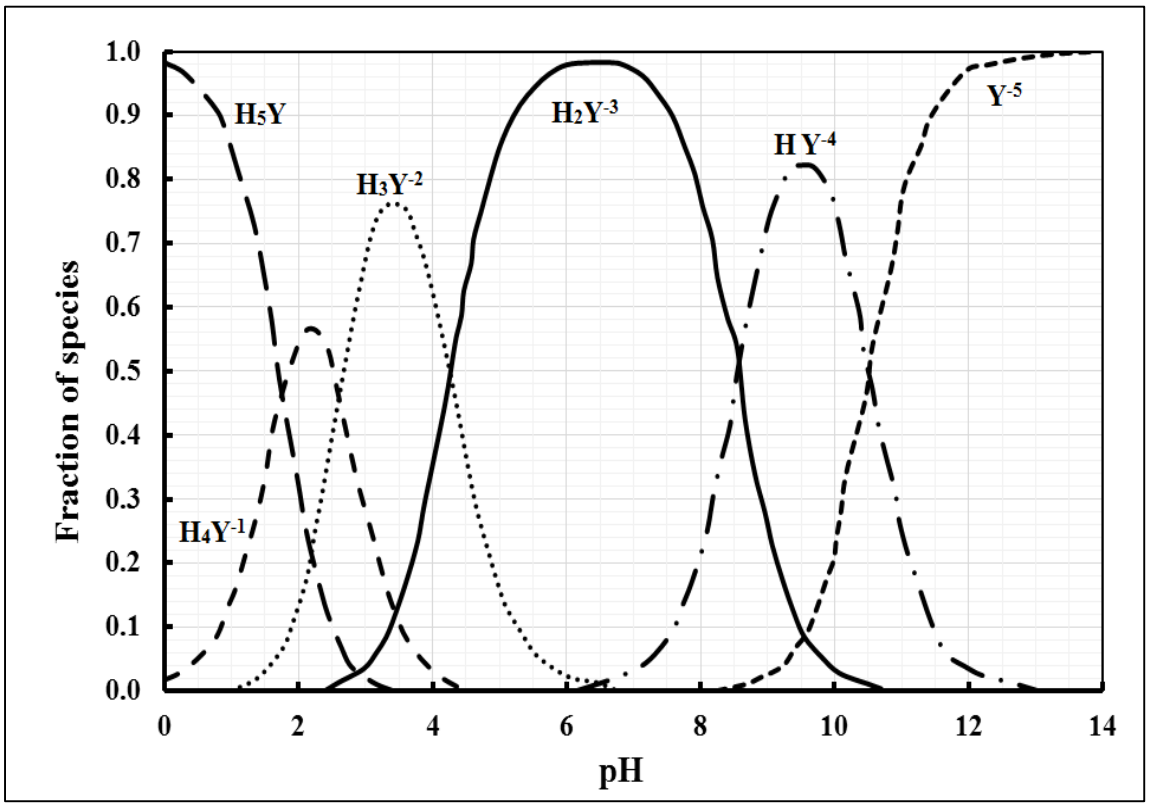

Figure 6. 2—DTPA ionic species distribution as a function of pH.

At a pH of 4.5, DTPA consists of two species H_3Y^{-2} and H_2Y^{-3} at 40% and 60%, respectively. In this pH range, the DTPA reaction rate with calcite is much higher compared to the high pH one because of the presence of protons (hydrogen ions). Fredd and Fogler (1998) and Fredd (1998) reported that DTPA (at pH 4.3) and EDTA (at pH 13 and 4) have an optimum Damköhler number at which the number of pore volumes to break through the core is the minimum. They studied the effect of NaCl on the dissolution of calcite in the presence of EDTA. They observed that the rate of dissolution decreased as the NaCl concentration was increased from zero (deionized water) to 0.7M.

6.3 Experimental work

6.3.1 Rotating Disk Experiments

The dissolution rate of carbonate rock using DTPA is estimated using two sets of experiments in the rotating disk apparatus. In the first set, DTPA diluted from stock concentration of 40 wt% to 15 wt% using deionized water (DI) was used. In the second set of experiments, DTPA was diluted to the same concentration using synthetic seawater (SW) with the composition listed in **Table 6.1**. In both sets, HCl was used to adjust the pH of the solution to 4.5. The final composition of both fluids is listed in **Table 6.2**. Four experiments were carried out using each fluid system at constant pressure and temperature and at different disk speeds (500, 1000, 1500, and 2000 rpm). Every two minutes, samples were collected during

Table 6. 1—Synthetic seawater composition

Ions	Concentration (mg/l)
Sodium	18,300
Calcium	650
Magnesium	2,110
Sulfate	4,290
Chloride	32,200
Carbonate	0
Bicarbonate	120
TDS	57,670

Table 6. 2—Composition of the two fluid systems used in this study

Fluid System	DTPA 40 wt% (g/L)	Water (g)	HCL 37 wt% (g/L)	Viscosity (cp)	Density (g/cm^3)
DTPA/DI	357.14	588.36	54.50	0.865	1.052
DTPA/SW	357.14	598.54	44.31	0.005	1.107

The experiment and the reaction was stopped after collecting 10 samples of 3 ml each. After doing the required, inductively coupled plasma optical emission spectrometer Optima 8000 (ICP-OES) was used to determine calcium concentration in each sample. The experimental details are listed in **Table 6.3**; all experiments were conducted at 250^o and 1000 psi.

Table 6. 3—RDA Experimental parameters using DTPA and Indiana limestone samples at 250°F and 1000 psi.

Experiment No.	Disk Porosity (%)	Fluid	Disk Angular velocity (RPM)
1	17.6	DTPA/DI	500
2	16.7		1000
3	17.3		1500
4	17.5		2000
5	17.4	DTPA/SW	500
6	14.2		1000
7	18.2		1500
8	17.0		2000

One-foot Indiana limestone core sample was cut into small disks of 2 cm (0.8-inch) length and 3.81 cm (1.5-inch) diameter. Disk surfaces were prepared for reaction kinetic experiments using end face grinding, polishing, and sonic cleaning. This surface preparation was done to correctly estimate the surface area at which the reaction will take place. The porosity of each sample was calculated using dry and saturated weights and the cores were saturated with a fresh water of 1 g/cm^3 density.

6.3.2 Corrosion Test

In addition to reaction kinetics experiments, corrosion tests were conducted on actual coiled tubing coupons made of L-80 alloy placed in autoclave coated with hastelloy (acid resistant material) for 6 hours at 250^{o}F. The pressure was set to be 68 atm during the test; nitrogen was used to apply 54.4 atm while the remaining pressure was equally increased by CO_2, and H_2S. The corrosion rate was calculated by estimating the weight loss divided by the coupon surface area in the units of gm/cm^2. The industry standard for the corrosion rate is that it should not exceed 2.44×10^{-5} g/cm^2 (0.05 lb$_m$/ft^2) (Al-Mutairi et al., 2005 and Kalfayan at al., 2008). If the corrosion rate exceeds this value in 6 hours at the required temperature, the fluid cannot be used in the field operations.

6.3.3 Coreflooding

The aim of matrix acidizing treatment is to enhance the near-wellbore permeability. The injection rate of the acid at the surface is one of the key parameters that controls how deep a wormhole can penetrate. If the zone surrounding the wellbore has severe permeability reduction, a certain injection rate should be used to generate wormholes that can bypass the damaged zone. Four linear coreflooding experiments were performed to estimate the optimum flow rate using DTPA/SW system. A core sample of 1.5-inch diameter and 6-inch long Indiana limestone was used. Experimental parameters and flooding conditions

are listed in **Table 6.4**. The same coreflooding set-up described earlier in section (4.6.3) was used to perform the acid treatment experiments.

Table 6. 4—Properties of the core samples used for coreflooding experiments and flooding conditions at 250°F and 1000 psi.

Experiment	L (in)	D (in)	ϕ (%)	K (mD)	Q (cm^3/min)	PV (cm^3)	T (°F)	BP (psi)
1	6.0	1.5	9.60	0.79	4	16.5	250	1000
2	6.0	1.5	10.22	0.65	2	17.72	250	1000
3	6.0	1.5	9.75	0.64	0.5	16.8	250	1000
4	6.0	1.5	9.09	0.70	0.25	15.7	250	1000

(L) sample Length, (D) sample diameter, (ϕ) porosity, K permeability, (Q) Flow rate, (PV) pore volume, (T) Temperature BP (back Pressure)

6.4 Results and Discussion

6.4.1 Rotating Disk Experiments

Typical calcium concentration obtained from the ICP-OES analysis of the collected samples is shown in **Figure 6.3** for the first experimental set in which DTPA/DI system was used. For disk speeds above 1000 rpm, the slope of the straight lines remained constant regardless of the disk angular velocity, i.e. no mass transfer limitations for this reaction. Calcium concentration obtained from ICP-OES analysis of the collected samples is shown in **Figure 6.4** for the second set of experiments in which DTPA/SW fluid system was used. The slope of the straight lines increases as the disk angular velocity increases.

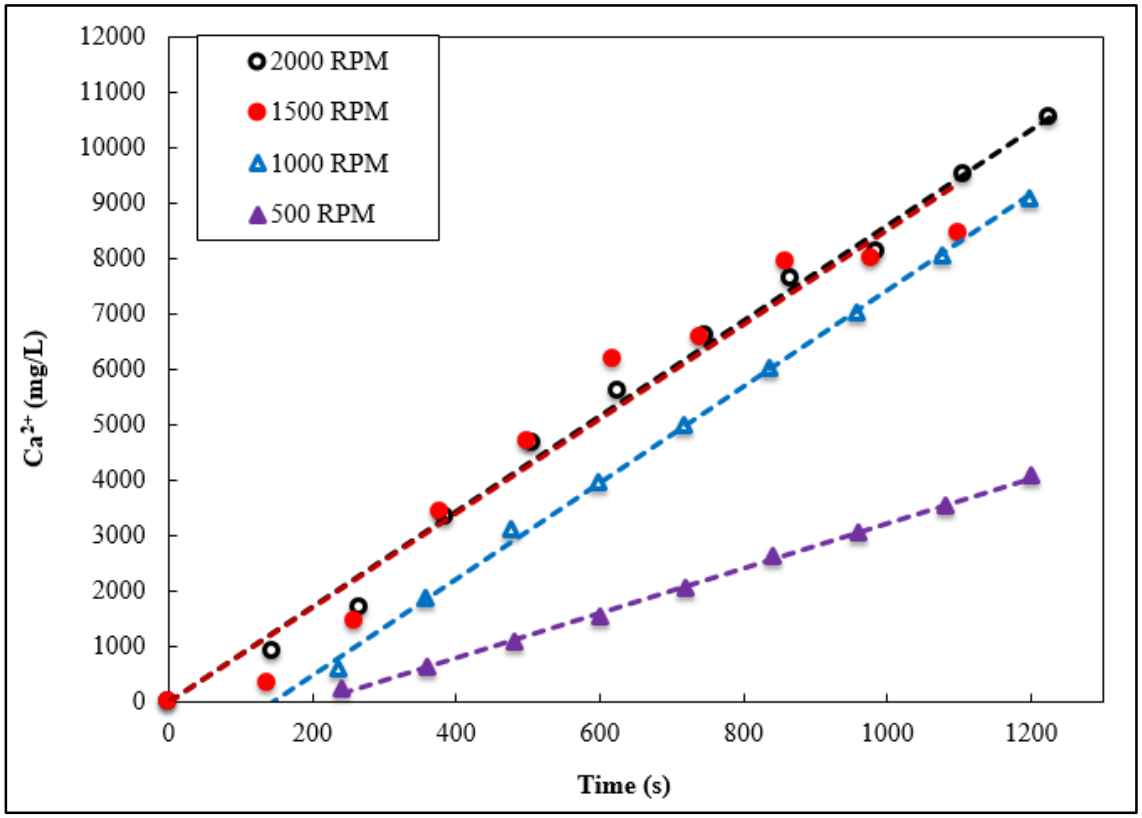

Figure 6. 3—Calcium concentration in the collected samples as a function of time and angular velocity using 15 wt% DTPA/DI water solution and Indiana limestone samples at 1000 psi and 250ºF .

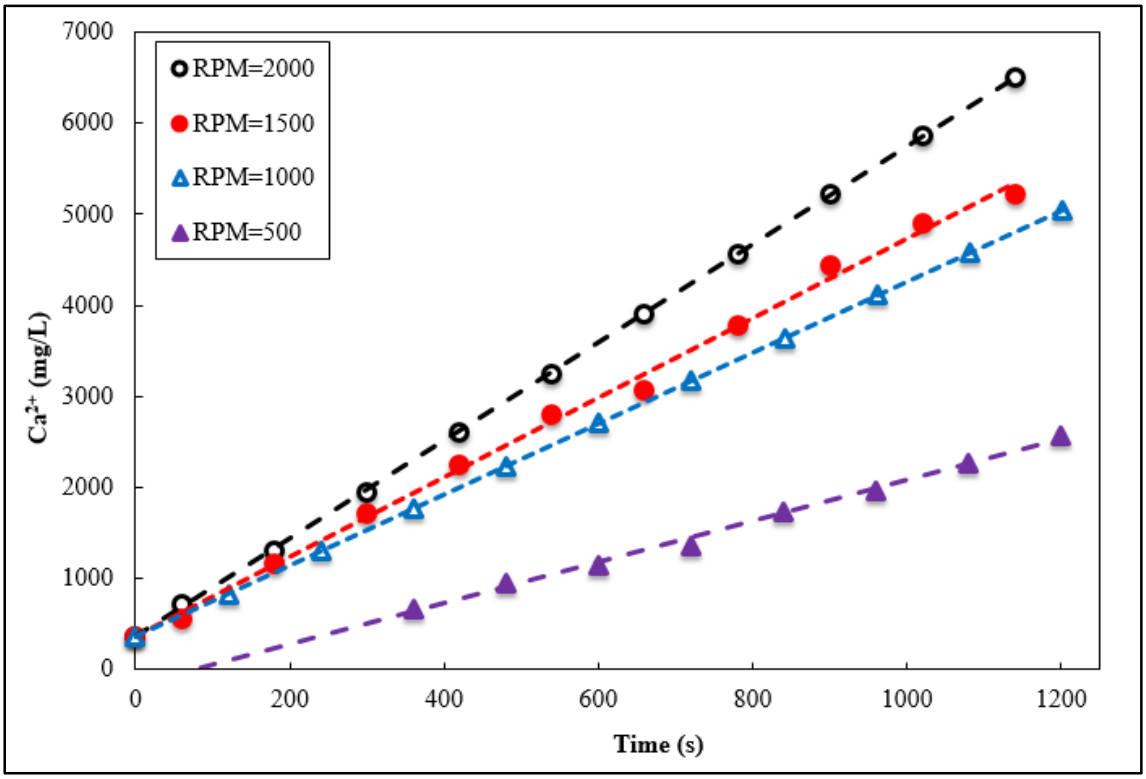

Figure 6. 4—Calcium concentration in the collected samples as a function of time and angular velocity using 15 wt% DTPA/SW water solution and Indiana limestone samples at 1000 psi and 250ºF.

When dissolution rates are extracted and plotted versus the square root of disk angular velocity, as shown in **Figure 6.5,** a surface reaction limited dissolution is obtained above 1000 rpm for the 15 wt% DTPA/DI water Solution at 1000 psi and 250ºF. This behavior is attributed to the slow reaction of the DTPA in comparison with HCl formulation and the low mass transfer resistance.

For 15 wt% DTPA/SW system at 1000 psi and 250ºF, the rates of dissolution were estimated and data in the mass transfer controlled regime is plotted versus the square root of disk angular velocity. Equation 5.7 is used to obtain the diffusion coefficient as 9.41 x 10^{-5} cm^2/s. The heavy matrix of seawater restricts the diffusion of DTPA to the rock surface, which explains why the reaction has changed from surface reaction limited for

DTPA/DI fluid system to mass transfer limited for DTPA/SW fluid system. If the same concentrations of DTPA are used, then changing the base of dilution from deionized water to seawater changed the reaction regime from surface reaction to mass transfer. This indicates the advantageous of kinetic study in accurately determining the reaction regime type that highly influences the whole design of the stimulation treatment.

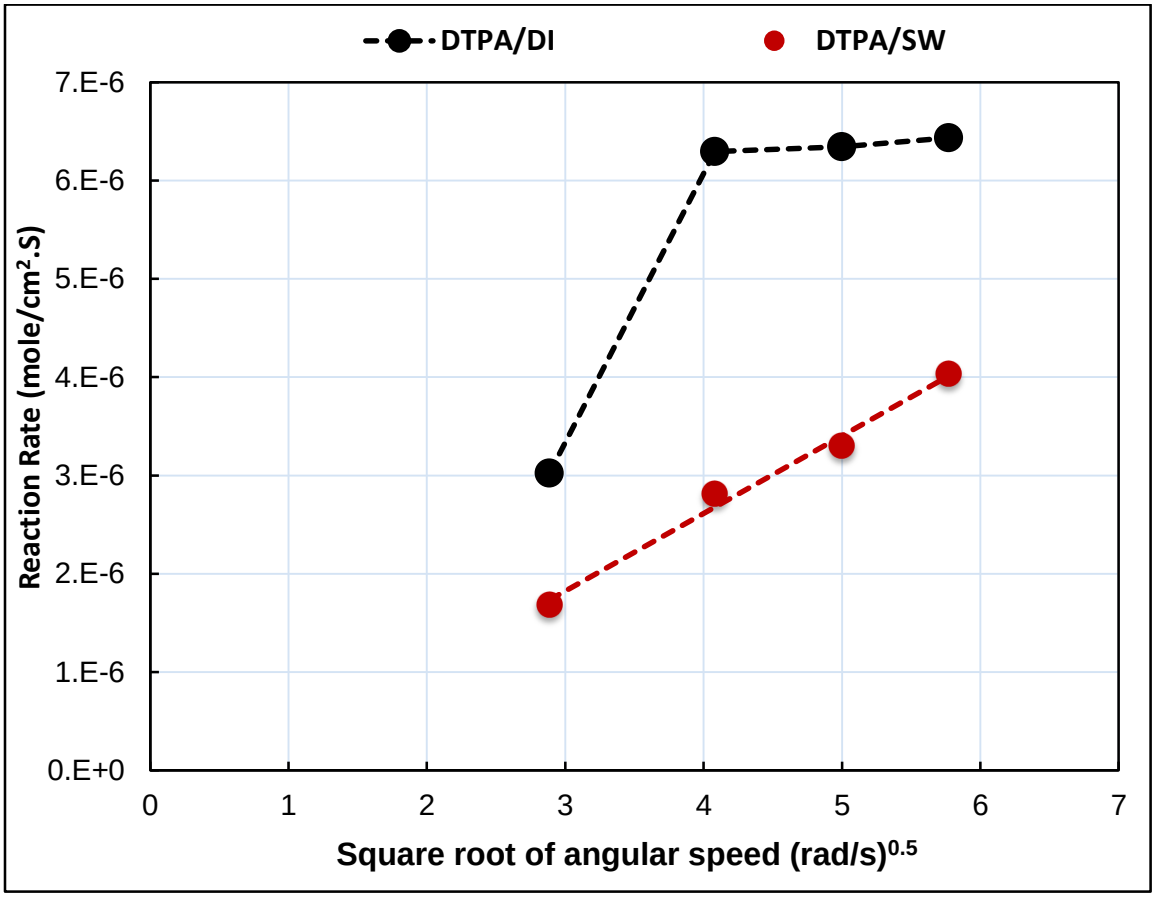

Figure 6. 5—Rate of calcite dissolution from Indiana limestone samples in 15 wt% DTPA/DI and 15 wt% DTPA/SW at pH 4.5, 1000 psi and 250°F.

6.4.2 Coreflooding Experiments

Liquid permeability was measured using 3 wt% KCl (potassium chloride) solution at room temperature, then the system was heated up to 250°F to allow temperature equilibration. The injection rate was then set to the desired rate (0.25, 0.5, 2 or 4 cm^3/min) with 3 wt% KCl solution. After steady state flow is achieved, the injected fluid is switched to DTPA/SW. The minimum pore volume required to create dominant wormhole in the core is used to identify the optimum injection rate (Huang at al. 2003). For each coreflooding experiment, the injected pore volume at the wormhole breakthrough (PV_{bt}) was reported corresponding to the pressure drop of near zero (**Figure 6.6).**

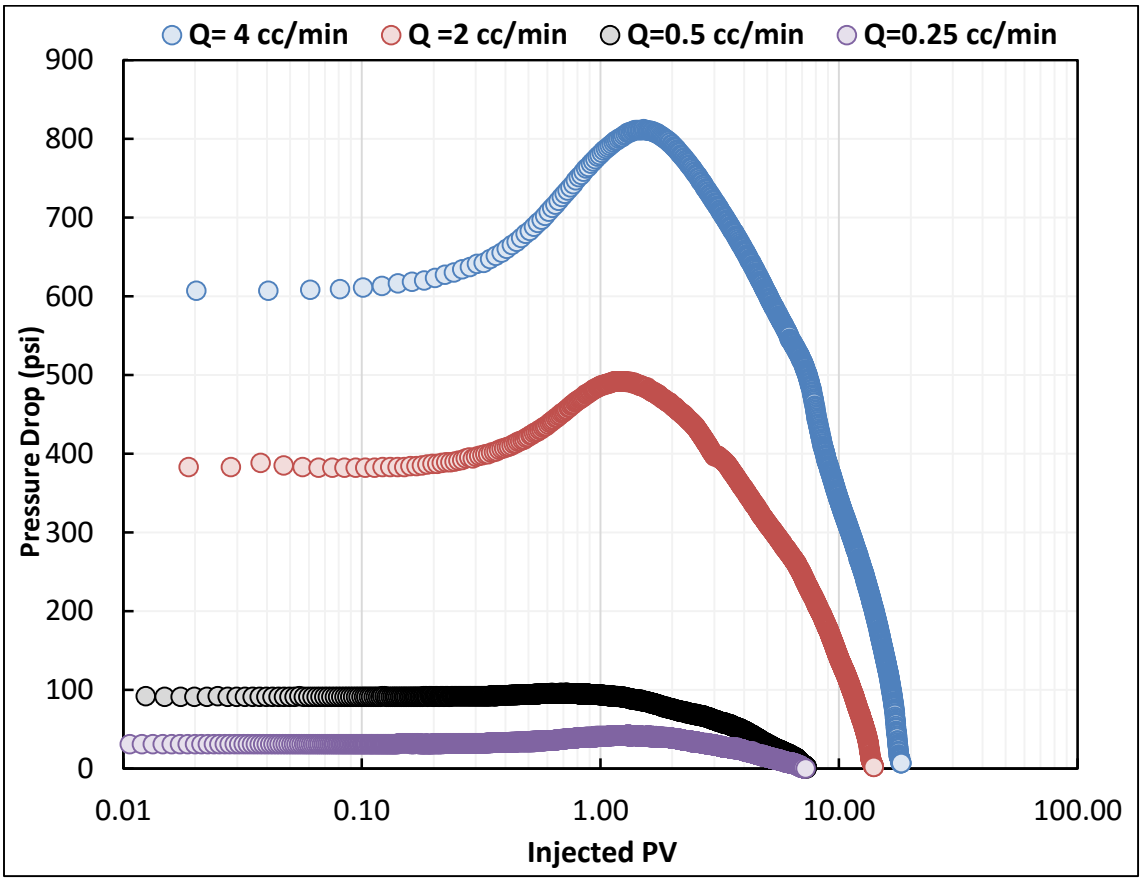

Figure 6. 6—Pressure drop variation during injection of 15 wt% DTPA/SW (pH=4.5) at 250°F at different injection rates using 6" Indiana Limestone rock samples.

The wormholes were characterized using computerized tomography (CT) scan the structure of the wormhole for each sample as well. CT-scans of the four samples were run at energy of 135kW/200mA with 1 mm resolution. **Figure 6.7** shows the wormhole path that confirmed the pressure drop results. The wormhole structures from CT-Scan showed that the optimum injection rate is between 0.25 and 0.5 cm^3/min injection rates with less ramified wormholes.

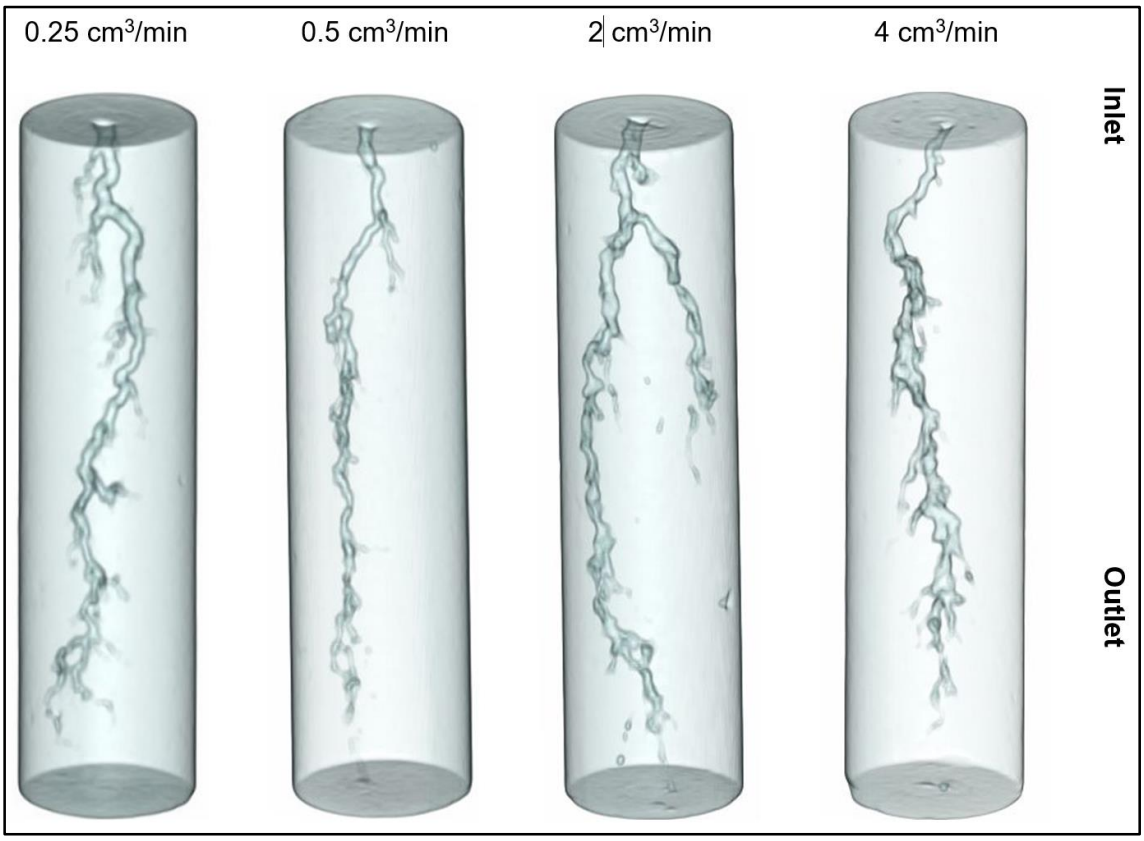

Figure 6. 7—Wormhole structure inside 6" Indiana Limestone Rock samples using CT scan for core samples stimulated using 15 wt% DTPA/SW at pH 4.5 at 250°F.

From the plot of injection rate versus injected PV_{bt} on a log-log plot (**Figure 6.8**) and at a rate of 0.5 cm^3/min, a wormhole can be generated at the minimum injected PV_{bt}. The cost of stimulation process in the field is controlled by the treatment time and the fluid volume.

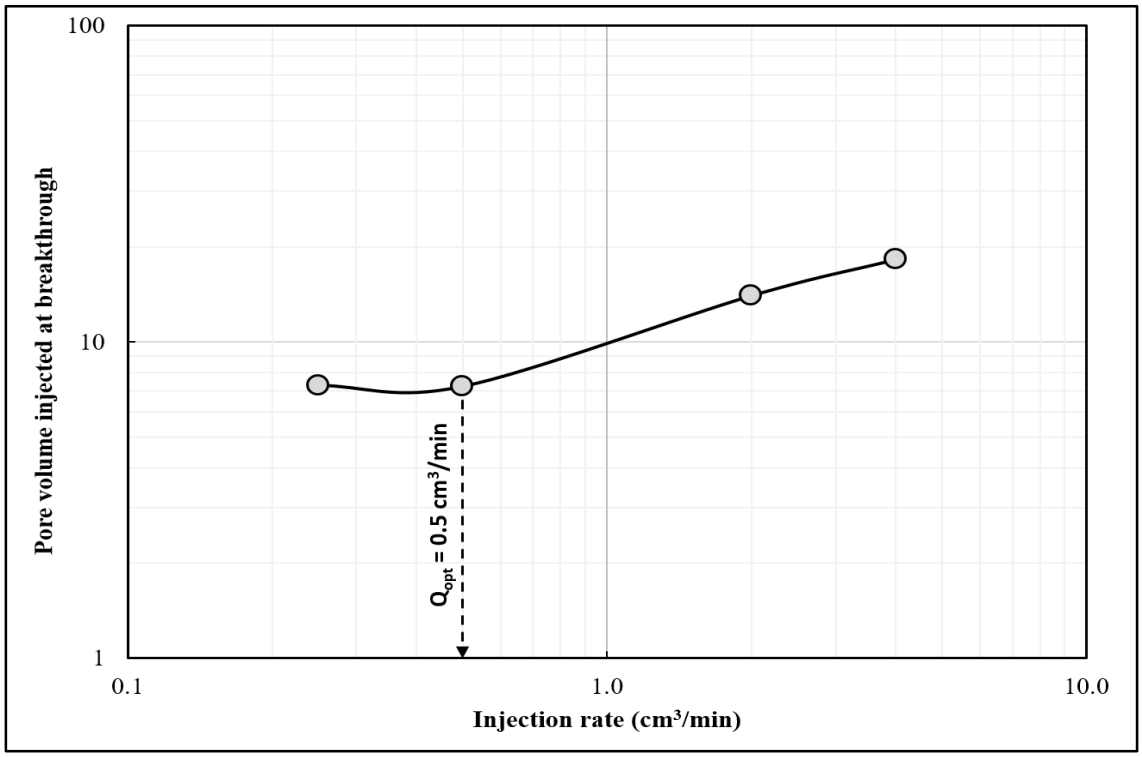

Figure 6. 8—Effect of acid injection rate of 15 wt% DTPA/SW (pH 4.5) on the required pore volume to breakthrough 6" Indiana Limestone rock samples at 1000 back pressure and 250ºF

As it become clear from Figure 6.8, unlike HCl, DTPA does not have a sharp optimum injection rate to be defined visually from the CT scans of the flooded core samples. A normalized pressure drop ratio (PDR) defined by Equation 5.12 is used in same way used before for GLDA to define the optimum injection rate. At the optimum injection rate, the minimum injected pore volume is used during the wormhole propagation to achieve the maximum value of pressure drop reduction from the maximum pressure drop encountered during the acid injection.

As shown in **Figure 6.9**, at injection rate of 0.5 cm^3/min about 3.0 PVs achieved 40% reduction of Δp_{max} where 5.5 PVs were required to achieve the same pressure drop reduction at 2.0 cm^3/min injection rate, 3.7 PVs at 0.25 cm^3/min and 7.5 PVs at 3.0 cm^3/min. Based on that, 0.5 cm^3/min can be selected as the optimum injection rate because of the earlier achieved PDR at minimum injected PVs compared to other injection rates which was the same result for GLDA as shown in chapter 5.

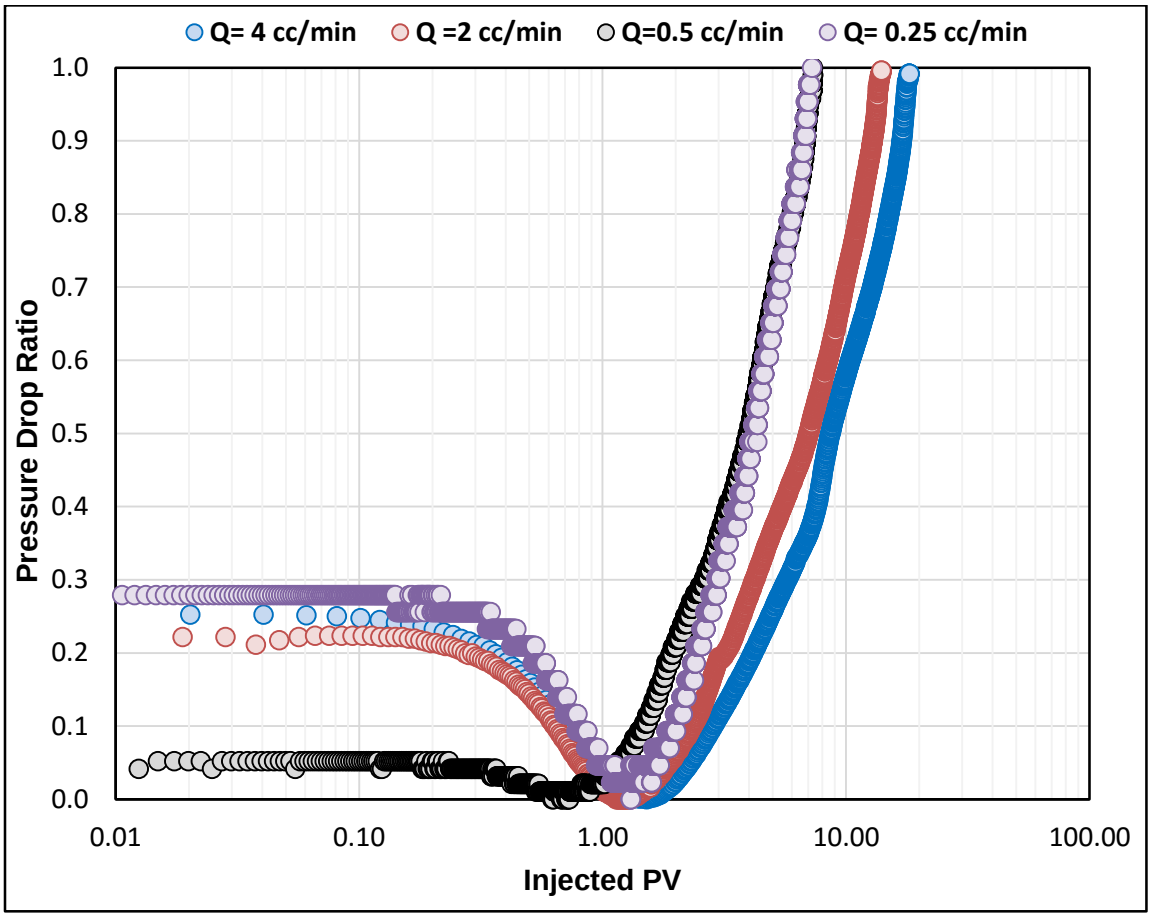

Figure 6. 9—Normalized pressure drop variation during injection of 15 wt% DTPA/SW (pH=4.5) at 250ºF at different injection rates using 6" Indiana Limestone rock samples.

For an effective stimulation treatment, the optimization process should include both factors, time and volume. In this study, new optimization tools were developed. Here, the normalized pore volume to breakthrough (NPV_{bt}) and the normalized time to breakthrough (NT_{bt}) were introduced. **Equations 6.6** and **6.7** are used to determine the two numbers.

$$NPV_{bt} = \frac{PV_{bt} - PV_{bt_{optimum}}}{PV_{bt_{max}} - PV_{bt_{optimum}}} \tag{6.6}$$

$$Nt_{bt} = \frac{t_{bt} - t_{bt_{min}}}{t_{bt_{max}} - t_{bt_{min}}} \tag{6.7}$$

Where PV_{bt} the pore volume to breakthrough at each rate, $PV_{bt_{optimum}}$ is the minimum pore volume to breakthrough from Figure 6.8, $PV_{bt_{max}}$ is the maximum pore volume required to breakthrough, t_{bt} is the time required to breakthrough at each injection rate, $t_{bt_{min}}$ is the time required to breakthrough at the maximum injection rate and $t_{bt_{max}}$ is the time required to breachthrough at the minimum injection rate. Both NPV_{bt} and NT_{bt} have a range from zero to one. A value of zero indicates minimum volume and maximum time to breakthrough while a value of one indicates maximum volume and minimum time to breakthrough. The coreflooding results listed in **Table 6.5** were used to calculate both NPV_{bt} and NT_{bt} for each experiment. The point of intersection of NPV_{bt} and NT_{bt} in **Figure 6.10** represents the injection rate at which the wormhole can breakthrough the 6-inch Indiana limestone rock sample at the minimum injected volume and time simultaneously. The optimum injection rate, considering injected acid volume and injection time, is 1.1 cm^3/min compared to 0.5 cm^3/min when optimization is based only on the injected pore volume alone.

Table 6. 5—Coreflooding experiments results for 15 wt% DTPA/SW at 250ºF using 6" Indiana Limestone rock samples.

Q (cm^3/min)	Pore Volume at breakthrough	Time to breakthrough (min)	NPV_{bt}	NT_{bt}
4	18.20	75.00	1	0
2	14.00	123.90	0.62	0.13
0.5	7.22	244.00	0.02	0.45
0.25	7.28	452.00	0.02	1

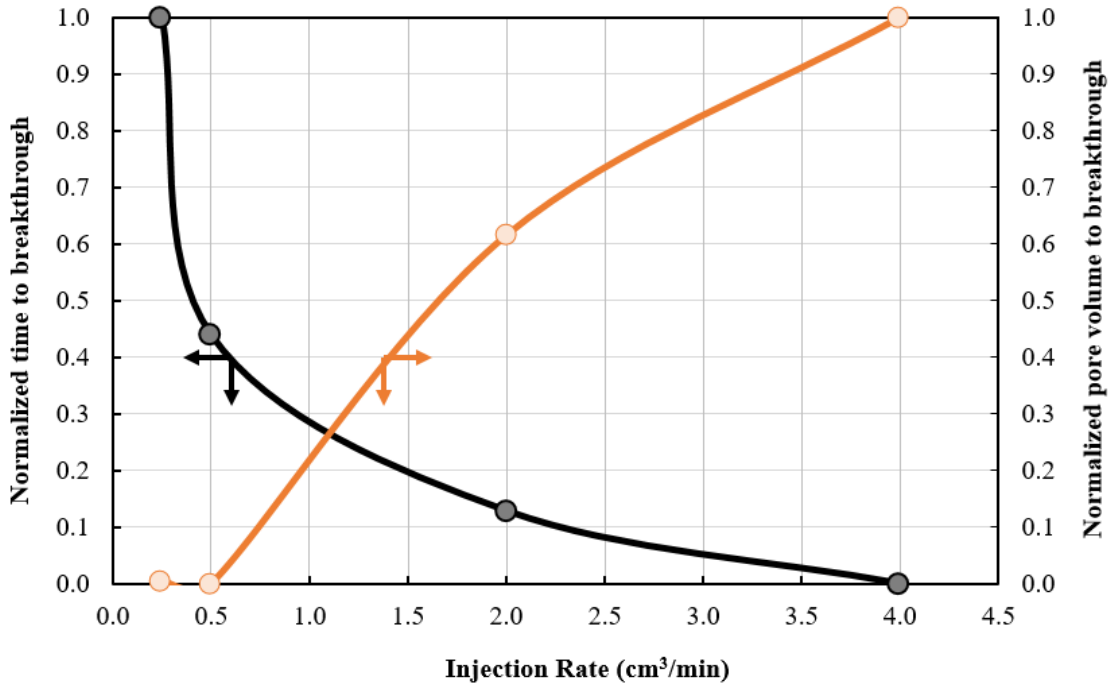

Figure 6. 10—Normalized pore volume and time to breakthrough for 15 wt% DTPA/SW at 250ºF using 6" Indiana Limestone rock samples

Equation 6.8 can be used to estimate the optimum radial injection rate of DTPA/SW. To scale-up linear coreflooding results to radial and then filed scale, equations 6.8 and 6.9 are used to determine the optimum injection rate in radial coreflooding experiments (q_{opt_R})

and the actual optimum injection rate in the well q_{opt_W} based on the laboratory results (Mostofizadeh and Economides 1994)

$$q_{opt\_R} = q_L \frac{2r_w L_c}{r_c^2} \tag{6.8}$$

$$q_{opt\_W} = q_R \frac{r_w H_f}{r_c L_c} \tag{6.9}$$

where H_f is the formation thickness, r_w is the well radius, r_c is the core radius, and L_c is the core length. For a HPHT gas well, such as KM-3 well (Al-Saeedi et al., 2006) to stimulate 18655 ft deep well with a thickness of 122 m (400 ft), the optimum injection rate of 15 wt% DTPA/SW stimulation fluid can be calculated using **Equation 6.9**. Optimum injection rate of 1.1 cm^3/min and parameters shown in **Table 6.6** were used to calculate the field injection rate. The optimum injection rate required in the field scale is 1.4 bbl/min, which enables stimulation of this interval in one stage compared to HCl which may require more than one stage due to the high reactivity with carbonate formation at HPHT condition with the operational injection rate limits and risk of exceeding formation fracture pressure. Using Darcy law, the injection pressure at the sand face for 0.1 md, 18655 ft deep formation is 11961 psi which is far away from the formation fracture pressure assuming (1 psi/ft) fracture gradient.

Table 6. 6—Design parameters for actual carbonate well.

Parameter	Value
Well radius (in)	3.0
Worm hole penetration (in)	6.0
L_c (in)	6.0
Temperature (^{o}F)	250
H_f (ft)	400
Pore pressure gradient (psi/ft)	0.64

6.4.3 Corrosion Test Results

The corrosion experiments were carried out using 15 wt% DTPA at 250ºF and 15 wt% HCl with 3 vol% corrosion inhibitor on actual coupons (**Figure 6.11**). The corrosion rate was determined by taking the weight loss of the coupon sample after soaking for 6 hours in the fluid and then the weight loss per unit surface area of the coupon was calculated. The results showed a corrosion rate of 0.0034 g/cm^2 in 6 hours (0.007 lbm/ft^2) for 15 wt% DTPA while the corrosion rate of the 15 wt% HCl, with 3 vol% corrosion inhibitor, is 0.205 g/cm^2 in 6 hours (0.42 lbm/ft^2) at the same conditions of pressure and temperature. The industry limit is 0.0244 g/cm^2.

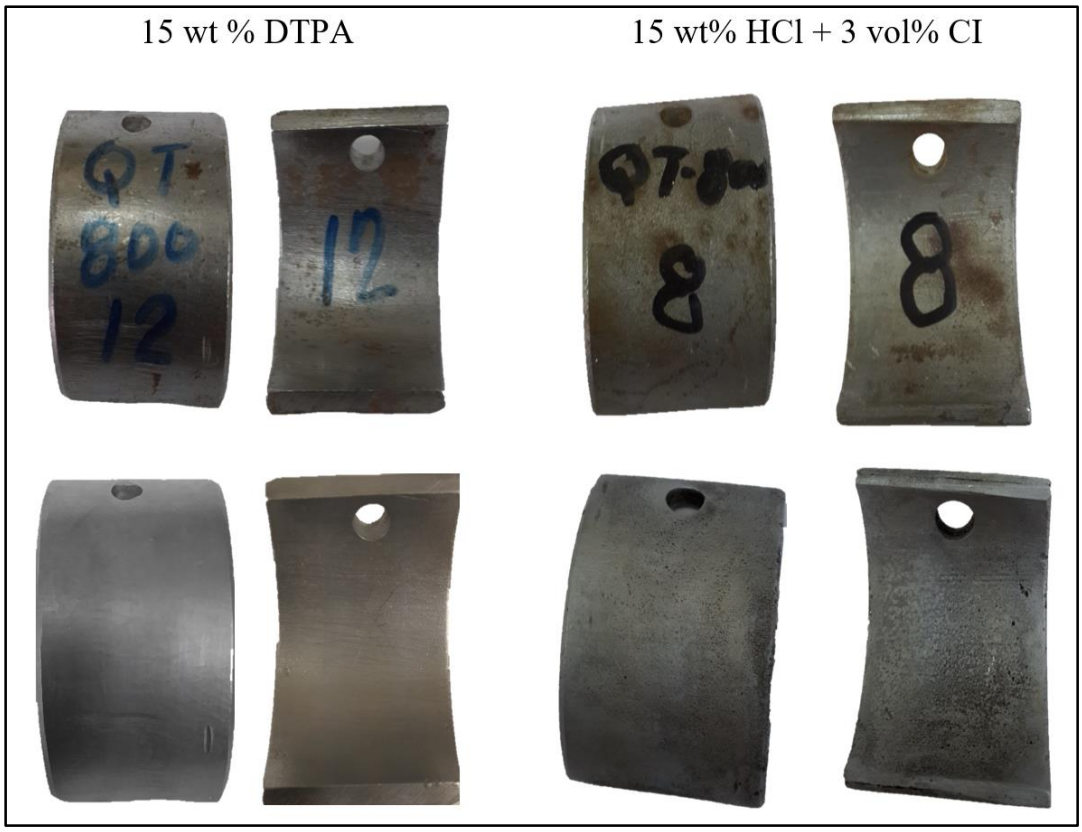

Figure 6. 11—Coiled tubing coupons before and after corrosion rate test using 15 **wt% DTPA and 15 wt% HCl with 3 vol% at 250ºF.**

HCl is very corrosive if used in this high temperature environment even in the presence of the corrosion inhibitor. Using DTPA/SW system will eliminate the cost associated with adding corrosion inhibitors and intensifiers at high temperature. The latter may cost up to 50% of the treatment cost in deep gas wells. DTPA/SW fluid system is gentle to the well tubulars and has very low corrosion rate compared to HCl-based fluids, which make it a good candidate for deep gas well stimulation operations.

6.5 Conclusions

The following conclusions are drawn based on the comparison between the reaction of DTPA/SW and DTPA/DI solutions with carbonate reservoir rock samples at 250^{o}F:

- In the base case where no seawater is used, the reaction rate of 15 wt% DTPA/DI solution at pH 4.5 is controlled by surface reaction.
- Unlike using HCl alone, HCl addition to adjust DTPA pH does not make the reaction a mass transfer limited reaction.
- The use of seawater with DTPA lowers the reaction rate and may require using higher amounts of DTPA in comparison with fresh water.
- DTPA/SW low reaction rate is favored for treating of deep gas wells and will eventually reduce the flow rate required for treatment in the field.
- The optimum injection rate of a stimulation fluid can be optimized based on the required acid volume to breakthrough and the injection time instead of only the required acid volume.
- 15 wt% DTPA/SW solution has very low corrosion rate far below the industry standard in comparison with the 15 wt% HCl acid which is commonly used in the industry.

CHAPTER 7

EDTA Chelating Agents: Reaction Kinetics Study

7.1 Diethylenetriaminepentaacetic Acid (EDTA)

EDTA is a merciful abbreviation for ethylenediaminetetraacetic acid which forms strong complexes with most metal ions. EDTA has a wide use in quantitative analysis, industrial processes, detergents and cleaning agents' production, and food additives that prevent metal-catalysed oxidation of food. It is also capable of combining stoichiometrically with virtually every metal in the periodic table (Chaberck and Martell, 1959). EDTA is one of the Aminopolycarboxylic acids, which are able to form stable complexes with alkali earth metals (Ca, Mg, etc.). EDTA is considered one of the most widely used chelating agent. In the presence of EDTA, the chelated metal is largely prevented from reacting with competing anions with an increased solubility. The stability constants for different metal–EDTA complexes vary considerably, and any metal that is capable of forming a strong complex with EDTA will at least partially displace another metal. EDTA plays a larger role as a strong metal-binding agent in industrial processes and in products such as detergents, cleaning agents, and food additives that prevent metal-catalysed oxidation of food. EDTA is an emerging player in environmental chemistry. EDTA has two amino groups and four carboxylic groups as shown in **Figure 7.1.**

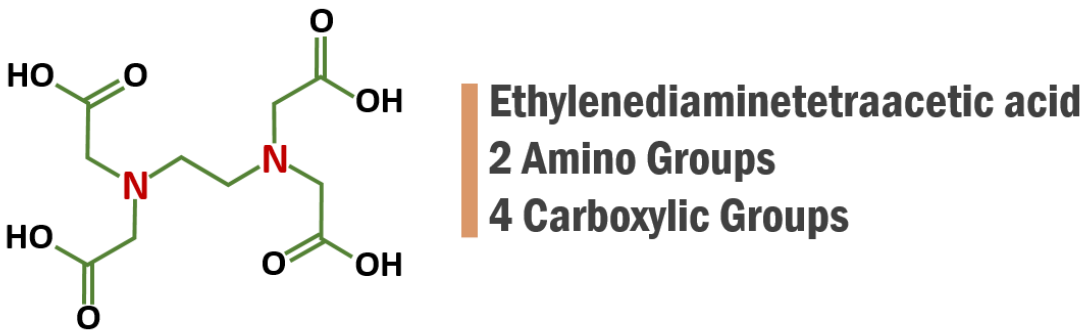

Figure 7. 1—Diethylenetriaminepentaacetic Acid (EDTA)chemical structure.

The distribution of ionic species for EDTA at room temperature is shown in **Figure 7.2**. At a pH of approximately 4.5, EDTA is in the form of H^2Y^{2-}. At higher pH values of about 8.5 and 13 EDTA successively deprotonates to the HY^{-3} and Y^{-4} species respectively. EDTA is valuable for applications application in the oil and gas upstream industry due to the high stability the metal/ligand formed by EDTA with common metal ions present in the reservoir system. The stability constants for different metal/ligand chelates of EDTA are listed in **Table 7.1**. Fredd and Fogler (1998) proved that EDTA is capable of forming wormholes in limestone when injected at pH values between 4 and 13 by combination of hydrogen ions attacking and chelating free calcium ions. They reported a mass transfer limited dissolution of limestone by EDTA with a diffusion coefficient of $6x10^{-6}$ cm^2/s, an order of magnitude lower than that of HCl ($4x10^{-5}$ cm^2/s) at room temperature and 500 psi.

In this chapter the reaction kinetics of EDTA prepared in fresh water (EDTA/Di) with carbonate reservoir rock will be studied using rotating disk. In addition, the effect of preparing EDTA in seawater will be investigated and compared to EDTA/DI. Coreflooding experiments also were carried out to investigate the effect of seawater on the wormholing ability of EDTA through carbonate rock samples. 4.5 pH at 15 wt% EDTA concentration

was selected for the EDTA based fluid systems to be used for the rotating disk experiments. At pH values below 4.5, EDTA is soluble in seawater but at lower concentration which is too low to be used in carbonate matrix acidizing applications.

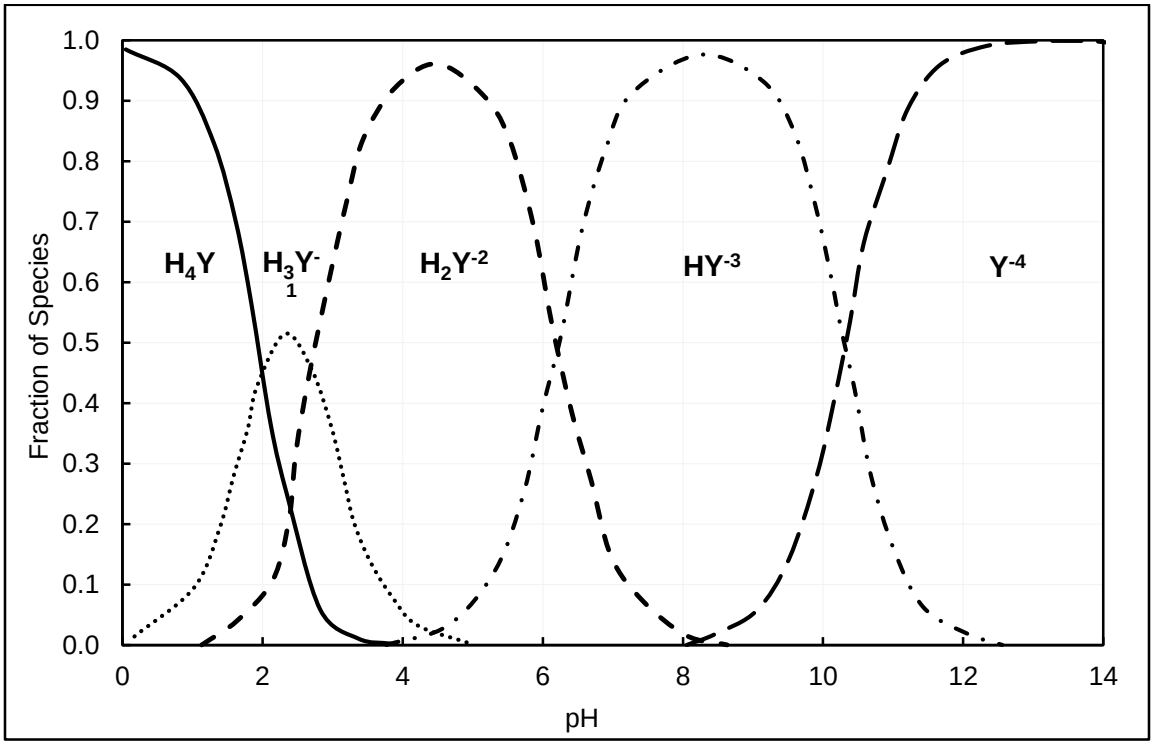

Figure 7. 2—Distribution of ionic species of EDTA at room temperature (Freiner 2001).

Table 7. 1— EDTA chelates Stability constants at 20°C and 0.1 ionic strength (Welcher, 1958)

Metal Ion	Log K
Fe^{3+}	25.1
Fe^{2+}	14.2
Mn^{2+}	13.5
Ca^{2+}	10.59
Mg^{2+}	8.69
Sr^{2+}	8.63
Ba^{2+}	7.76
Na^{+}	1.66

7.2 Experimental work

The dissolution rate of carbonate rock using EDTA is estimated using two sets of experiments in the rotating disk apparatus. In the first set, EDTA diluted from stock concentration of 40 wt% to 15 wt% using deionized water (EDTA/DI) was used. In the second set of experiments, EDTA was diluted to the same concentration using synthetic seawater (EDTA/SW). In both sets, HCl was used to adjust the pH of the solution to 4.5. Four experiments were carried out using each fluid system at constant pressure and temperature and at different disk speeds (500, 750, 1000, 1500, and 2000 rpm). Every two minutes, samples were collected during the experiment and the reaction was stopped after collecting 10 samples of 3 ml each.

After doing the required, inductively coupled plasma optical emission spectrometer Optima 8000 (ICP-OES) was used to determine calcium concentration in each sample. The experimental details are listed in **Table 7.2**; all experiments were conducted at 250^{o}F and 1000 psi. One-foot Indiana limestone core sample was cut into small disks of 2 cm (0.8-inch) length and 3.81 cm (1.5-inch) diameter. Disk surfaces were prepared for reaction kinetic experiments using end face grinding, polishing, and sonic cleaning. This surface preparation was done to correctly estimate the surface area at which the reaction will take place. The porosity of each sample was calculated using dry and saturated weights and the cores were saturated with a fresh water of 1 g/cm^3 density.

Table 7. 2—RDA Experimental using EDTA with Indiana Limestone at 250°F and 1000 psi

Experiment No.	Disk Porosity (%)	Fluid	Disk Angular velocity (RPM)
1	9.37	15 wt% EDTA/DI pH 4.5	500
2	9.07		750
3	9.48		1000
4	9.43		1500
5	9.01		2000
6	10.88	15 wt% EDTA/SW pH 4.5	500
7	11.56		750
8	9.76		1000
9	9.73		1500
10	12.74		2000

7.3 Results and Discussion

7.3.1 Reaction with Indiana Limestone

Typical calcium concentration obtained from the ICP-OES analysis of the collected samples is shown in **Figure 7.3** for the first experimental set in which 15wt% EDTA/DI system was used. The slope of the straight lines increases as the disk angular velocity increases. For the 15wt% EDTA/SW calcium concentration obtained from the ICP-OES analysis is shown in **Figure 7.4**.

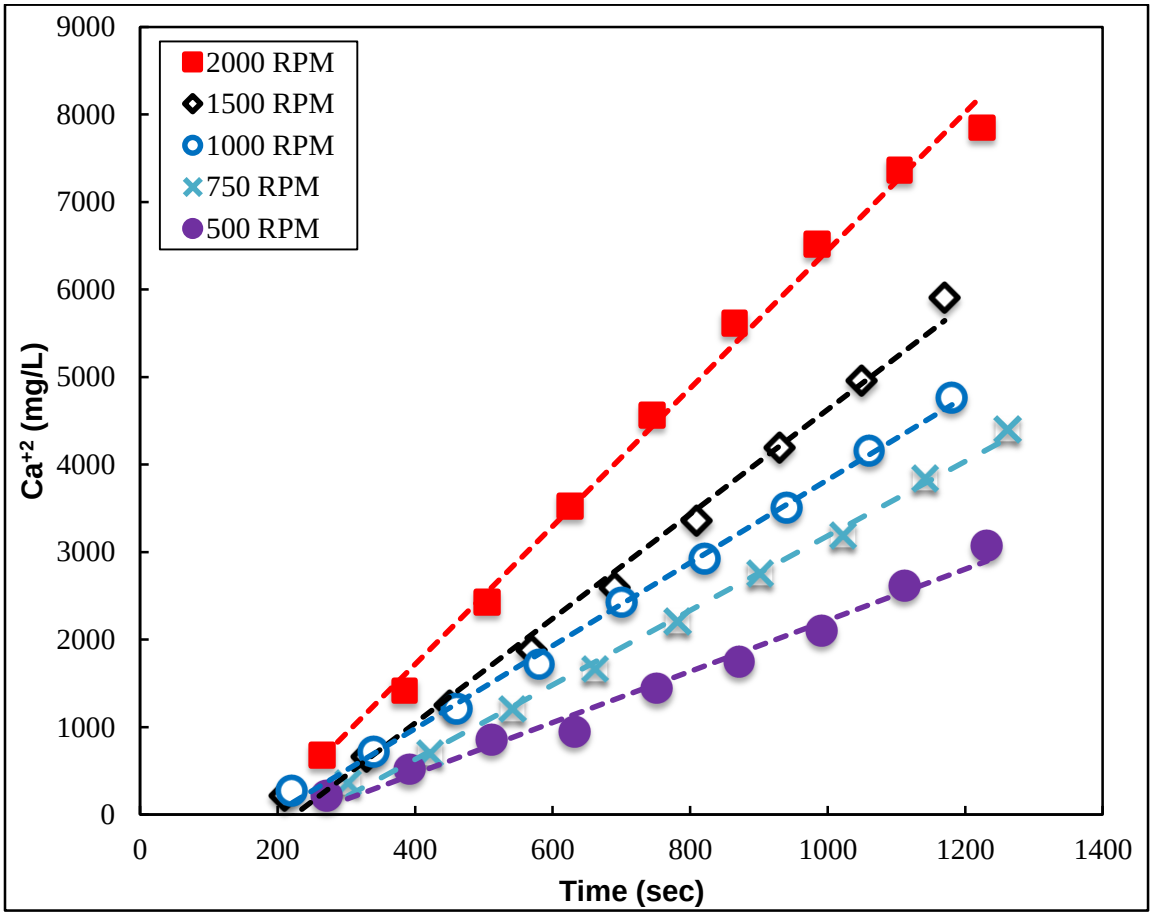

Figure 7. 3—Calcium concentration in the collected samples as a function of time and angular velocity using 15 wt% EDTA/DI water solution at 1000 psi and 250ºF.

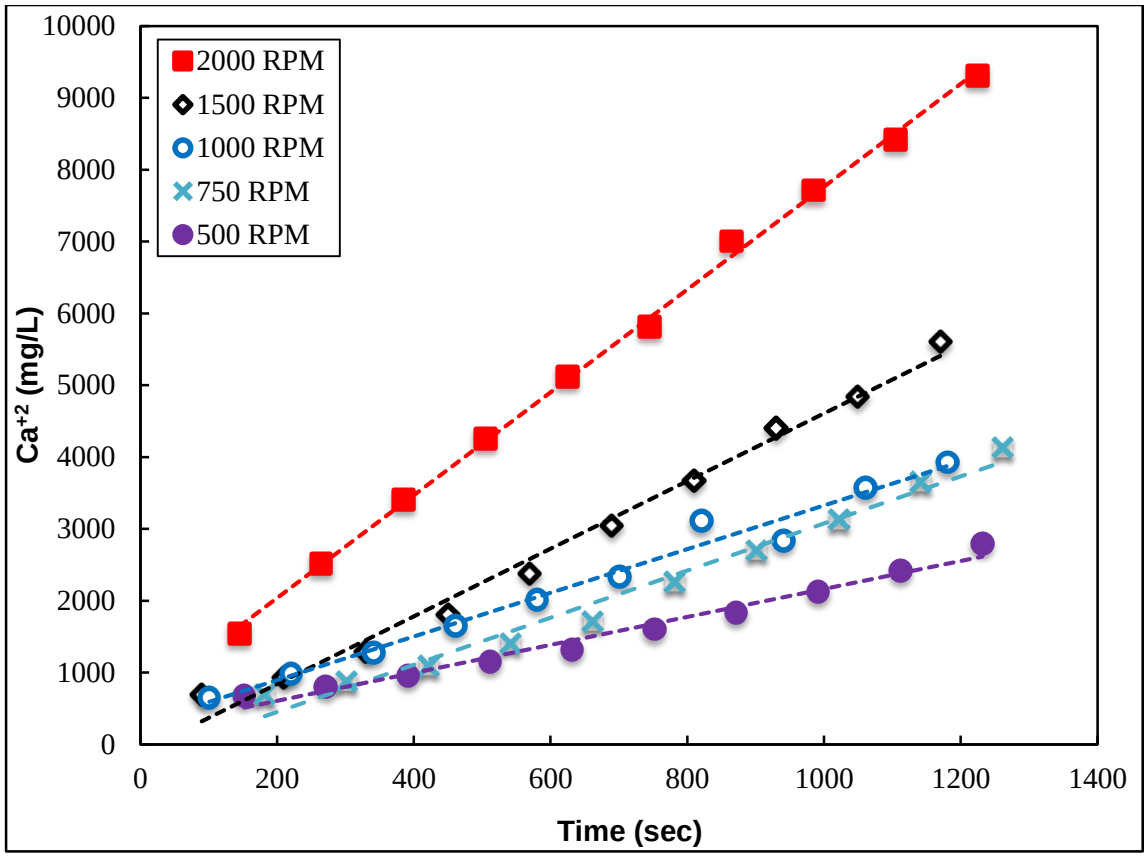

Figure 7. 4—Calcium concentration in the collected samples as a function of time and angular velocity using 15 wt% EDTA/SW water solution at 1000 psi and 250ºF.

The reaction rate for both cases was calculated as a function of angular speed using the calcium ion concentration change and plotted in **Figure 7.5** (left) for both EDTA/DI and EDTA/SW. Initially at low RPM the seawater highly affected the reaction rate. with increasing the rpm, the seawater system approaches the DI system. At 2000 rpm the two fluid system have the same reaction rate. This can be explained in the way that at seawater effect was canceled due to higher convection. The EDTA acid reaction with Indiana limestone is mass transfer limited in both cases (EDTA/SW and EDTA/DI). Applying **equation 5.7**, diffusion coefficients of 4.07 $x10^{-5}$ and 5.72 $x10^{-5}$ cm^2/s are obtained at 250^{o}F for EDTA/DI and EDTA/SW respectively as shown in figure (right).

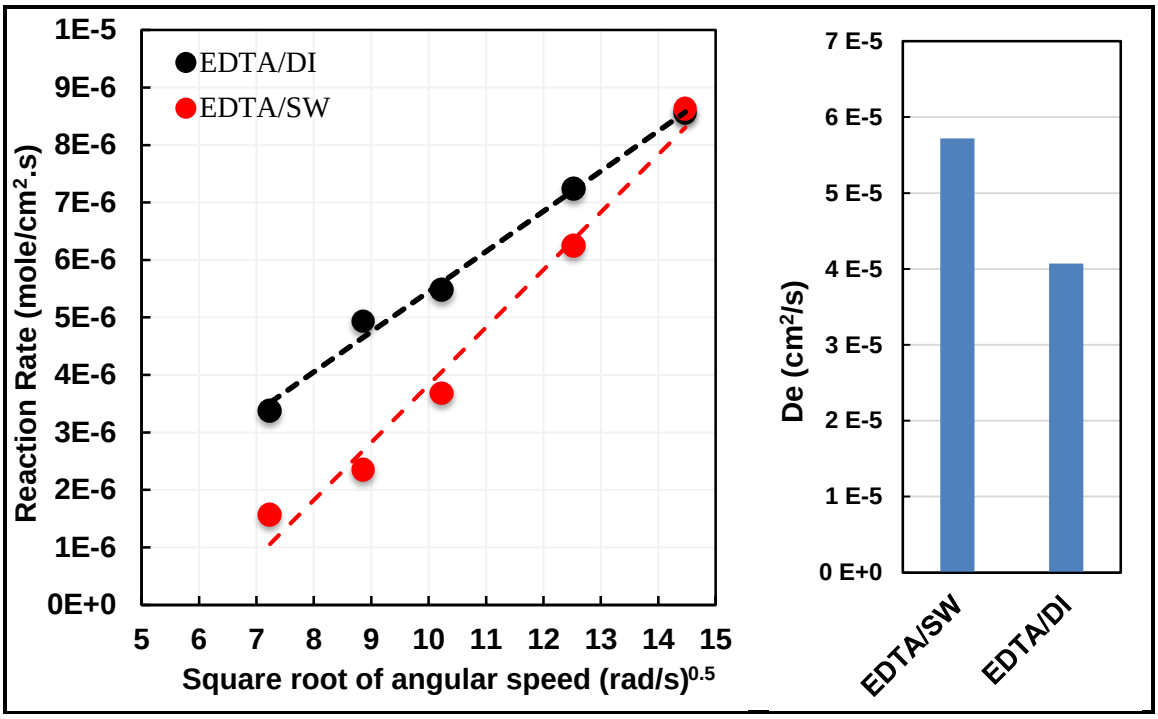

Figure 7. 5—Reaction rate of 15 wt% EDTA/DI and EDTA/SW with Indiana limestone at 1000 psi and 250°F as a function of Square root of angular speed (left), and Diffusion coefficient for the two fluid systems (right).

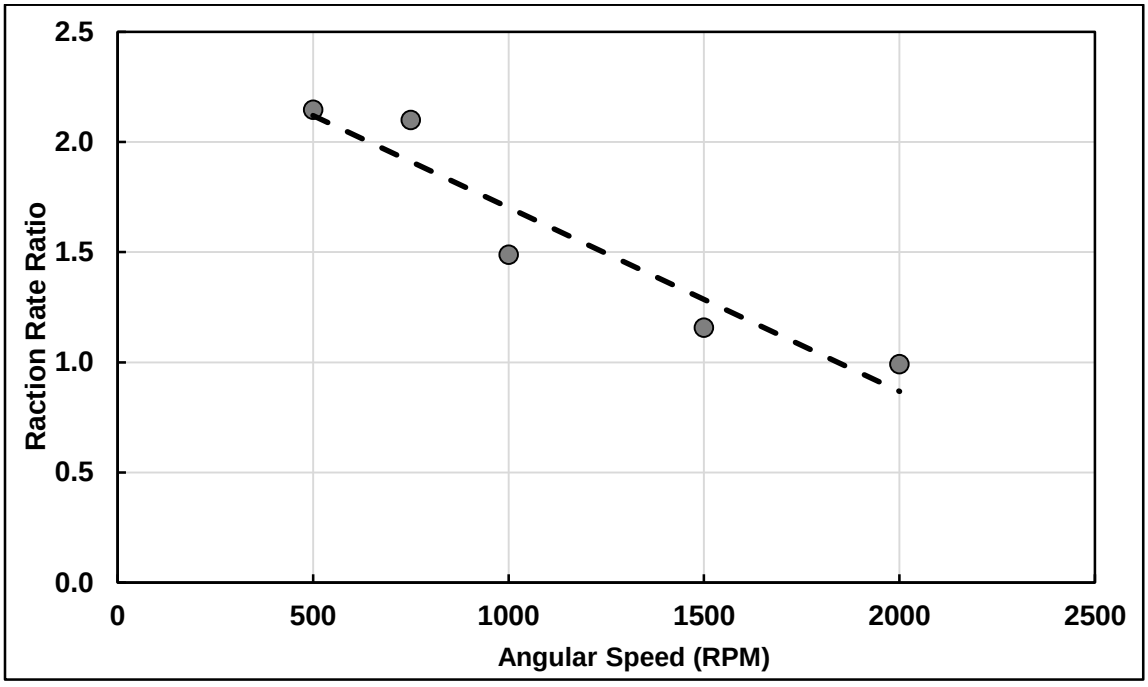

Figure 7. 6—Reaction rate ratio of 15 wt% EDTA/DI with Indiana limestone with respect to 15 wt% EDTA/SW at 1000 psi and 250°F as a function disk angular speed.

Figure 7.6 is showing the Reaction rate ratio of 15 wt% EDTA/DI with Indiana limestone with respect to 15 wt% EDTA/SW at 1000 psi and 250°F as a function of disk angular speed. At 500 and 750 RPM the reaction of EDTA/DI with Indiana limestone is almost double the reaction of EDTA/SW which reflects the fast reaction of EDTA/DI at low RPM. At higher RPM the two systems reaction rate converges to each other and almost same at 2000 RPM. These results can be better explained by The model introduced by Conway et al. (1999) which introduced the effect of the calcium concentration on the diffusion coefficient. The relation is given by the following equation:

$$D = EXP\begin{Bmatrix} \left(\frac{2918.54}{T}\right) - 0.589\sqrt{\frac{[Ca^{2+}]}{[H^+]}} \\ -0.789\sqrt{\frac{[Mg^{2+}]}{[H^+]}} + 0.452[H^+] - 4.995 \end{Bmatrix} \quad (7.1)$$

In case of reaction with Indiana limestone (magnesium free) there will be no Mag^{2+}, Conway et al. equation can be written as:

$$D = EXP\left\{\left(\frac{2918.54}{T}\right) - 0.589\sqrt{\frac{[Ca^{2+}]}{[H^+]}} + 0.452[H^+] - 4.995\right\} \quad (7.2)$$

Due to the initial fast reaction of EDTA/DI system, Ca^{2+} will build up quickly in the solution and according to Conway et al. the diffusion coeffiecnt will decrease resulting in a lower reaction rate observed at high RPM.

7.4 Conclusions

After studying the reaction of Indiana limestone with EDTA chelating agent diluted using seawater and fresh water, the reaction limiting process is defined for each system at reservoir conditions. The following conclusions can be drawn:

- The reaction between 4.5 pH 15% EDTA/DI and EDTA/SW and Indiana limestone is mass transfer limited at 250^{o}F.
- At lower RPM the reaction of EDTA/DI with Indiana limestone is almost double the reaction of EDTA/SW.
- At higher RPM the two systems reaction rate converges to each other and become almost same at 2000 RPM.
- The rapidly chelated Ca^{+2} in to the solution in case of EDTA/SW fluid system causes a reduction in the diffusion coeffiecnt.
- The injection rate of EDTA/SW into carbonate rock samples should be higher than the inaction rate of EDTA/DI system.

CHAPTER 8

Conclusions and Recommendations

8.1 Conclusions

In conclusion, HCl can cause formation damage when diluted in seawater for stimulation treatments by disconnecting different pore systems in the carbonate rock. Chelating agents can be used safely (No induced formation damage) for stimulation treatments when diluted in seawater. The reaction of different chelating agents with carbonate rock samples was studied at HPHT by conduction reaction kinetics and coreflooding experiments.

For the reaction of Indiana limestone and Austin chalk with GLDA chelating agent diluted using seawater and fresh water, the limiting process is defined for each system at reservoir conditions. The effect of porosity system was studied using Indiana limestone and Austin chalk which have almost has the same chemical composition of Indiana limestone but different porosity type resulted from the grain size distribution with in the rock matrix. The following conclusions can be drawn:

- The porosity type of the rock sample significantly affects the reaction rate with the same acid system even for the same chemical composition (Indiana limestone and Austin chalk as an example)
- The reaction between 3.8 pH 20% GLDA/DI and Indiana limestone is surface reaction limited at 150^{o}F and mass transfer limited at 200 and 250^{o}F, however the reaction of 20% GLDA/SW with the same rock is mass transfer limited at 150-250^{o}F.

- The overall reaction of GLDA/SW with Indiana limestone rock surface is inhibited with the presence of salt ions from seawater compared to GLDA/DI.
- Using pressure drop ration enables an accurate determination of optimum injection rate of GLDA/SW which does not show a sharp optimum injection rate from the coreflooding results.
- The reaction between 3.8 pH 20% GLDA/SW and Austin chalk is surface reaction limited at 200^{o}F.
- 0.5 cm^{3}/min was estimated as an optimum injection rate for 20 wt. % SW/GLDA at 1000 psi and 250^{o}F from coreflooding experiments analysis compared to 0.43 cm^{3}/min using a mathematical model.

For the reaction of Indiana limestone DTPA chelating agent diluted using seawater and fresh water, the limiting process is defined for each system at 1000 psi and 250^{o}F. The following conclusions are drawn:

- In the base case where no seawater is used, the reaction rate of 15 wt% DTPA/DI solution at pH 4.5 is controlled by surface reaction.
- Unlike using HCl alone, HCl addition to adjust DTPA pH does not make the reaction a mass transfer limited reaction.
- The use of seawater with DTPA lowers the reaction rate and may require using higher amounts of DTPA in comparison with fresh water.
- DTPA/SW low reaction rate is favored for treating of deep gas wells and will eventually reduce the flow rate required for treatment in the field.

- The optimum injection rate of a stimulation fluid can be optimized based on the required acid volume to breakthrough and the injection time instead of only the required acid volume.
- 15 wt% DTPA/SW solution has very low corrosion rate far below the industry standard in comparison with the 15 wt% HCl acid which is commonly used in the industry.

For the reaction of Indiana limestone EDTA chelating agent diluted using seawater and fresh water, the limiting process is defined for each system at 1000 psi and 250^{o}F. The following conclusions are drawn:

- The reaction between 4.5 pH 15% EDTA/DI and EDTA/SW and Indiana limestone is mass transfer limited at 250^{o}F.
- At lower RPM the reaction of EDTA/DI with Indiana limestone is almost double the reaction of EDTA/SW.
- At higher RPM the two systems reaction rate converges to each other and almost same at 2000 RPM.
- The rapidly Chelate Ca^{+2} in to the solution in case of EDTA/DI fluid system causes a reduction in the diffusion coeffiecnt resulting a higher diffusion coeffiecnt in case of EDTA/SW.
- The injection rate of EDTA/SW into carbonate rock samples should be higher than the inaction rate of EDTA/Di system.

Figures 8.1, **8.2** and **8.3** summarizes the reaction kinetics experiments between the different chelating agents and Indiana limestone at 1000 psi and 250^{o}F.

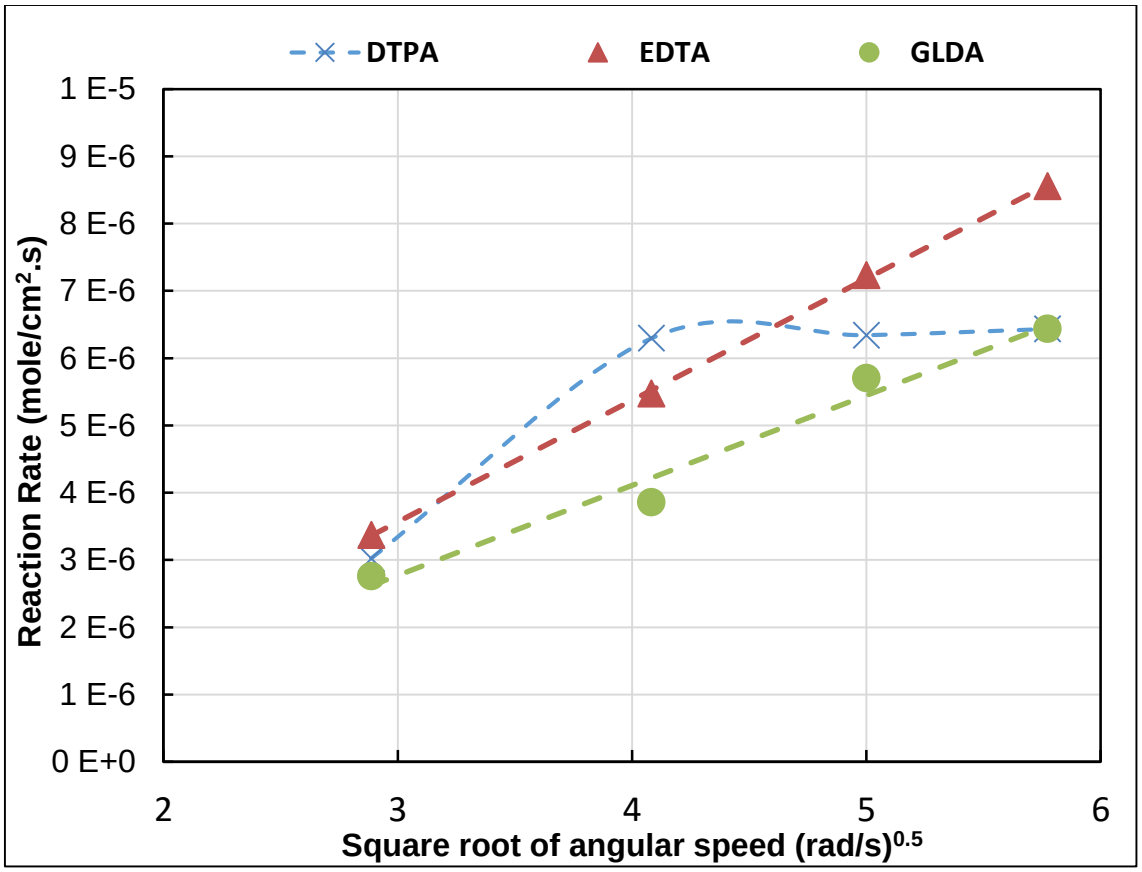

Figure 8. 1—Reaction rate of different chelating agents (15 wt% EDTA, 15 wt% DTPA and 20 wt% GLDA) diluted using DI water at 1000 psi and 250°F vs. Square root of angular speed.

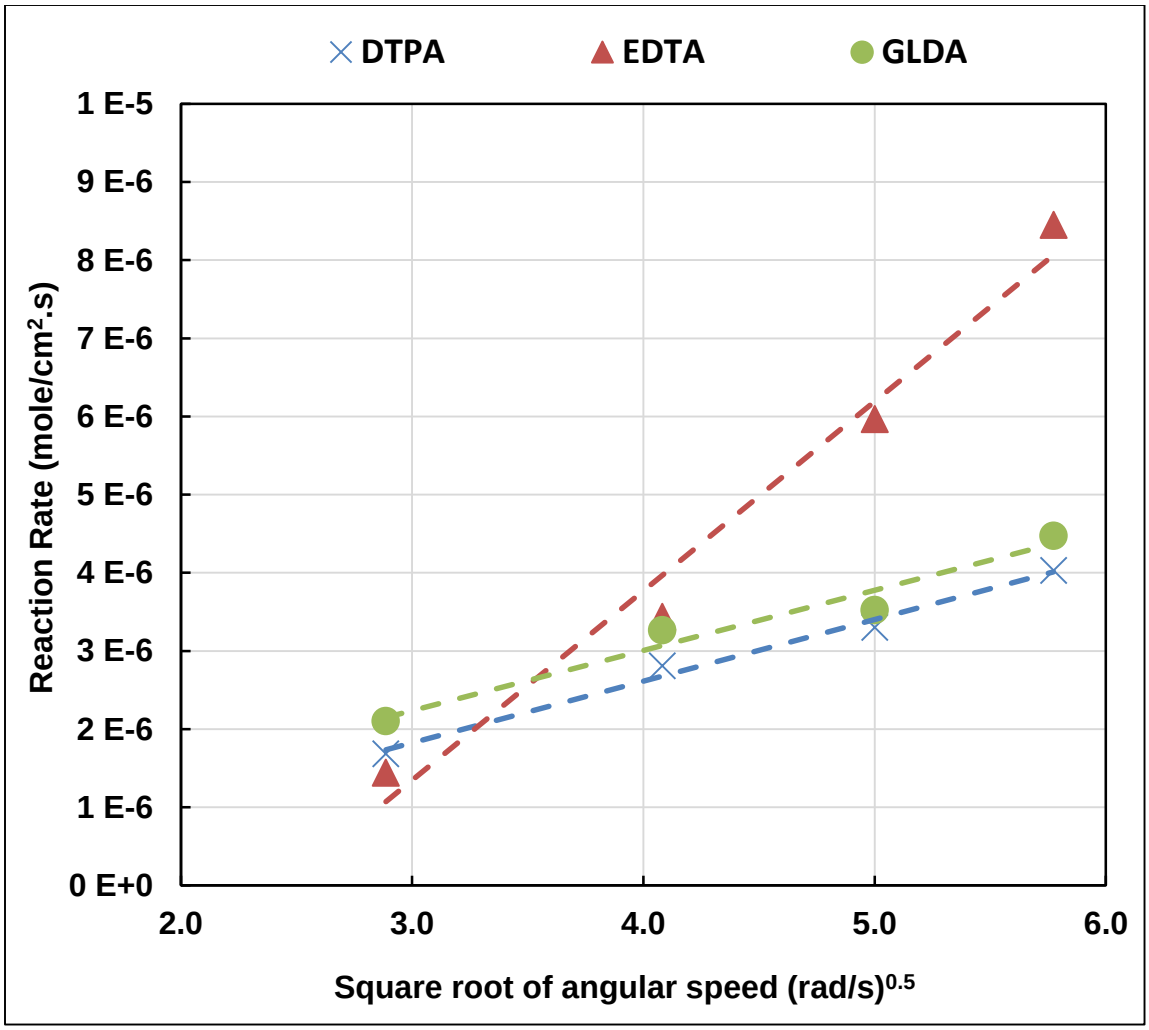

Figure 8. 2—Reaction rate of different chelating agents (15 wt% EDTA, 15 wt% DTPA and 20 wt% GLDA) diluted using seawater at 1000 psi and 250°F vs. Square root of angular speed.

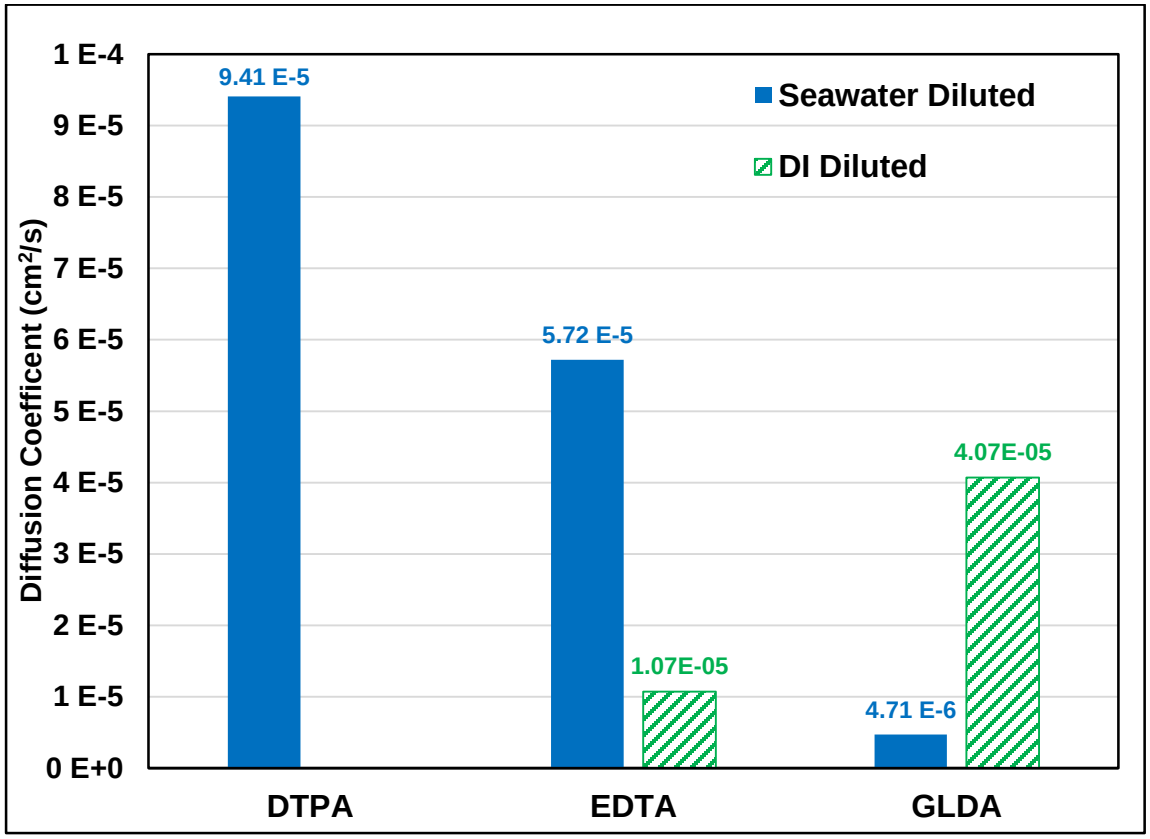

Figure 8. 3—Reaction rate of different chelating agents (15 wt% EDTA, 15 wt% DTPA and 20 wt% GLDA) diluted using seawater at 1000 psi and 250ºF vs. Square root of angular speed.

8.2 Future Work

Raw seawater from different areas should be collected and used for the experiments after required treatment and filtration. Results then can be compared to Synthetic seawater used in this study. Also it was planned to used HEDTA chelating agents due to is excellent performance with fresh water as published in the literature but unfortunately due to custom regulations we could not get it. If HEDTA sample are available in the future, Reaction kinetics experiments can be run to study the effect of seawater on the chemical reaction rate with Indiana limestone as an example. More investigation is required in the reaction of Chelating agents with dolomitic reservoir rock (Khuff reservoir rocks are an example).

References

[1] Al-Ghamdi, A. H., Mahmoud, M., Hill, A. D., and Nasr-El-Din, H. A. 2010. When Do Surfactant-Based Acids Work as Diverting Agents? Paper SPE 128074 presented at the SPE International Symposium and Exhibiton on Formation Damage Control, 10-12 February, Lafayette, Louisiana, USA.

[2] Al-Ghamdi, A., Mahmoud, M.A., A, Wang, G., Hill, A.D., and Nasr-El-Din, H.A. 2014. Acid Diversion Using Viscoelastic Surfactants: The Effects of Flow Rate and Initial Permeability Contrast. *SPE Journal* **19** (6): 1203 – 1216.

[3] Al-Ghamdi, A., Nasr-El-Din, M. A., Hill, A. D., and Nasr-El-Din, H. A. 2009. Diversion and Propagation of Viscoelastic Surfactant Based Acid in Carbonate Cores. Paper SPE 121713 presented at the SPE International Symposium on Oilfield Chemistry, 20-22 April, The Woodlands. Texas. doi:10.2118/121713-MS.

[4] Al-Harthy, S., Bustos, O.A., Samuel, M. et al. 2008 Options for high-temperature well stimulation. *Oil Field Rev* **20**(4):52–62

[5] Frenier, W. W., Fredd, C. N., and Chang, F. 2001. Hydroxyaminocarboxylic Acids Produce Superior Formulations for Matrix Stimulation of Carbonates at High Temperatures. Presented at the SPE Annual Technical Conference and Exhibition, 30 September-3 October, New Orleans, Louisiana.

[6] Ali, A. H. A., Frenier, W. W., Xiao, Z. et al. 2002. Chelating Agent-Based Fluids for Optimal Stimulation of High-Temperature Wells. Presented at the SPE Annual Technical Conference and Exhibition, San Antonio, Texas, 29 September-2 October.

[7] Aliaga, D. A., Wu, G., Sharma, M. M., and Lake, L. W. 1992. Barium and Calcium Sulfate Precipitation and Migration Inside Sandpacks. *SPE Formation Evaluation Journal* **7**(1):79- 86.

[8] Alkhaldi MH, Nasr-El-Din HA, Sarma HK. 2010. Kinetics of the Reaction of Citric Acid with Calcite. **15**(3):704–13.

[9] Anderegg, G., Arnaud-Neu, F., Delgado, R., et al. 2009. Critical evaluation of stability constants of metal complexes of complexones for biomedical and environmental applications. *Pure and Appl Chem* **77**(8):1445–1495.

[10] Al-Mutairi, S. H., Nasr-El-Din, H. A., Aldriweesh, S. M., and Al-Muntasheri, G. A., 2005. Corrosion Control during Acid Fracturing of Deep Gas Wells: Lab Studies and Field Cases. In: SPE International Symposium on Oilfield Corrosion, Aberdeen, United Kingdom.

[11] Al-Saeedi, M. J., Singh, J. R., Sounderrajan, M., Al-Ajmi, H. S., & Mckinnell, D. C. 2006. Drilling and Testing of an HPHT Deep Gas Prospect from an Existing Well: Case History of Kra-Al-Maru 3 Deepening. In: IADC/SPE Asia Pacific Drilling Technology Conference and Exhibition, Bangkok, Thailand.

[12] Archie, G. E., 1952, Classification of carbonate reservoir rocks and petrophysical considerations: *The American Association of Petroleum Geologists Bulletin*, **36**(2):278-298.

(13) Attia, M., Mahmoud, M. A., Al-Hashim. H. S. et al. 2014. Shifting to a New EOR Area for Sandstone Reservoirs with High Recovery, No Damage, and Low Cost.

Presented at the SPE EOR Conference at Oil and Gas West Asia, Muscat, Oman, 31 March-April 2.

[14] Bakken, V., & Schoffel, K. 1996. Semi-quantitative study of chelating agents suitable for removal of scale. *Revue de l'Institut francais du Petrole*. Paris, **51**(1):151–159.

[15] Barri A.A. and Mahmoud M. M.Sc. Thesis. Identifying optimum conditions for stable wormholes created by chelating agents, KFUPM, Dhahran. May 10, 2015.

[16] Bazin, B. 2001. From matrix acidizing to acid fracturing: A laboratory evaluation of acid/rock interactions. *SPE Prod & Fac* **16**(1): 22 – 29.

[17] Beaumont EA, Foster NH. 1999. Exploring for Oil and Gas Traps. American Association of Petroleum Geologists.

[18] Boomer DR. 1972. Rotating Disk Apparatus for Reaction Rate Studies in Corrosive Liquid Environments. *Rev. Sci. Instrum*. **43**(2):225.

[19] Budd, D. A., Saller, A. H., and Harris, P. M., eds., Unconformities and porosity in carbonate strata: *American Association of Petroleum Geologists, AAPG Memoir* **63**:279–300.

[20] Buijse, Adriaan A., and Glasbergen, G. 2005. A Semi-Empirical Model to Calculate Wormhole Growth in Carbonate Acidizing. Paper SPE-96892-MS presented at the SPE Annual Technical Conference and Exhibition, 9-12 October, Dallas, Texas.

[21] Chaberck S. A., Martell A. E. 1959. Organic sequestering agents. New York, NY, John Wiley & Sons, Inc.

[22] Cheng, H., Zhu, D., and Hill, A. D. 2016. The Effect of Evolved CO_2 on Wormhole Propagation in Carbonate Acidizing. *SPE Production and Operations Journal*, **32**(3):325- 332

[23] Choquette, P.W. and Pray, L.C. 1970. Geologic nomenclature and classification of porosity in sedimentary carbonates, *AAPG Bulletin*, **54**(2):207-250.

[24] Conway, M. W., Asadi, M., Penny, G. S. et al. 1999. A Comparative Study of Straight/Gelled/Emulsified Hydrochloric Acid Diffusivity Coefficient Using Diaphragm Cell and Rotating Disk. Presented at the SPE Annual Technical Conference and Exhibition, Houston, Texas, 3-6 October.

(25) Crabetree, M., Eslinger, D., Fletcher P. et al. 1999. Fighting scale-removal and prevention. *Schlumberger Oil Field Review*, Autumn.

[26] Daccord, G. 1997. Chemical dissolution of a porous medium by a reactive fluid Phys. *Physical review letters* **58**(5):479-482.

[27] Daccord, G., Liétard, O., and Lenormand, R. 1993. Chemical dissolution of a porous medium by a reactive fluid—II. Convection vs reaction, behavior diagram. Chemical Engineering Science. **48** (1): 179-186.

[28] Daccord, G., Touboul, E., and Lenormand, R. 1989. Carbonate Acidizing: Toward a Quantitative Model of the Wormholing Phenomenon. *SPE Production Engineering Journal* **4**(1): 63 – 68.

[29] Daccord, Gérard, and Roland Lenormand. 1987. Fractal Patterns from Chemical Dissolution. *Nature* **325**(6099): 41–43.

[30] Darren, M., Shuchart, C., Jackson, S., Postl, D. et al. 2010. Understanding Wormholes in Carbonates: Unprecedented Experimental Scale and 3D Visualization. *Journal of Petroleum Technology* **62**(10): 78–81.

[31] De Rozieres, J., Chang, F. F., and Sullivan, R. B. 1994. Measuring Diffusion Coefficients in Acid Fracturing Fluids and Their Application to Gelled and Emulsified Acids. Paper SPE-28552-MS Presented at the SPE Annual Technical Conference and Exhibition, New Orleans, 25–28 September.

[32] De Wolf, C. A., Nasr-El-Din, H. A., Bouwman, A. et al. 2017. Corrosion rates of Cr- and Ni-based alloys with organic acids and chelating agents used in stimulation of deep wells. *SPE Prod & Oper* **32**(2): 208 - 217.

[33] Dwyer, F.P.J., and Mellor, D.P. 1964. Chelating agents and metal chelates. Academic Press.

[34] Economides, M. J., Hill, A.D., Economides, C. E., and Zhu, D. 2014. Petroleum Production System. 2nd Edition, Prentice Hall Publishing company, Houston, Texas, USA.

[35] Ellison, B. T. and Cornet, I. 1970. Mass transfer to a Rotating disk. *J. Electrochem. Soc.* **118**(1):68-72.

[36] Fredd C.N., Miller M. 2000. Validation of carbonate matrix stimulation models. Paper SPE 58713 presented at the SPE International Symposium on Formation Damage Control, Lafayette, Louisiana, 23-24 February.

[37] Fredd CN, Fogler HS. 1998. Alternative Stimulation Fluids and Their Impact on Carbonate Acidizing. *SPE Journal*. **3**(1):34–41.

[38] Fredd, C. N. and Fogler, H. S. 1999. Optimum Conditions for Wormhole Formation in Carbonate Porous Media: Influence of Transport and Reaction. *SPE Journal*, **4** (3): 196 – 205.

[39] Fredd, C. N. and Fogler, H. S.1997. Chelating Agents as Effective Matrix Stimulation Fluids for Carbonate Formations. Paper presented at the International Symposium on Oilfield Chemistry, 18-21 February, Houston, Texas.

[40] Fredd, C.N. 1998. The influence of transport and reaction on wormhole formation in carbonate porous media: a study of alternative stimulation fluids. Ph.D. Dissertation, University of Michigan, Ann Arbor, MI.

[41] Fredd, C.N. and Fogler, H.S. 1998. Influence of transport and reaction on wormhole formation in porous media." *AIChE Journal* **44**(9): 1933-1949.

[42] Fredd, C.N. and Fogler H.S. 1998. The Influence of Chelating Agents on the Kinetics of Calcite Dissolution. *J. Colloid Interface Sci.* **204** (1):187-197.

[43] Fredd, C.N. and Fogler, H.S. 1998. The Kinetics of Calcite Dissolution in Acetic Acid Solutions. *Chem. Eng. Sci.,* **53** (22):3863-3874.

[44] Freeman, J.J., Appel, M., Perkiins, R.B., et al. Restricted Diffusion and Internal Field Gradient. SPWLA, 1999, FF.

[45] Freiner, W.W., Fredd, C.N., and Chang, F. 2001. Hydroxyaminocarboxylic Acids Produce Superior Formulations for Matrix Stimulation of Carbonates at High Temperatures, Paper SPE 71696 presented at annual Technical Conference and Exhibition. New Orleans, Louisiana, 30 September-3 October.

[46] Frick, T. P., Kurmayr M., and Economides M. J. 1994. An Improved Modeling of Fractal Patterns in Matrix Acidizing and Their Impact On Well Performance. *SPE Production & Facilities* **9**(1): 61–68.

[47] Friedmann, F. 1986. Surfactant and Polymer Losses during Flow through Porous Media. SPE *Reservoir Engineering Journal* **1**(3): 261-271.

[48] Furui, K., Burton, R.C., Burkhead, D.W. et al. 2012. A Comprehensive Model of High-Rate Matrix-Acid Stimulation for Long Horizontal Wells in Carbonate Reservoirs: Part I--Scaling Up Core-Level Acid Wormholing to Field Treatments. *SPE Journal*, **17**(1): 271–279.

[49] Glasbergen, G., Kalia, N., and Talbot, M. S. 2009. The Optimum Injection Rate for Wormhole Propagation: Myth or Reality? Paper Presented at the 8th European Formation Damage Conference, Scheveningen, The Netherlands, 27-29 May.

[50] Golfier, F., Zarcone, C., Bazin, B., Lenormand, R., Lasseux, D., and Quintard, M., 2002. On the ability of a Darcy-scale model to capture wormhole formation during the dissolution of a porous medium. *Journal of Fluid Mechanics* **475**:213-254.

[51] Gomaa, A. M. and Nasr-El-Din, H. 2010a. New Insights into Wormhole Propagation in Carbonate Rocks Using Regular, Gelled and In-Situ Gelled Acids. Paper SPE 133303 presented at the SPE Production and Operations Conference and Exhibition, 8-10 June, Tunis, Tunisia.

[52] Gomaa, A. M., and Nasr-El-Din, H. 2010b. Rheological and Core Flood Studies of Gelled and In-Situ Gelled Acids. Paper SPE 128056 presented at the North Africa Technical Conference and Exhibition, 14-17 February, Cairo, Egypt.

[53] Gomaa, A. M., and Nasr-El-Din, H. A. 2010c. Propagation of Regular HCl Acids in Carbonate Rocks: The Impact of an In-Situ Gelled Acid Stage. Paper SPE 130586 presented at the International Oil and Gas Conference and Exhibition in China, 8-10 June, Beijing, China.

[54] Gomaa, A. M., Mahmoud, M. A., and Nasr-El-Din, H. A. 2011. Laboratory Study of Diversion Using Polymer-Based In-Situ-Gelled Acids. *SPE Production & Operations Journal* **26**(3): 278 – 290.

[55] Gong, M., and El-Rabaa, A. M. 1999. Quantitative Model of Wormholing Process in Carbonate Acidizing. Paper SPE 52165 presented at the SPE Mid-Continent Operations Symposium, 28-31 March, Oklahoma City, Oklahoma.

[56] Grunewald, E. and Knight, R. 2011. The effect of pore size and magnetic susceptibility on the surface NMR relaxation parameters T2. *Near Surf. Geophys.*, **9**:169-178.

[57] Hansford, G.S. and Litt, M. 1968. Mass Transport from a Rotating Disk into Power Law Liquids," *Chem. Eng. Sci*. **23**: 849-864.

[58] Hill, D.G. 2005. Gelled Acid. United States Patent Application Publication, US2005/0065041 Al, 24 March.

[59] Hoefner, M.L. and Fogler, B.S. 1988. Pore Evolution and Channel Formation During Flow and Reaction in Porous Media. *AIChE J*., **34**(1):45-54.

[60] Huang, T., & Crews, J. B. 2008. Do Viscoelastic-Surfactant Diverting Fluids for Acid Treatments Need Internal Breakers? Paper SPE-112484-MS presented at the SPE

International Symposium and Exhibition on Formation Damage Control, 13-15 February, Lafayette, Louisiana, USA.

[61] Huang, T., Hill, A. D., and Schechter, R. S. 2000a. Reaction Rate and Fluid Loss: The Keys to Wormhole Initiation and Propagation in Carbonate Acidizing. *SPE Journal* **5**(3):287–292.

[62] Huang, T., McElfresh, P.M., and Garbrysch, A.D. 2003. Carbonate Acidizing Fluids at High Temperatures: Acetic Acid, Chelating Agents or Long-Chained Carboxylic Acids? Paper SPE 82268 presented at the SPE European Formation Damage Conference, The Hague, 13-14 May.

[63] Hubicki. H., and Kołodyńska, D. 2012. Selective Removal of Heavy Metal Ions from Waters and Waste Waters Using Ion Exchange Methods, Ion Exchange Technologies, Ayben Kilislioglu (Ed.), InTech.

[64] Ivanov, V.A., Timofeevskaya, V.D., Gorshkov, V.I., Drozdova, N.V. 1996. The role of temperature in ion exchange processes of separation and purification, *Journal of Radioanalytical and Nuclear Chemistry*, **208**(01)23-45.

[65] Johnson, D.E., Fox, K.B., Burns, L.D., and O'Mara, E.M. 1988. Carbonate production decline rates are reduced through improvements in gelled acid technology. Paper SPE 17297 presented at the Permian Basin Oil and Gas Recovery Conference, Midland, Texas, 10-11 March.

[66] Kalfayan, L. J., & Martin, A. N. 2009. The Art and Practice of Acid Placement and Diversion: History, Present State, and Future. Paper SPE 124141-MS presented at the

SPE Annual Technical Conference and Exhibition, 4-7 October, New Orleans, Louisiana.

[67] Kenyon WE. 1992. Nuclear Magnetic Resonance as a Petro- physical Measurement. Nuclear *Geophysics* **6**(2): 153-171.

[68] Kalfayan, L., 2008. Production Enhancement with Acid Stimulation. PennWell Corporation, Tulsa, Oklahoma, US.

[69] Klaewkla, R., Arend, M., and Hoelderich, W. F. 2011. A Review of Mass Transfer Controlling the Reaction Rate in Heterogeneous Catalytic Systems. Mass Transfer - Advanced Aspects, first Edition, H. Nakajima, Chapter 29 667-684. Rijeka, Croatia: INTECH.

[70] Kleinberg, R.L., Kenyon, W.E., and Mitra, P.P. 1994. Mechanism of NMR Relaxation of Fluids in Rock," J. of Magn. Reson. Ser.A, **108**:206-214.

[71] Korringa, J., Seevers, D.O., and Torrey, H.C. 1962. Theory of Spin Pumping and Relaxation in Systems with a Low Concentration of Electron Spin Resonance Centers," Phys. Rev. **127**(4):1143-1150.

[72] LePage, J.N., De Wolf, C.A., Bemelaar, J.H., Nasr-El-Din, H.A., 2009. An Environmentally Friendly Stimulation Fluid for High Temperature Applications. In: SPE International Symposium on Oilfield Chemistry, The Woodlands, Texas, USA.

[73] Levich V.G. 1962**.** Physicochemical hydrodynamics. Transl. by scripta technica, inc. Prentice-Hall.

[74] Li, Y., Liao, Y., Zhao, J., Peng, Y., and Pu, X. 2017. Simulation and analysis of wormhole formation in carbonate rocks considering heat transmission process. *Journal of Natural Gas Science and Engineering* **42**: 120-132.

[75] Lucia, F. J. 1995**.** Rock fabric/petrophysical classification of carbonate pore space for reservoir characterization: *American Association of Petroleum Geologists Bulletin*, **79**(9):1275–1300

[76] Lund K, Fogler HS, McCune CC. 1973. Acidization—I. The dissolution of dolomite in hydrochloric acid. *Chem. Eng. Sci*. **28**(3):691–IN1.

[77] Lund, K., H.S. Fogler, C.C. McCune, and Ault, J.W. 1975. Acidization - II. The Dissolution of Calcite in Hydrochloric Acid. *Chem. Eng. Sci*. **30**:825.

[78] Lungwitz, B. R., Fredd, C. N., Brady, M. E., Miller, M. J., Ali, S. A., & Hughes, K. N. 2007. Diversion and Cleanup Studies of Viscoelastic Surfactant-Based Self-Diverting Acid. *SPE production operation journal*, **22**(1): 121-127.

[79] Lynn, J.D. and Nasr-El-Din, H.A. 2001. A Core-Based Comparison of the Reaction Characteristics of Emulsified and In-Situ Gelled Acids in Low Permeability, High Temperature, Gas Bearing Carbonates. Paper SPE 65386 presented at the SPE International Symposium on Oilfield Chemistry, Houston, 13-16 February.

[80] MaGee, J., Buijse, M.A., and Pongratz, R. 1997. Method for Effective Fluid Diversion when Performing a Matrix Acid Stimulation in Carbonate Formations. Paper SPE 37736 presented at the Middle East Oil Show, Bahrain, 15-18 March.

[81] Maheshwari, P., and Balakotaiah, V. 2013. Comparison of Carbonate HCl Acidizing Experiments with 3D Simulations. *SPE Prod & Oper*. **28**(04): 402 – 413.

[82] Mahmoud M.A. 2017. Determination of the optimum wormholing conditions in carbonate acidizing using NMR. *Journal of Petroleum Science and Engineering*, **159**:952-969.

[83] Mahmoud, M. A. 2014. Evaluating the Damage Caused by Calcium Sulfate Scale Precipitation During Low- and High-Salinity-Water Injection. Journal of Canadian Petroleum Technology 53 (3): 141 – 150.

[84] Mahmoud, M. A., and Abdelgawad, K. Z. 2015. Chelating-Agent Enhanced Oil Recovery for Sandstone and Carbonate Reservoirs. *SPE Journal.* **20** (3) 483 – 495.

[85] Mahmoud, M. A., Nasr-El-Din, H. A., De Wolf, C. et al. 2011. Evaluation of a New Environmentally Friendly Chelating Agent for High-Temperature Applications. *SPE Journal* **16** (3): 559 – 574.

[86] Mahmoud, M. A., Nasr-El-Din, H. A., De Wolf, C., and LePage, J. 2011. Optimum Injection Rate of a New Chelate That Can Be Used to Stimulate Carbonate Reservoirs. *SPE Journal* **16**(4): 968 – 980.

[87] Mahmoud, M. A., Nasr-El-Din, H. A., LePage, J. N. et al. 2011. Optimum Injection Rate of a New Chelate That Can Be Used to Stimulate Carbonate Reservoirs. *SPE Journal*. **16** (4): 968 - 980.

(88) Mahmoud, M., Abdelgawad, K. Z., Elkatatny, S. M. et al. 2016. Stimulation of *Seawater* Injectors by GLDA (Glutamic-Di Acetic Acid). *SPE Drill & Compl* **31**(3) 178 - 187.

[89] Mahmoud, M., Al-Duailej, Y., Al-Khaldi, M. et al. 2016. NMR as a Characterization Tool for Wormholes. *SPE Prod & Oper* **31**(4): 362 – 373.

[90] Mahmoud, M.A. and Nasr-El-Din, H.A. 2014. Modeling Flow of Chelating Agents During Stimulation of Carbonate Reservoirs. *Arab J Sci Eng* **39**: 9239–9248.

[91] Mahmoud, M.A. with Nasr-El-Din, H.A., De Wolf, C.A., and LePage, J.N. 2011b. Optimum Injection Rate of a New Chelate That Can Be Used to Stimulate Carbonate Reservoirs. *SPE Journal* **16**(4): 968-980.

[92] Mahmoud, M.A., Barri, A., and Elkatatny. S.M. 2017. Mixing Chelating Agents with Seawater for Acid Stimulation Treatments in Carbonate Reservoirs. *Journal of Petroleum Science and Engineering*, **152**: 9–20.

[93] Mahmoud, M.A., Nasr-El-Din, H.A., De Wolf, C.A., LePage, and J.N., Bemelaar, J. H. 2011a. Evaluation of a New Environmentally Friendly Chelating Agent for High Temperature Applications. *SPE Journal* **16** (3): 559-574.

[94] Mostofizadeh, B. and Economides, M. J. 1994, January 1). Optimum Injection Rate from Radial Acidizing Experiments. Paper SPE 28547 presented at the SPE Annual Technical Conference and Exhibition, 25-28 September, New Orleans, Louisiana.

[95] Muskat, M.: Physical Principles of Oil Production, McGraw-Hill Book Co. Inc., New York City (1947) 242.

[96] Nasr-El-Din HA, Al-Mohammed AM, Al-Aamri AD, Al-Fahad MA, Chang FF. 2009. Quantitative Analysis of Reaction-Rate Retardation in Surfactant-Based Acids. SPE Prod. Oper. **24**(1):107–16.

[97] Nasr-El-Din, H. A., Al-Ghamdi, A. H., Al-Qahtani, A. A., & Samuel, M. M. (2008, March 1). Impact of Acid Additives on the Rheological Properties of a Viscoelastic Surfactant and Their Influence on Field Application. SPE Journal **13**(1): 35 – 47.

[98] Nasr-El-Din, H. A., de Wolf, C. A., Stanitzek, T. et al. 2013. Field Treatment to Stimulate a Deep, Sour, Tight-Gas Well Using a New, Low Corrosion and Environmentally Friendly Fluid. *SPE Prod & Oper* **28**(03): 277 – 285.

[99] Newman J. 1966. Schmidt Number Correction for the Rotating Disk. J. Phys. Chem. **70**(4):1327–8.

[100] Nierode, D. E. and Williams, B. B. 1971. Characteristics of Acid Reaction in Limestone Formations. *SPE J*. **11**(04):406-418.

[101] Nuñez, W., Bautista, O., Cepeda, F. A. et al. 2017. Field Treatment of an Injector Well in a Sandstone Formation Using a Low Corrosive Environmentally Friendly Fluid that Does Not Require Flow-Back. Presented at the SPE Latin America and Caribbean Petroleum Engineering Conference, Buenos Aires, Argentina, 17-19 May.

[102] Qiu XW, Zhao W, Dyer SJ, Al Dossary A, Khan S, Sultan AS. 2014. Revisiting Reaction Kinetics and Wormholing Phenomena During Carbonate Acidizing. Paper IPTC-17285-MS presented at International Petroleum Technology Conference, Doha, Qatar, 19-22 January.

[103] Rabie AI, Shedd DC, Nasr-El-Din HA. 2014. Measuring the Reaction Rate of Lactic Acid with Calcite and Dolomite by Use of the Rotating-Disk Apparatus. *SPE Journal*, **19**(6):1192–202.

[104] Ramakrishnan, T.S., Schwartz, L.M., Fordhan, E.J., Kenyon, E.J., and Wilkinson, D.J.: "Forward Models for Nuclear Magnetic Resonance in Carbonate Rocks," SPWLA, 1998, SS.

[105] Sayed M, Nasr-El-Din HA, Nasrabadi H. 2013. Reaction of Emulsified Acids with Dolomite. *J. Can. Pet. Technol*. **52**(3):164–75.

[106] Sayed, M. A. I., and Nasr-El-Din, H. A. 2013. Acid Treatments in High Temperature Dolomitic Carbonate Reservoirs Using Emulsified Acids: A Coreflood Study. Paper SPE 164487 presented at the SPE Production and Operations Symposium, 23-26 March, Oklahoma City, Oklahoma, USA.

[107] Sayed, M., Nasr-El-Din, H. A., and Nasrabadi, H. 2013. Reaction of Emulsified Acids with Dolomite. *Journal of Canadian Petroleum Technology* **52**(3): 164 – 175.

[108] Scholle, Peter A., and Dana S. Ulmer-Scholle. 2003. A Color Guide to the Petrography of Carbonate Rocks: Grains, Textures, Porosity, Diagenesis, AAPG Memoir 77.

[109] Sørland, G.H., Djurhuus, K., Widerøe, H.C., et al. 2017. Absolute Pore Size Distributions from NMR. *Diffusion Fundamentals*, **5**:24.1-1.15

[110] Straley, C., Rossini, D., Vinegar, H., et al. 1997 Core Analysis by Low-Field NMR. *The Log Analyst*, **38**(2):84-95.

[111] Taylor KC, Al-Ghamdi AH, Nasr-El-Din HA. 2003. Effect of Rock Type and Acidizing Additives on Acid Reaction Rates Using the Rotating Disk Instrument. Paper SPE-80256-MS presented at the International Symposium on Oilfield Chemistry, Houston, Texas, 5-7 February.

[112] Taylor KC, Nasr-El-Din HA. 2009. Measurement of Acid Reaction Rates with the Rotating Disk Apparatus. J. Can. Pet. Technol. **48**(6):66–70.

[113] Taylor KC, Al-Ghamdi AH, Nasr-El-Din HA. 2003. Effect of Rock Type and Acidizing Additives on Acid Reaction Rates Using the Rotating Disk Instrument. Paper SPE-80256-MS presented at the International Symposium on Oilfield Chemistry, Houston, Texas, 5-7 February.

[114] Taylor, K. C., Al-Ghamdi, A. H., and Nasr-El-Din, H. A. 2004. Effect of Additives on the Acid Dissolution Rates of Calcium and Magnesium Carbonates. *SPE Prod & Fac* **19**(03): 122 - 127.

[115] Toumelin, E., Torres-Verdin, C., Chen, S., et al. "Analysis of NMR Diffusion Coupling Effects in Two-Phase Carbonate Rocks: Comparison of Measurements with Monte Carlo Simulations," SPWLA, 2002, JJJ.

[116] Toumelin, E., Torres-Verdin, C., Chen, S., et al. 2003. Reconciling NMR Measurements and Numerical Simulations: Assessment of Temperature and Diffusive Coupling Effects on Two-Phase Carbonate Samples. *Petrophysics*, **44**(2):91-107.

[117] Wang, X., Qu, Q., Cutler, J.L. et al. 2009. Nonaggressive Matrix Stimulation Fluids for Simultaneous Stimulation of Heterogeneous Carbonate Formations. Paper SPE 121712 presented at the SPE International Symposium on Oilfield Chemistry, The Woodlands, Texas, 20-22 April.

[118] Wang, Y., A.D. Hill, and R.S. Schechter. 1993. The Optimum Injection Rate for Matrix Acidizing of Carbonate Formations. Paper SPE 26578-MS presented at the SPE Annual

[119] Warren, E.A. and Pulham, A.J. 2001. Anomalous Porosity and Permeability Preservation in Deeply Buried Tertiary and Mesozoic Sandstones in Cusiana Field, Llanos Foothills, Colombia. *Journal of Sedimentology Research* **71** (1): 2-14.

[120] Williams, B., Gidley, J., and Schechter, R., 1979. Acidizing Fundamentals. SPE Monograph Series, Richardson.

[121] Yen, S.C, Wang J.S., and Chapman, T. W. 1992. Experimental Mass Transfer at a Forced-Convective Rotating-Disk Electrode. *J. Electrochem. Soc.* **139**(8):2231-2238.

[122] Yu, M., Mahmoud, M.A., and Nasr-El-Din, A.H. 2011. Propagation and Retention of Viscoelastic Surfactants Following Matrix-Acidizing Treatments in Carbonate Cores. *SPE Journal* **16** (4): 993-1001.

[123] Zakaria, A. S., Sayed, M. A., and Nasr-El-Din, H. A. 2012. Propagation of Emulsified Acids in Vuggy Dolomitic Rocks. Paper SPE 163288 presented at the SPE Kuwait International Petroleum Conference and Exhibition, 10-12 December, Kuwait City, Kuwait.

Vitae

Name	:Khaled Z. Abdelgawad
Nationality	:Egyptian
Date of Birth	:8/9/2017
Email	:Abouzidan@icloud.com
Address	: Dhahran, Saudi Arabia
Academic Background	:B.S., in petroleum engineering from Suez University, Egypt, 2009, M.Sc. in petroleum engineering from KFUPM, Saudi Arabia, 2013, and Ph.D., in petroleum engineering, from KFUPM, Saudi Arabia, 2017

Peer-reviewed journal articles

1) Abdelgawad, K.Z., Mahmoud, M., Elkatatny, S.M. 2017. Stimulation of High Temperature Carbonate Reservoirs using Seawater and GLDA Chelating Agent: Reaction Kinetics and Coreflooding Study. *SPE production operations journal (accepted).*
2) Abdelgawad, K.Z., Mahmoud, A.M., and Ibnelwaleed H. 2017. Stimulation of High Temperature Carbonate Gas Reservoirs using Seawater and Chelating Agents: Reaction Kinetics. *Journal of Natural Gas Science & Engineering*, in Press.
3) Mahmoud, M., Abdelgawad, K.Z., Elkatatny, S. M., Akram, A., & Stanitzek, T. 2016. Stimulation of Seawater Injectors by GLDA (Glutamic-Di Acetic Acid). *SPE Journal Drilling & Completion* **31**(3): 483 – 495.
4) Mahmoud, M., Abdelgawad, K.Z. **2015**. Chelating-Agent Enhanced Oil Recovery for Sandstone and Carbonate Reservoirs. *SPE Journal* **20**(3): 483 – 495.

Papers Submitted to journals

1) Ba-geri, B.S., Mahmoud, M., Abdelgawad, K.Z., et al. 2017. Evaluation of the Reaction Kinetics of Chelating Agents with Barium Sulfate (Barite) Using Rotating Disk Apparatus. *Journal of Petroleum Science e and Engineering.*

Conference Papers & Presentations

1) Mahmoud, M., Abdelgawad, K.Z., Elkatatny, S. M., Akram, A., & Stanitzek, T. **2015**. Non- Coiled Tubing Stimulation of Water Injectors. Paper SPE 172572 presented at SPE MEOS, Manama, Bahrain, 8-11 March.
2) Abdelgawad, K.Z. and Mahmoud, A.M. **2017**. Seawater Stimulation fluid system for High Temperature Carbonate reservoirs: Reaction Kinetics Study. Paper SPE 177448 to be presented at the SPE KOGS, Kuwait City, Kuwait, 15-18 October.